Instrument Familiarization Plan for ground based observations of SPSS. II. Calibration Frames Study and Recommendations

prepared by: S. Marinoni, S. Galleti, G. Cocozza, E. Pancino, G. Altavilla
approved by: F. van Leeuwen
authorized by: M.G. Lattanzi
reference: GAIA-C5-TN-OABO-SMR-002
issue: 1
revision: 0
date: 18 Apr 2013
status: Issued

Abstract

When trying to build a large set of ground based SpectroPhotometric Standard Stars (SPSS) for calibrating Gaia BP/RP spectra and G-Band images to a few % in absolute flux, it is essential to maintain the maximum homogeneity in data quality, acquisition and treatment. This IFP Protocol concerns the calibration frames stability monitoring of all instruments used in the ground-based campaigns aimed at building the grid of Gaia SPSS. The result of this protocol provide clear guidelines for our observations and data reduction strategies.

Document History

Issue	Revision	Date	Author	Comment
1	0	18-Apr-2013	SMR	Corrections and suggestions from FVL implemented. Document ready for Livelink.
D	5	20-Mar-2013	SMR	Corrections from co-authors implemented and document authorized by Lattanzi
D	4	20-Jan-2013	SMR	Study of all CCDs used with LaRuca
D	3	15-Jul-2012	SMR	New figures from pipeline and Marconi1 CCD study
D	2	24-Nov-2011	SMR	Correction post-PhD Thesis and post automatic pipeline version implemented
D	1	11-Feb-2011	SMR	EP corrections implemented
D	0	17-Jan-2011	SMR	Creation

Acronym	**Description**
ADU	Analogue-to-Digital Unit
BFOSC	Bologna Faint Object Spectrograph & Camera
BP	Blue Photometer
CAFOS	Calar Alto Faint Object Spectrograph
CAHA	Centro Astronómico Hispano Alemán
CCD	Charge-Coupled Device
DoLoRes	Device optimized for Low Resolution spectroscopy
EFOSC2	ESO Faint Object Spectrograph & Camera
ESO	European Southern Observatory
IFP	Instrument Familiarization Plan
IRAF	Image Reduction and Analysis Facility (NOAO)
LaRuca	Rueda Cachanilla
NTT	New Technology Telescope (ESO)
QA	Quality Assurance
QC	Quality Control
REM	Rapid-Eye Mount
RON	Read-Out Noise (CCD)
ROSS	REM Optical Slitless Spectrograph
RP	Red Photometer
SPM	San Pedro Mártir Observatory
SPSS	Spectro-Photometric Standard Star
TNG	Telescopio Nazionale Galileo

Contents

1 Introduction

Our task is to build a grid of *Spectro-Photometric Standard Stars* (SPSS), see GA-001, GA-003, and Pancino et al. (2012), suitable for the absolute calibration of the BP/RP spectrophotometers and of the G-Band of Gaia (see MBZ-001). The precision required for the Gaia SPSS grid is a few percent in flux at most, relative to Vega. The ground-based observations of SPSS represent an enormous observational effort, that must rely on different telescopes and instruments (see LF-001 and GA-002). Therefore, we must ensure the maximum homogeneity in the observation procedures (EP-001, EP-003, and EP-006), in the data reduction (SMR-001 and GCC-001) and analysis (SMR-003, SMR-004, and GA-006).

As a first step, because we are interested in accurate and precise spectrophotometry, it is mandatory to test the capabilities of each telescope/instrument combination and to devise methods to keep systematics under control, and eventually to correct for the typical instrumental effects that can affect the high precision required for the Gaia SPSS grid.

Four kinds of tests form the so-called *Instrument Familiarisation Plan* (IFP):

1. *CCD Performance Tests*: even if most telescope staffs measure regularly their CCD performances, we need to perform very high quality photometry and spectroscopy. Therefore we must know the Instrument Shutter characteristics and the CCD Linearity very well (see GA-004).
2. *Calibration Frames Monitoring Tests*: concern the stability and reliability of both the calibration frames that we use to remove the instrument signature, and the lamps to provide the wavelength calibration of our spectra (this document).
3. *Instrument Performance Tests*: are only required for instruments with spectroscopic capabilities, and are aimed at understanding and correcting for effects like the second order light contamination and polarization added by the mirrors inside each instrument (see GA-005).
4. *Photometricity and Extinction Monitoring Tests*: aimed at determining zero points and extinction coefficients for all clear nights or nights that were judged photometric by the observers (in preparation).

The Instrument Familiarization Plan is of fundamental importance since its results can affect both the observing and data reduction strategies, as shown in Fig. 1. For example, a stability monitoring of calibration frames (over at least one run) is necessary to evaluate if, when appropriate calibrations are missing for one night, those taken in adjacent nights can be safely used to pre-reduce scientific data. This allows to build a *calibration plan* for all the instruments we use. In addition, because we are interested in accurate and precise spectrophotometry, instrumental

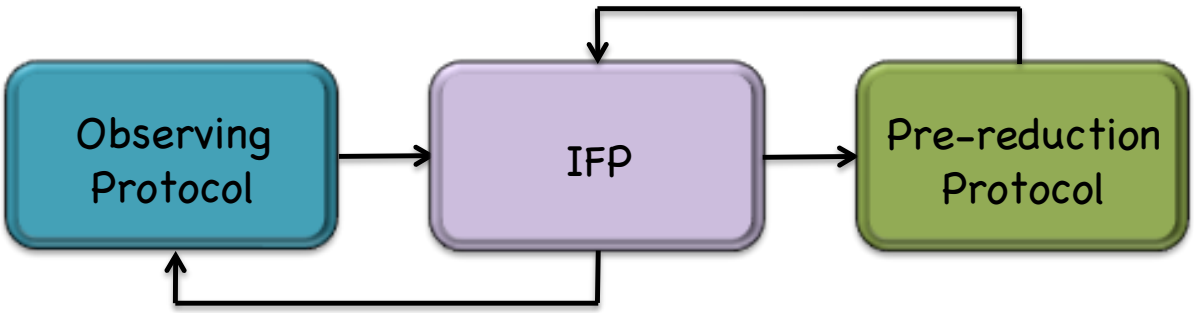

FIGURE 1: Schematic view of how the IFP is related with both the observing and reduction strategies.

effects which may affect our measurements, as for example the CCD linearity, must be investigated. The result of the CCD linearity test obviously affects the observing protocols, because it defines the CCD range we can exploit in our observations and the quality control criteria for our data reduction protocols.

In this document we report the results of the Calibration Monitoring, showing the study of the short-term (one run) and long-term (covering a period of at least one year) stability of the calibration masterframes.

2 IFP strategy

When pre-reducing images and spectra (see SMR-001 and GCC-001), a quality assurance is performed by defining and measuring a set of Quality Control (QC) parameters[1]. These same parameters are used here to study the masterframes stability on timescales longer than a single night. A short-term[2] stability monitoring is necessary to evaluate if, when appropriate calibrations are missing for one night, the ones acquired in adjacent nights can be safely used in the pre-reduction process. Together with a long-term[3] stability monitoring, it is also useful to build a *calibration plan* for the instruments used. In the following sections we describe how the monitoring is performed, and we summarize the results in Section 9. Detailed monitoring of the various instruments is described in the instrument-specific Appendices. The complete set of monitoring plots can be found as usual in Wiki-Bo[4], while here we present just a few examples.

[1] `http://yoda.bo.astro.it/wiki/index.php/IFP_QC_Parameters`
[2] In the present context, *short-term* means one run.
[3] In the present context, *long-term* means more than one run.
[4] `http://yoda.bo.astro.it/wiki/index.php/IFP_Calibration_Frames_Summary`

3 Masterbias Monitoring

The details of the production of masterbias frames, as well as both the QC parameters evaluation and the short-term monitoring of the intensity level and 2D structure of these calibration frames, are described in SMR-001. An example is shown in Fig. 2. In brief, five areas on the surface of each masterbias are defined (one for each corner and one for the centre) and the ratio between the median value of each corner and the median value of the centre is the QC parameter which allows us to monitor the 2D shape of a masterbias. The stability of the bias level over one run can be checked together with the 2D structure stability using the appropriate pipeline[5] available in Wiki-Bo. The same parameters and pipeline can be used to visualize the long-term stability trend over more than one run. An example is shown in Fig. 3.

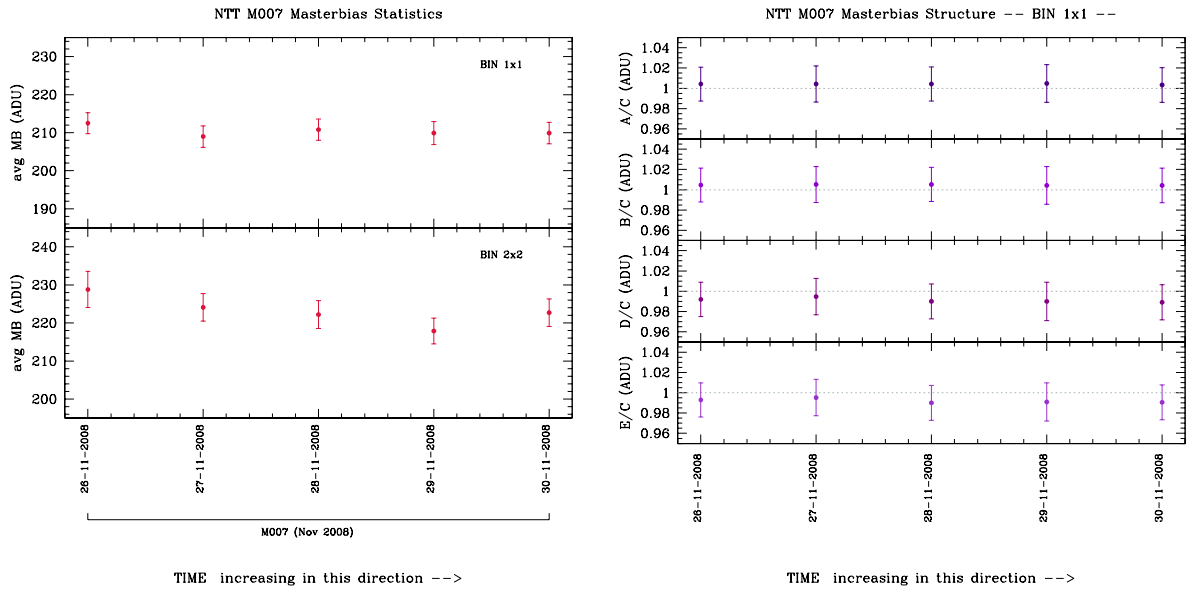

FIGURE 2: Example of a short-term masterbias stability monitoring. In the *left panel* the statistics of all masterbias frames produced using the data acquired with EFOSC2@NTT during run M-007 (and with different binning factors) are used to produce the *bias level* plot. In the *right panel* the *2D structure stability* plot is produced using the same data set (only the example for BIN 1x1 is shown): A, B, D, E labels refer to the areas at the corners, C at the central area (see SMR-001 for more details).

[5] http://yoda.bo.astro.it/wiki/index.php/QC_MasterBiaspipe

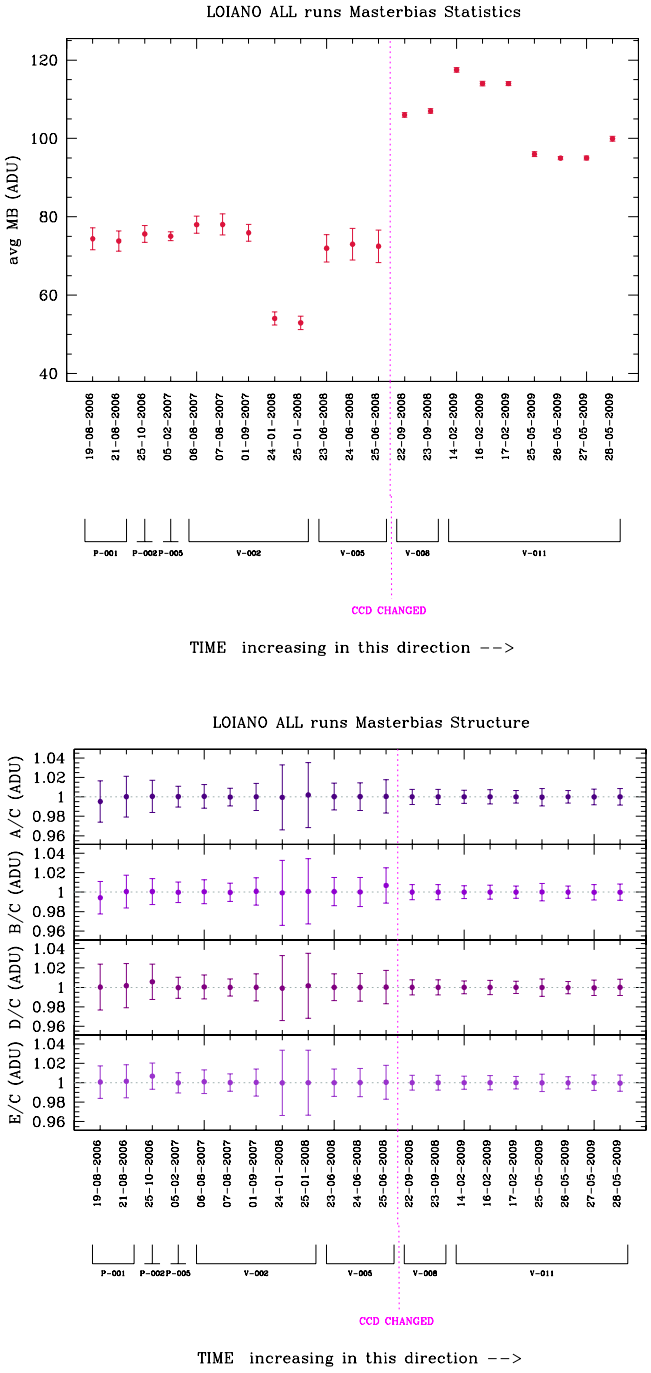

FIGURE 3: Long-time trend monitoring of the bias level (*upper panel*) and two-dimensional structure (*bottom panel*) produced using data acquired in our first seven runs with BFOSC@Cassini. Between runs V-005 and V-008, a new CCD was mounted : the improvement in data quality is clearly visible in the two-dimensional stability trend plot. Anyway, for both CCDs, the masterbias frames appear to be sufficiently stable (within 1-2%) in their 2D shape, although the absolute global level may vary from night to night.

4 Masterflat Monitoring

As for bias frames, the production and QC parameters evaluation, as well as the short-term monitoring of masterflat frames, are performed together with the data pre-reduction as described in SMR-001 and GCC-001. Summarizing, of the three stability tests used to monitor the short-term photometric flat stability and described in detail in SMR-001[6], two are of interest for the calibration frames monitoring: the *large scale variability*, which provides information on the "global" variation of the masterflat shape in comparison with a reference flat (assuming the variation uniformly distributed all over the pixels), and the *9 areas* check-plot which provides information on "where" and "how much" is the variation of the flat shape in comparison with a reference flat. Examples of these two plots in the short term monitoring framework are reported in Fig. 4 and Fig. 5. The long-term monitoring of masterflats is not strictly needed, since we generally exclude the possibility to use masterflat frames produced in one run to pre-reduce data acquired during other runs. Nevertheless, the photometric masterflat QC pipeline allows to perform this kind of test and two examples are shown in Fig. 6 and Fig. 7. The results of the long term monitoring performed for our instruments used in photometric mode are reported in the instrument-specific Appendices.

For spectroscopic flats, because they are flattened to remove the shape of the lamp spectrum (see GCC-001), a monitoring of large-scale variations similar to the one performed on photometric flats is not necessary.

5 Masterdark Monitoring

The details of masterdark production and QC parameters evaluation are described in SMR-001. In brief, the trend of dark counts with exposure time is checked and the extrapolation at zero exposure time is compared with the bias level (see, for example, Fig. 8). The long-term monitoring of masterdark is essential only for ROSS@REM: the CCD is not nitrogen-cooled and dark currents become important[7]. As an example, we report in Fig. 9 and Fig. 10 respectively the dark level and the two-dimensional stability trends for the 60 sec masterdarks during the first three REM runs (V-001, V-004 and V-007). Masterdark frames, for both exposure times, are very stable in shape, but the counts level show seasonal changes. Therefore, our pre-reduction protocol (SMR-001) foresees the use of the closest available masterdark, which is produced monthly by the REM staff. This is not the case for all other instruments used in our campaigns: correction for masterdark is not necessary. However a series of dark frames with increasing exposure time are taken every 1-2 years in order to monitor the instrument: the resulting plots are shown in the instrument-specific appendices.

[6]The pipeline to perform all the tests is available in Wiki-bo at: `http://yoda.bo.astro.it/wiki/index.php/QC_MasterFlatPhotopipe`.

[7]Bias frames are not acquired with ROSS: dark frames already include the bias level and pattern (see EP-003).

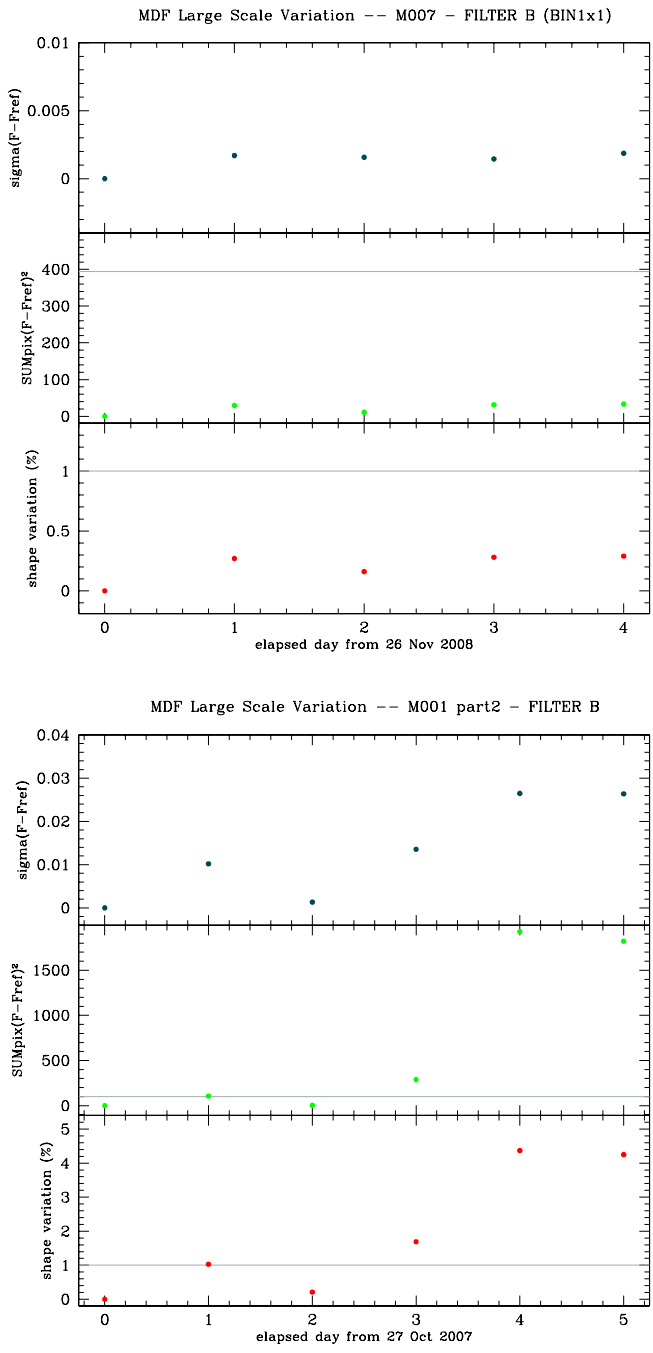

FIGURE 4: Examples of *large scale variability* plot on a short timescale (one run), see SMR-001 for details. The plot is divided in 3 window reporting respectively the parameter $\Delta S/S$ (the so called *Shape Variation*, in the bottom panel), the function K_{stab} (in the middle panel) and the sigma of each "difference frame" (in the upper panel). The *upper plot* shows the very good case of M-007@NTT: the global shape variation for all masterflats is always lower than 0.3%. In the *bottom plot* the situation is not so good: the shape of the masterflats obtained during the run M-001@CAHA is changing every night and also the global shape variation is high, reaching almost 4.5% in the worst case.

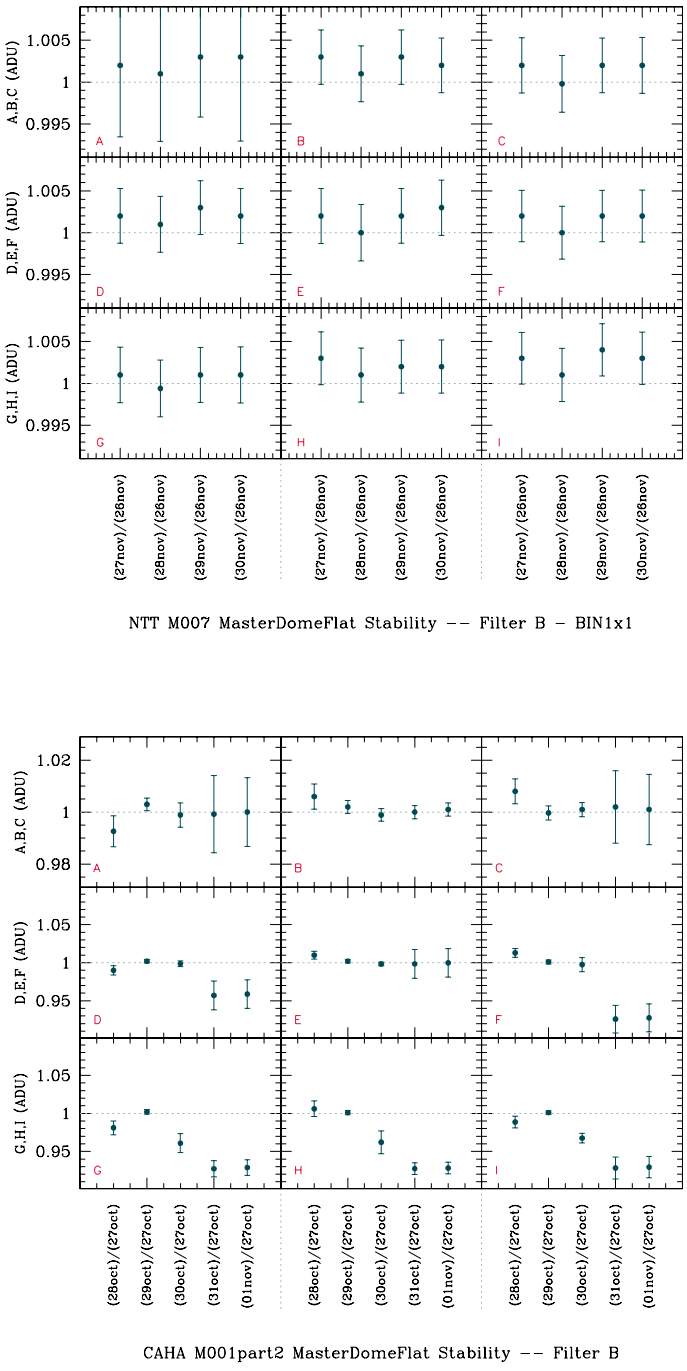

FIGURE 5: Examples of *9 areas* plot on a short timescale (one run), see SMR-001 for details. In both panels, the plot is built considering the same data used in Fig. 4. The plot is divided in 9 windows in which the mode and standard deviation of each "ratio frame" are shown. The *upper plot* shows the very good example of M-007@NTT. The *bottom plot* shows the less good case of M-001@CAHA: the most important variation of the masterflat shape occurs in the bottom part of the frames.

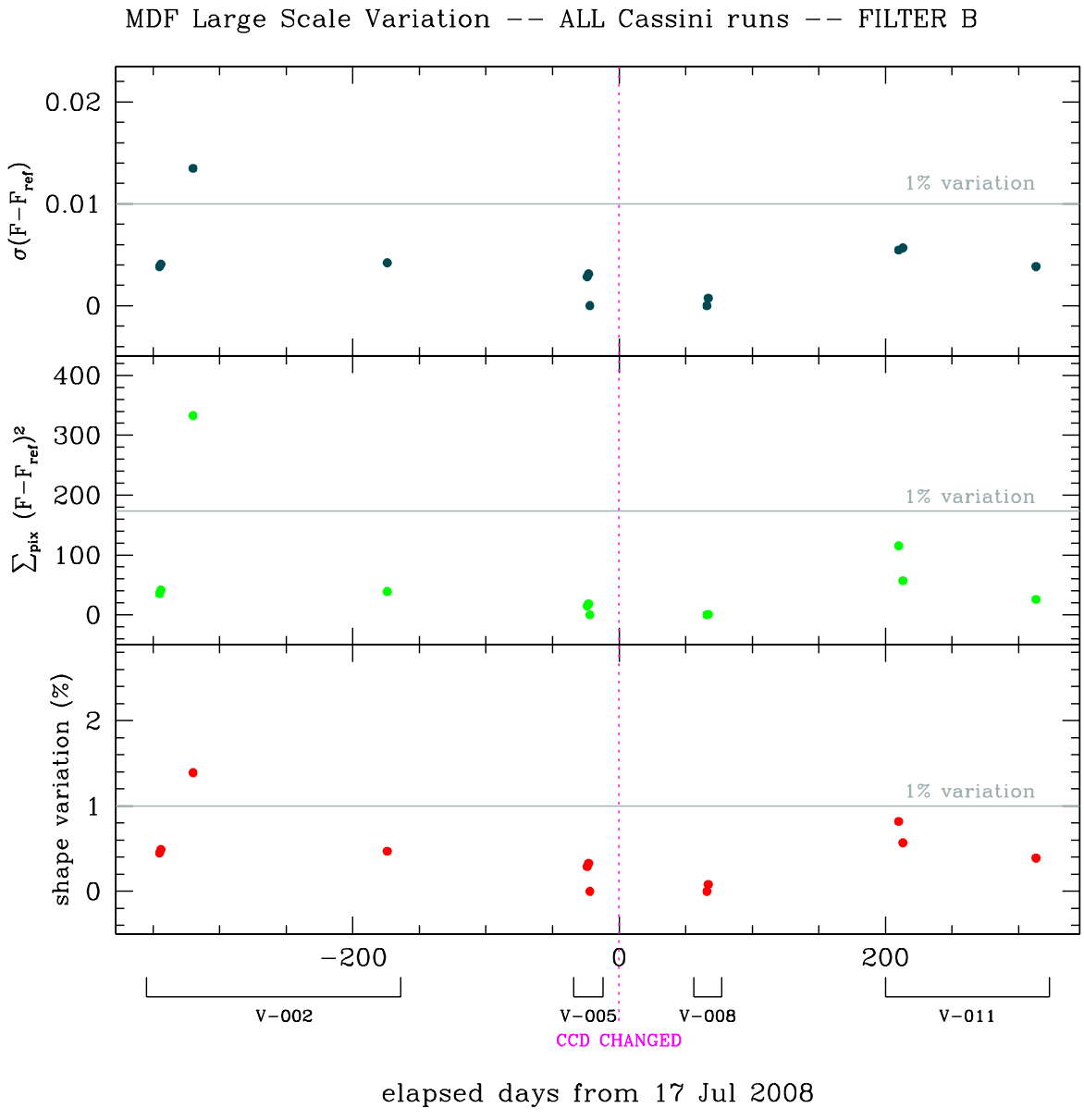

FIGURE 6: Long-time large scale variability test performed on all imaging dome-masterflats produced with the B filter during three consecutive runs in Loiano (BFOSC@Cassini). Owing to the CCD change between run V-005 and V-008, two reference frames were chosen: the dome-masterflat of the last night of run V-005 is used as a reference for the old CCD, while that of the first night of run V-008 is the reference for the new CCD. The time-lenght stability of masterflats is very good for both CCDs, reaching about 300 days.

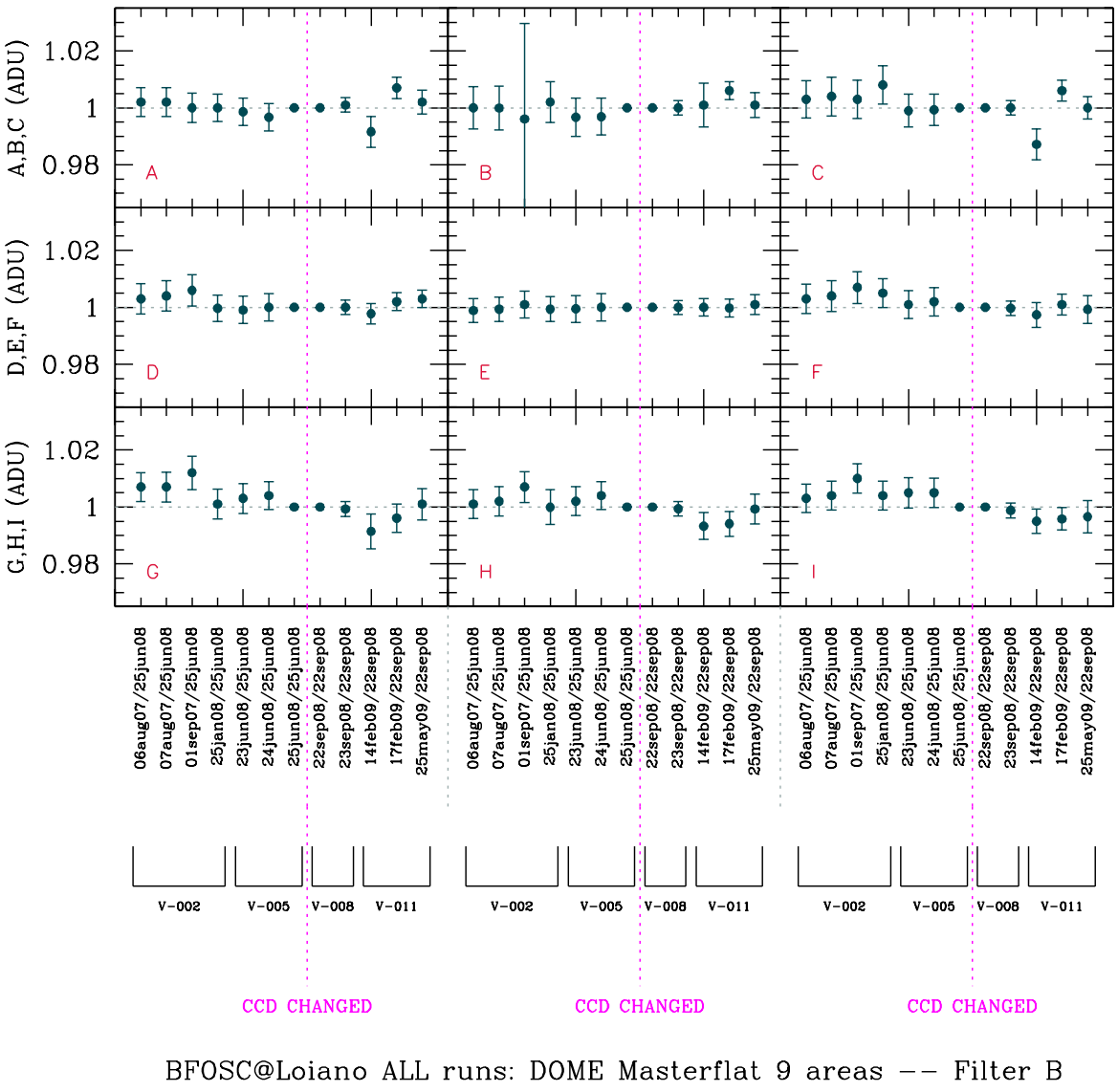

FIGURE 7: Long-time 9 areas test performed on all dome masterflat produced with the B filter during the first four V-runs in Loiano. The reference frames for each CCD used are the same of Fig. 6. The B panel of this plot shows the "bad" region of the dome masterflat produced using data acquired on 01-09-2008: this is due to a very big grain of dust on the CCD window.

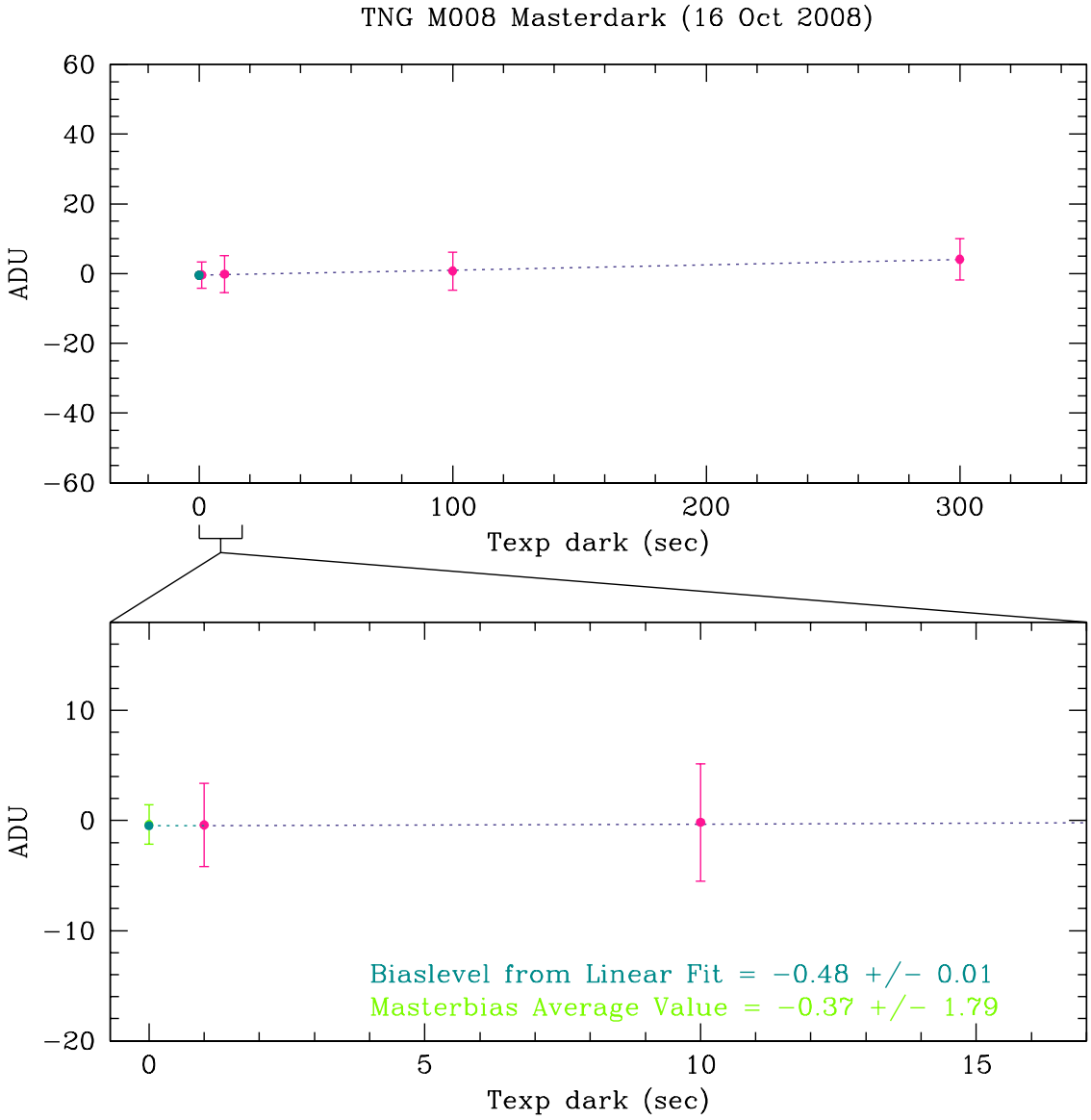

FIGURE 8: Example of masterdark growth plot (see SMR-001 for details) for one dark sequence obtained in run M-008@TNG. The points and errorbars in the plot represent respectively the median value and the standard deviation computed for each masterdark on the whole frame (see SMR-001 for further details). In the *bottom panel* a zoom is shown in order to compare the bias level extrapolated from the linear fit (dark green point) with that measured directly from the masterbias (light green point). The dotted line is the linear fit.

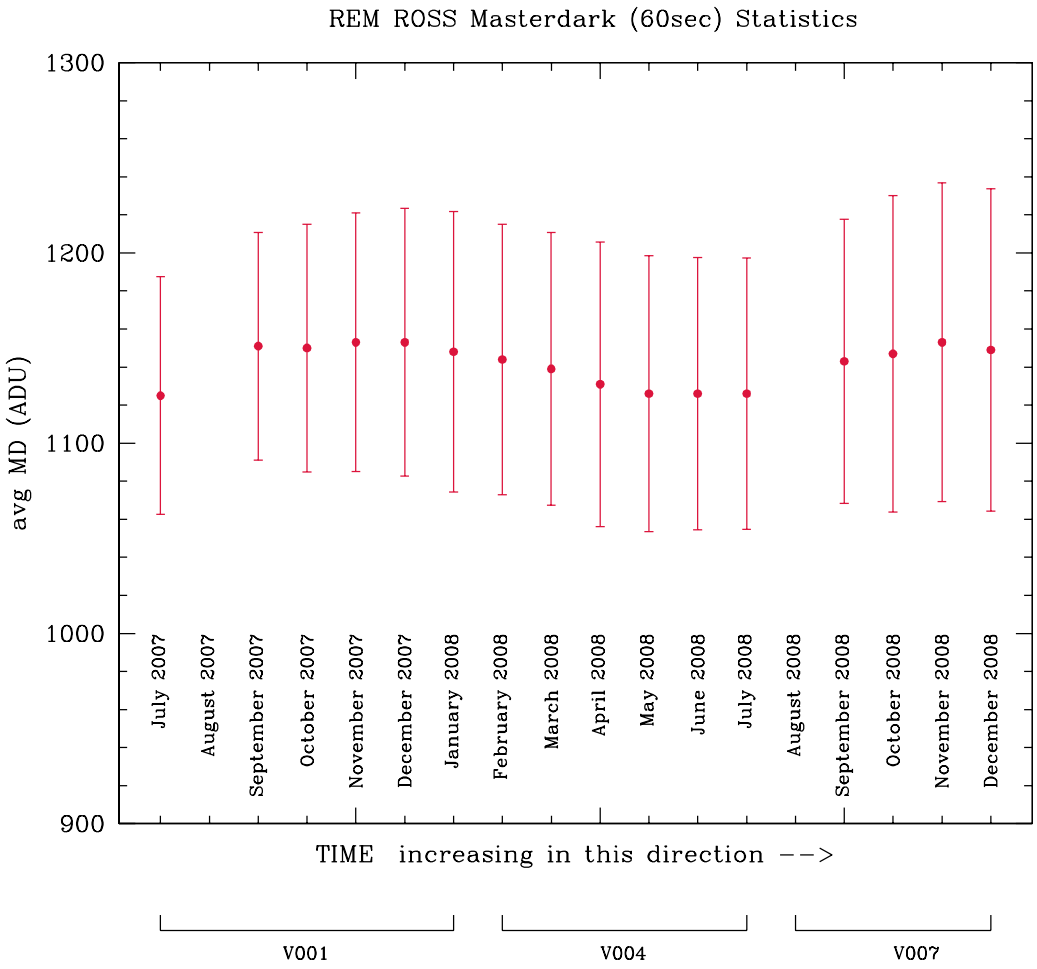

FIGURE 9: Long-time trend of the 60 sec dark level produced using data acquired with ROSS@REM in the first three runs. This plot is produced only for ROSS monthly masterdarks following the same strategy used to monitor the intensity level of masterbias (see Sec. 3 and SMR-001). The plot is produced using the statistics of all monthly masterdark frames for each specific exposure time (in this case, 60 sec).

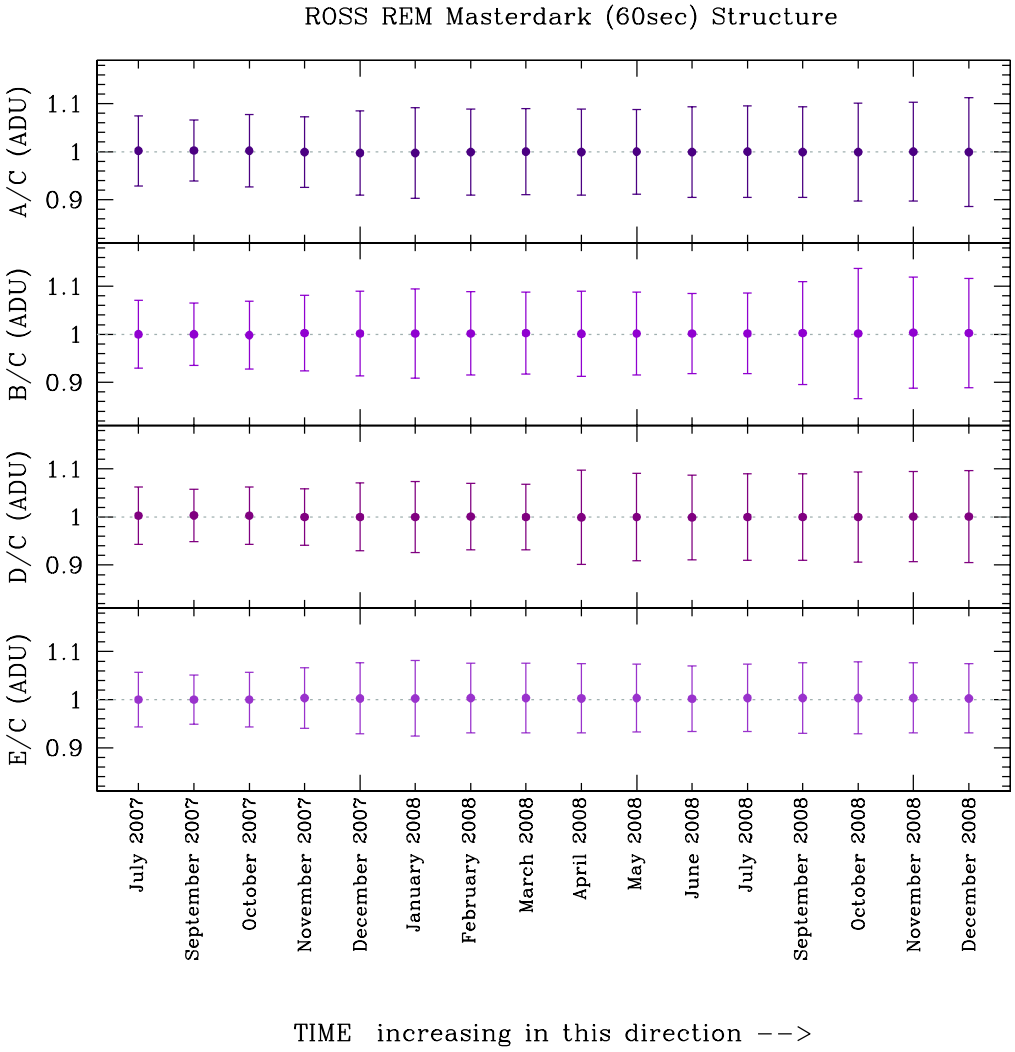

FIGURE 10: Long-time trend of the two-dimensional structure produced using data acquired with ROSS@REM in the first three runs. This plot is produced only for ROSS monthly masterdarks using the same technique which allows us to monitor the 2D shape of a masterbias (see Sec. 3): five areas on the surface of each ROSS monthly masterdark are defined (one for each corner and one for the centre) and the statistics on these areas are computed. The points in the plot are ratio between the median value of each corner and the median value of the centre, while the errorbars are computed using the error propagation law (see and SMR-001 for further details) considering as errors on the median values the standard deviation computed in the corresponding areas.

6 Bad Pixel Mask

The detailed procedure to obtain the bad pixel mask is described in SMR-001, where examples can be found for each instrument. The cosmetics of CCDs used in our campaigns is not always optimal, therefore data required to build BPMs are taken every 1-2 years in order to allow for the best correction possible for bad pixels and columns during the pre-reduction process.

7 Fringing

In the case of photometric observations, the fringing mask for the filter R (or for the I filter, when used) can be obtained using all R (or I, if any) scientific images acquired during the night, following the simple procedure described in SMR-001. In the same document some examples of fringing mask can be found for each instrument. In the imaging case, exposure times are always quite short with all the used instruments: the sky is not so strong to produce a significant fringing pattern. As a result, the fringing correction is not needed in our pre-reduction pipeline. For the spectroscopic case, fringing is one of the major problems in data reduction because no fringing mask can be produced and no specific correction performed (but a partial correction is provided by flat fielding). Both spectroscopic masterflats and scientific frames acquired using red grisms are strongly contaminated by fringing. At least when the wide slit is adopted to acquire spectra, the corresponding masterflat seems to present a stable and almost constant fringing pattern. Nevertheless, the result in the correction for the fringing in the scientific spectra (when the masterflat correction is performed) will depend on the star position in the slit. A detailed discussion on the effects which the flat correction produce on scientific frames is presented in GCC-001.

8 Wavelength Lamp Flexures

Low resolution spectrographs are usually mounted at the telescope or at the telescope derotator, and they move during observations. At each different position, the varying projection of the gravitational force leads to mechanical distortions, either negligible or important. These mechanical distortions are seen on the wavelength calibration frames, where they produce shifts of the lamp emission lines which can be linear or non-linear in wavelength.
To evaluate mechanical distortions, lamps must be taken at different positions of the telescope. Depending on the instrument/telescope combination, the position can be parametrized with a single angle (the derotator angle) if the instrument is attached to a fixed derotator (as at a Nasmyth focus), or with two different angles if the instrument is mounted at the telescope. In the simplest case, lamp flexures can be measured with one full circle of the derotator angles, by moving the derotator both in the clockwise and anti-clockwise directions, with respect to a reference position, for an ideal total of $\sim$70-140 wavelength lamp exposures (steps of $\sim$5-10 deg). The choice of the lamp depends on the expected kind of distortion. One lamp with a relatively

good wavelength coverage is sufficient if only linear distortions are expected. If, after a first set of measurements, non-linear distortions are suspected, measurements could be repeated with at least two different lamps, to evenly sample the whole spectral range covered by Gaia (330-1050 nm).
A test was performed with DoLoRes, measuring line shifts at different positions of the derotator (see Appendix C, Section C.4). The result of the test was that a linear shift was sufficient to report all spectra to the same wavelength scale. The observing protocol (EP-003) and the spectroscopic pre-reduction protocol (GCC-001) foresee a conservative strategy, where lamps are taken during the night close to each observed (narrow slit) spectrum, whenever possible.

9 Results and Recommendations

All the results concerning the Calibration Frames, for each telescope/instrument configuration, are reported in a dedicated table hosted by Wiki-Bo[8] (see Fig. 11). In this table, each active link can be followed to open specific dedicated pages for each kind of calibration frames and for each instrument.

SUMMARY						
	BFOSC	CAFOS	DoLoRes	EFOSC2	LaRuca	ROSS
DARK	Short Time Trend at Dark_Loiano NO Long Time Trend	Short Time Trend at Dark_CAHA NO Long Time Trend	Short Time Trend at Dark_TNG NO Long Time Trend	Short Time Trend at Dark_NTT NO Long Time Trend	Short Time Trend at Dark_SPM NO Long Time Trend	Short Time Trend at Dark_REM Long Time Trend at Dark_REM
BIAS	Short Time Trend at Bias_Loiano Long Time Trend at Bias_Loiano	Short Time Trend at Bias_CAHA Long Time Trend at Bias_CAHA	Short Time Trend at Bias_TNG Long Time Trend at Bias_TNG	Short Time Trend at Bias_NTT Long Time Trend at Bias_NTT	Short Time Trend at Bias_SPM Long Time Trend at Bias_SPM	NO BIAS
BAD PIXEL MASK	BPM_Loiano	BPM_CAHA	BPM_TNG	BPM_NTT	BPM_SPM	no BPM
FRINGING MASK	correction not needed	correction not needed	correction not needed	correction not needed	correction not needed	correction not needed
PHOT DOME FLAT	Short Time Trend at Domeflat_Loiano Long Time Trend at Domeflat_Loiano	Short Time Trend at Domeflat_CAHA Long Time Trend at Domeflat_CAHA	NO DOME FLAT	Short Time Trend at Domeflat_NTT Long Time Trend at Domeflat_NTT	NO DOME FLAT	NO DOME FLAT
PHOT SKY FLAT	Short Time Trend at Skyflat_Loiano Long Time Trend at Skyflat_Loiano	Short Time Trend at Skyflat_CAHA Long Time Trend at Skyflat_CAHA	Short Time Trend at Skyflat_TNG Long Time Trend at Skyflat_TNG	Short Time Trend at Skyflat_NTT Long Time Trend at Skyflat_NTT	Short Time Trend at Skyflat_SPM Long Time Trend at Skyflat_SPM	correction not performed
SPEC LAMP FLAT	NO SPECTRA	Short Time Trend at SpecLampflat_CAHA	Short Time Trend at SpecLampflat_TNG	Short Time Trend at SpecLampflat_NTT	NO SPECTRA	NO SPECTRA
SPEC SKY FLAT	NO SPECTRA	Short Time Trend at Illumflat_CAHA	Short Time Trend at Illumflat_TNG	Short Time Trend at Illumflat_NTT	NO SPECTRA	NO SPECTRA

FIGURE 11: Portion of the Calibration Frames IFP summary table.

The typical stability time scale for each kind of calibration frame is reported in Table 1. A calibration plan for each instrument used during our Campaigns, as derived from IFP tests, is reported in Table 2.

[8]The specific section on calibration frames study results is available at: `http://yoda.bo.astro.it/wiki/index.php/IFP_Calibration_Frames_Summary`.

TABLE 1: Typical Calibration Frames stability time scale

Instrument Telescope	Bias	Photometric Dome Flat	Photometric Sky Flat	Spectroscopic Flat	Dark
BFOSC Cassini 1.5m	1 run ($\simeq$ 4 days)	$\sim$ 300 days	OLD CCD: 1 run ($\simeq$ 4 days) NEW CCD: $\sim$ 100 days	-	-
CAFOS CAHA 2.2m	1 run ($\simeq$ 7 days)	$\simeq$ 1 day until run M-006 $\simeq$ 1 run from run M-006	1 day	1 day	-
DoLoRes TNG 3.58m	1 day	-	$\simeq$ 250 days	1 run ($\simeq$ 5 days)	-
EFOSC2 NTT 3.58m	1 run ($\simeq$ 5 days) for photometry 1 day for spectroscopy	$\sim$ 250 days	$\simeq$ 250 days	1 day	-
LaRuca SPM 1.5m	from 1 to $\simeq$ 7 days depending on CCD used	-	4-5 days for each CCD	-	-
ROSS REM 0.6m	-	-	-	-	$\sim$1 month

TABLE 2: Calibration Plan

Instrument Telescope	CCD	Bias	Photometric Dome Flat	Photometric Sky Flat	Spectroscopic Flat	Spectroscopic Illumination Flat	Wavelenght calib. Lamp	Dark
BFOSC Cassini 1.5m	EEV 1300 × 1340B (old) EEV 1300 × 1340B (new)	daily daily	daily daily	daily daily	-	-	-	once for year once for year
CAFOS CAHA 2.2m	CCD#40 LORAL/LESSER	daily	daily	daily	daily	once per run	for each star	once for year
DoLoRes TNG 3.58m	E2V4240(new)	daily	-	daily	daily	once per run	Ar+Ne+Hg+Kr for each star He, Ar+Ne+Hg+Kr in day time	once for year
EFOSC2 NTT 3.58m	SITE#1d_15	daily	daily	daily	daily + for each star in the red grism	once per run	for each star	once for year
LaRuca SPM 1.5m	SITE#1 Photometrics Marconi e2vm E2V-4240	daily daily	- -	daily daily	- -	- -	- -	once for year once for year
ROSS REM 0.6m	Marconi 47-10	-	-	-	-	-	-	daily (*)

(*) : daily darks are acquired by REM team and used to produce monthly Masterdark frames.

References

[SMR-003], Marinoni, S., et al., 2010, *Data Reduction Protocol for Ground Based Observations of SpectroPhotometric Standard Stars. III. Quality Control on SPSS Photometric Frames and Photometric Catalogues Production*,
GAIA-C5-TN-OABO-SMR-003,
DRAFT

[SMR-004], Marinoni, S., et al., 2010, *Short Variability Monitoring: Light Curves production and analysis*,
GAIA-C5-TN-OABO-SMR-004,
DRAFT

[GA-001], Altavilla, G., Bellazzini, M., Pancino, E., et al., 2007, *The Primary standards for the establishment of the GAIA Grid of SPSS. Selection criteria and a list of candidates.*,
GAIA-C5-TN-OABO-GA-001,
URL http://www.rssd.esa.int/llink/livelink/open/2736914

[GA-003], Altavilla, G., Bragaglia, A., Pancino, E., et al., 2010, *Secondary standards for the establishment of the Gaia Grid of SPSS. Selection criteria and a list of candidates.*,
GAIA-C5-TN-OABO-GA-003,
URL http://www.rssd.esa.int/llink/livelink/open/3033479

[GA-002], Altavilla, G., Federici, L., e Pancino, E., et al., 2010, *Absolute calibration of Gaia spectro-photometric data. III. Observing facilities for ground-based support*,
GAIA-C5-TN-OABO-GA-002,
URL http://www.rssd.esa.int/llink/livelink/open/3012989

[GA-004], Altavilla, G., Pancino, E., Marinoni, S., et al., 2011, *Instrument Familiarization Plan for ground based observations of SPSS. I. CCD Shutter Characterization and Linearity Evaluation*,
GAIA-C5-TN-OABO-GA-004,
URL http://www.rssd.esa.int/llink/livelink/open/3075673

[GA-005], Altavilla, G., et al., 2013, *Instrument Familiarization Plan for ground based observations of SPSS. III. Second Order Contamination and Polarization Effects*,
GAIA-C5-TN-OABO-GA-005,
DRAFT

[GA-006], Altavilla, G., et al., 2013, *Data Reduction Protocol for Ground Based Observations of SpectroPhotometric Standard Stars. IV. Spectroscopy reductions up to relative flux calibration*,
GAIA-C5-TN-OABO-GA-006,
DRAFT

[MBZ-001], Bellazzini, M., Bragaglia, A., Federici, L., et al., 2006, *Absolute calibration of Gaia photometric data. I. General considerations and requirements.*,
GAIA-C5-TN-OABO-MBZ-001,
URL http://www.rssd.esa.int/llink/livelink/open/1145146

[GCC-001], Cocozza, G., Altavilla, G., Carrasco, J.M., et al., 2012, *Data Reduction Protocol for Ground Based Observation of Spectrophotometric Standard Stars. II. Spectroscopy Pre-reduction up to extraction and wavelength calibration*,
GAIA-C5-TN-OABO-GCC-001,
URL http://www.rssd.esa.int/llink/livelink/open/3143422

[LF-001], Federici, L., Bragaglia, A., Diolaiti, E., et al., 2006, *Absolute calibration of Gaia photometric data. II. Observing facilities for ground-based support (pilot program)*,
GAIA-C5-TN-OABO-LF-001,
URL http://www.rssd.esa.int/llink/livelink/open/2706141

[SMR-001], Marinoni, S., Pancino, E., Altavilla, G., et al., 2012, *Data Reduction Protocol for Ground Based Observations of SpectroPhotometric Standard Stars. I. Imaging Pre-reduction*,
GAIA-C5-TN-OABO-SMR-001,
URL http://www.rssd.esa.int/llink/livelink/open/3117618

[EP-001], Pancino, E., Altavilla, G., Bellazzini, M., et al., 2008, *Protocol for Ground Based Observations of SpectroPhotometric Standard Stars. I. Instrument Familiarization Tests*,
GAIA-C5-TN-OABO-EP-001,
URL http://www.rssd.esa.int/llink/livelink/open/2858529

[EP-003], Pancino, E., Altavilla, G., Carrasco, J.M., et al., 2009, *Protocol for Ground Based Observations of SpectroPhotometric Standard Stars. II. Variability Searches and Absolute Photometry Campaigns Photometry Campaigns*,
GAIA-C5-TN-OABO-EP-003,
URL http://www.rssd.esa.int/llink/livelink/open/2908205

[EP-006], Pancino, E., Altavilla, G., Carrasco, J., et al., 2011, *Protocol for Ground Based Observations of SpectroPhotometric Standard Stars. III. Main Spectrophotometric Campaign*,
GAIA-C5-TN-OABO-EP-006,
URL http://www.rssd.esa.int/llink/livelink/open/3072732

Pancino, E., Altavilla, G., Marinoni, S., et al., 2012, MNRAS, 426, 1767, ADS Link

A BFOSC@Cassini Calibration Frames IFP results

A.1 Masterbias

We monitored the bias level and the two-dimensional stability trend during the first seven runs (P-001, P-002, P-005, V-002, V-005, V-008 and V-011) performed in Loiano using BFOSC at Cassini Telescope. Between runs V-005 and V-008, a new CCD was mounted[9]: the improvement in data quality is clearly visible in the two-dimensional stability trend plot (see Fig. 12). Anyway, for both CCDs, the masterbias frames appear to be sufficiently stable (within 1-2%) in their 2D shape, although the absolute global level may vary from night to night. For this reason, we recommend not to use masterbias frames produced during one run to pre-reduce data acquired during other runs. A correction for the overscan level would be beneficial, but unfortunately no overscan strip is present in BFOSC data.

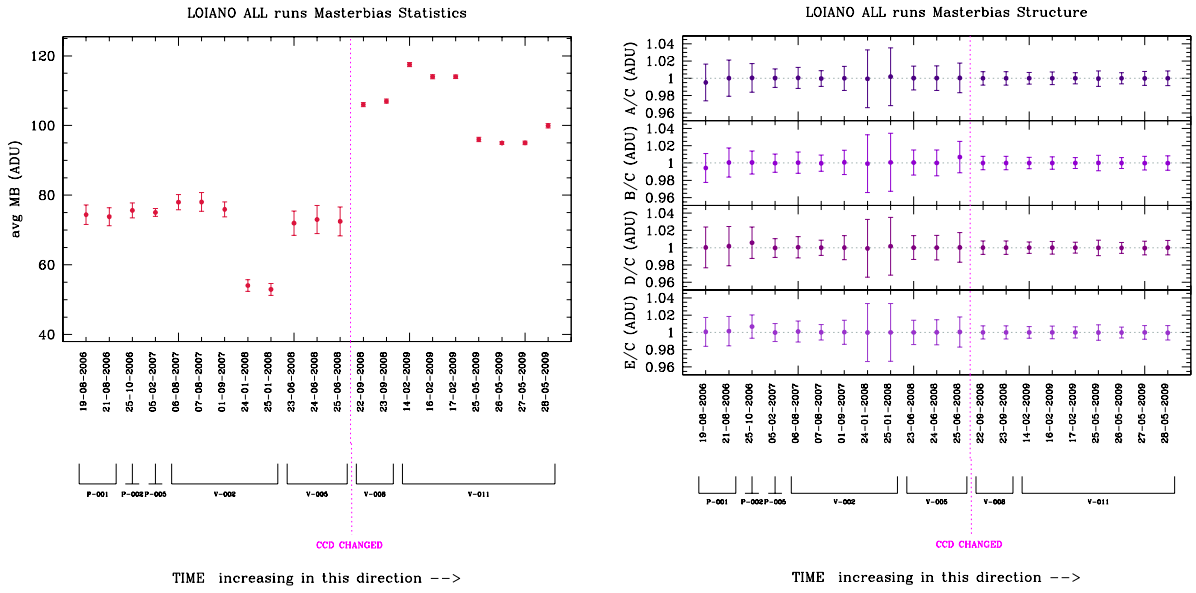

FIGURE 12: Long-time trend monitoring of the bias level (*left panel*) and two-dimensional structure (*right panel*) produced using the data acquired in the first seven runs with BFOSC@Cassini.

[9]The new CCD is an EEV 1300x1400 B, as well as the old one.

A.2 Photometric Masterflat

An example of the two tests of interest here, performed in order to study the short-term stability of photometric flats produced during runs V-002 to V-011, is shown both for dome and sky masterflats using the B filter (see Fig. 13). As usual, the short-term monitoring plots for all runs are available in WikiBo. In each run, the global shape of dome masterflat frames appears to be very stable, with global variation of $\sim$1% in the worst case. In the calibration plan we still recommend to acquire flat frames every night for safety reasons. However, if flats for a specific night are lacking for some reason, those of adjacent nights can be safely used in data pre-reduction.
In Fig. 14 we show, as an example, the long-time trend study on the large scale variation performed on dome masterflat frames in filter B, produced during runs V-002, V-005, V-008 and V-011[10]. The long-time trend of the *9 areas* plot for the B dome masterflats produced during the same runs is shown, as an example, in Fig. 15. The same plots are shown for sky B masterflats in Fig. 16 and Fig. 17 respectively.

The stability of dome masterflats is quite good for both CCDs: the variation in shape showed by dome masterflats acquired with the new CCD is lower than 1% over a period greater than 300 days. For sky masterflats produced using the old CCD (at least in the B and V filter) the stability can be considered very good only for each single part of run V-002: comparing the first part with the last part of this run, the shape changes of about 2% in the worst case. The situation still remains very good for the sky masterflats produced using the new CCD: their variation in shape is lower than 1% over a period greater than 100 days.
Similar studies (and similar results), both for short and long-time trends, performed for filter V and R dome and sky masterflats can be found in Wiki-Bo.

A.3 Masterdark

In Fig. 18 the check on the linear growth of masterdark frames with the exposure time is shown using data acquired during run V-011. With increasing exposure time, the BFOSC dark frames are very stable, and no dark correction is needed for scientific data. We suggest to repeat the test once every year in order to monitor the dark current behaviour.

[10]Owing to the CCD change between run V-005 and V-008, two reference frames have been chosen: the dome masterflat produced using frames acquired in the last night of run V-005 is the reference frame for all dome masterflats produced using the old CCD data, while those acquired in the first night of run V-008 are used to produce the reference frame for the new CCD.

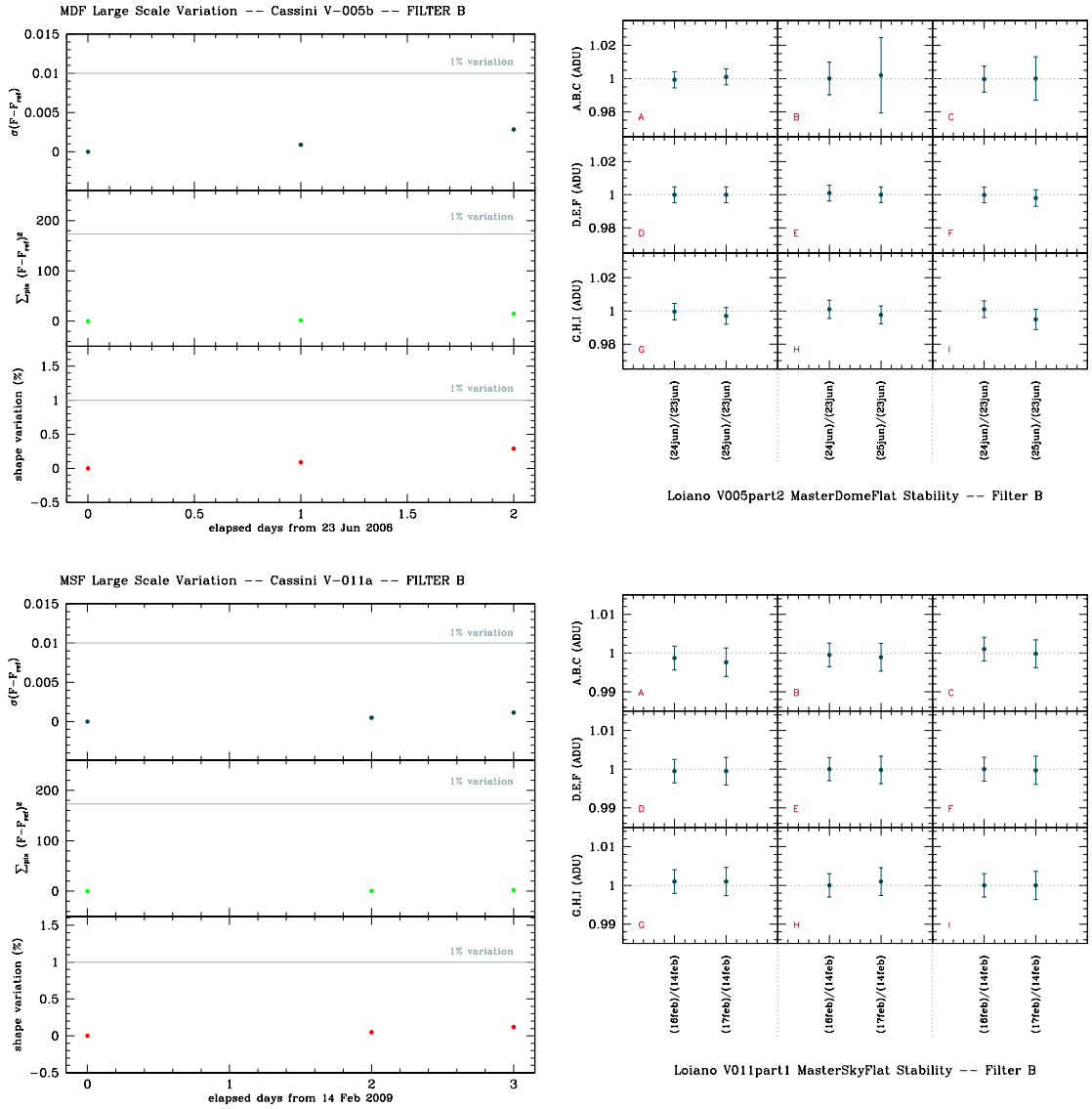

FIGURE 13: Short-time stability monitoring (see SMR-001) for dome and sky masterflat frames produced during runs V-005b and V-011a respectively using the B filter. As usual, the short-term monitoring plots for all runs are available in WikiBo.

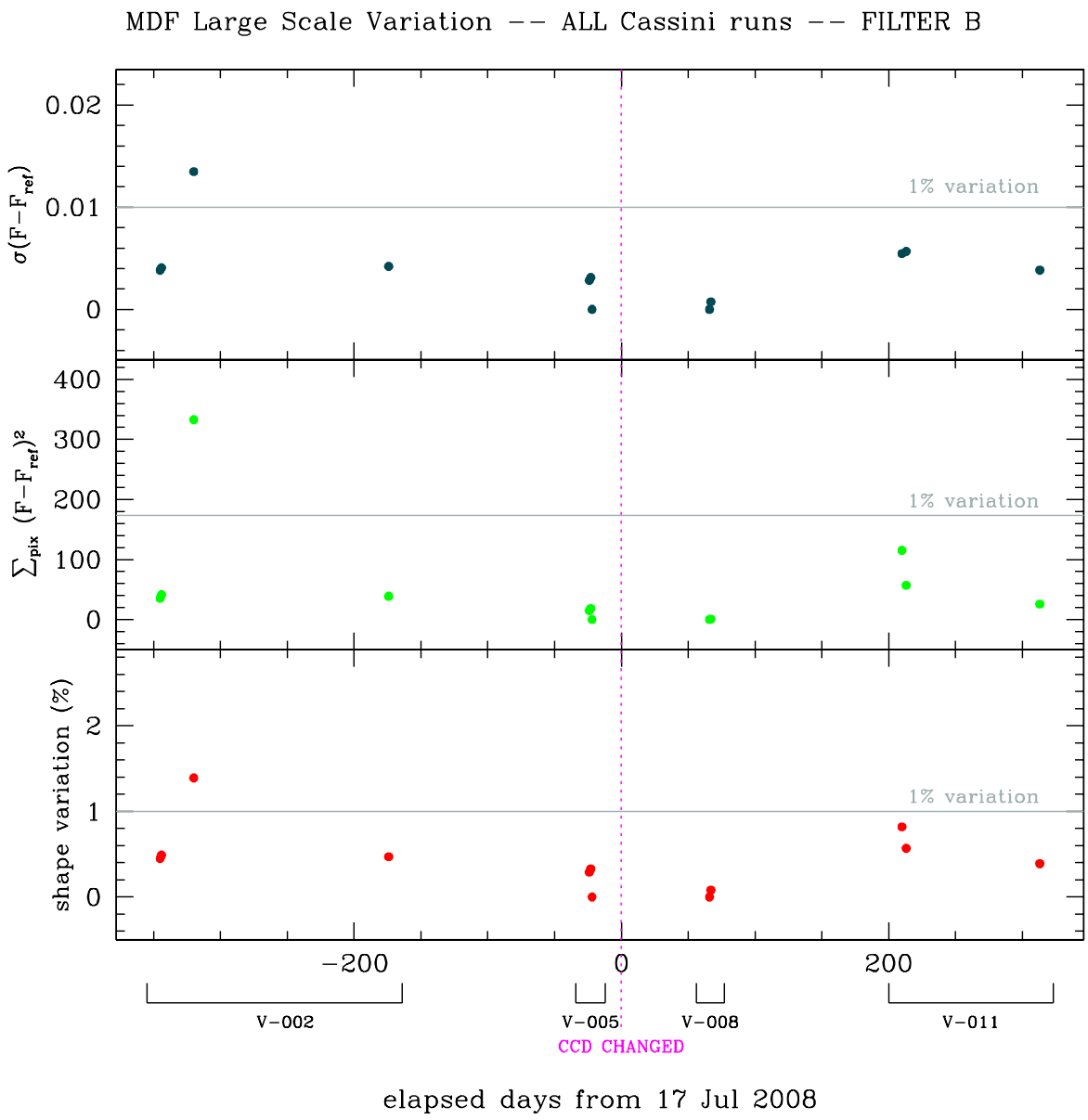

FIGURE 14: Long-time large scale variability test performed on all dome masterflats produced with the B filter during the first four V-runs in Loiano. Owing to the CCD change between run V-005 and V-008, two reference frames have been chosen: the dome masterflat produced using frames acquired in the last night of run V-005 is the reference frame for all dome masterflats acquired using the old CCD, while those acquired in the first night of run V-008 is the reference frame for the new CCD. The stability of dome masterflats is very good for both CCDs (almost always within 1%).

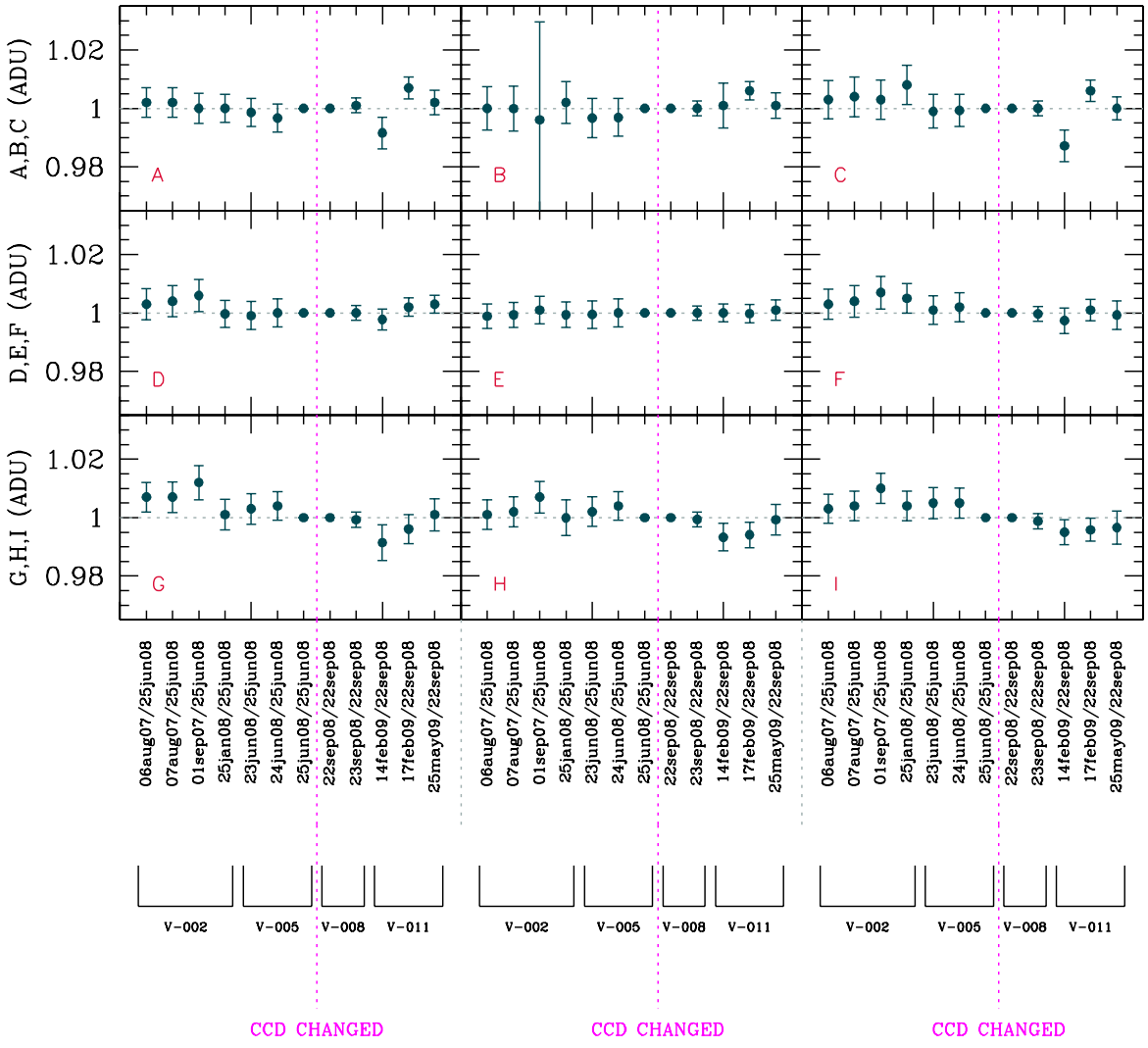

FIGURE 15: Long-time 9 areas test performed on all dome masterflats produced with the B filter during the first four V-runs in Loiano. The reference frames for each CCD used are the same of Fig. 14. The panel B of this plot shows the "bad" region of the dome masterflat produced using data acquired on 01-09-2008: this is due to a very big grain of dust on the CCD window.

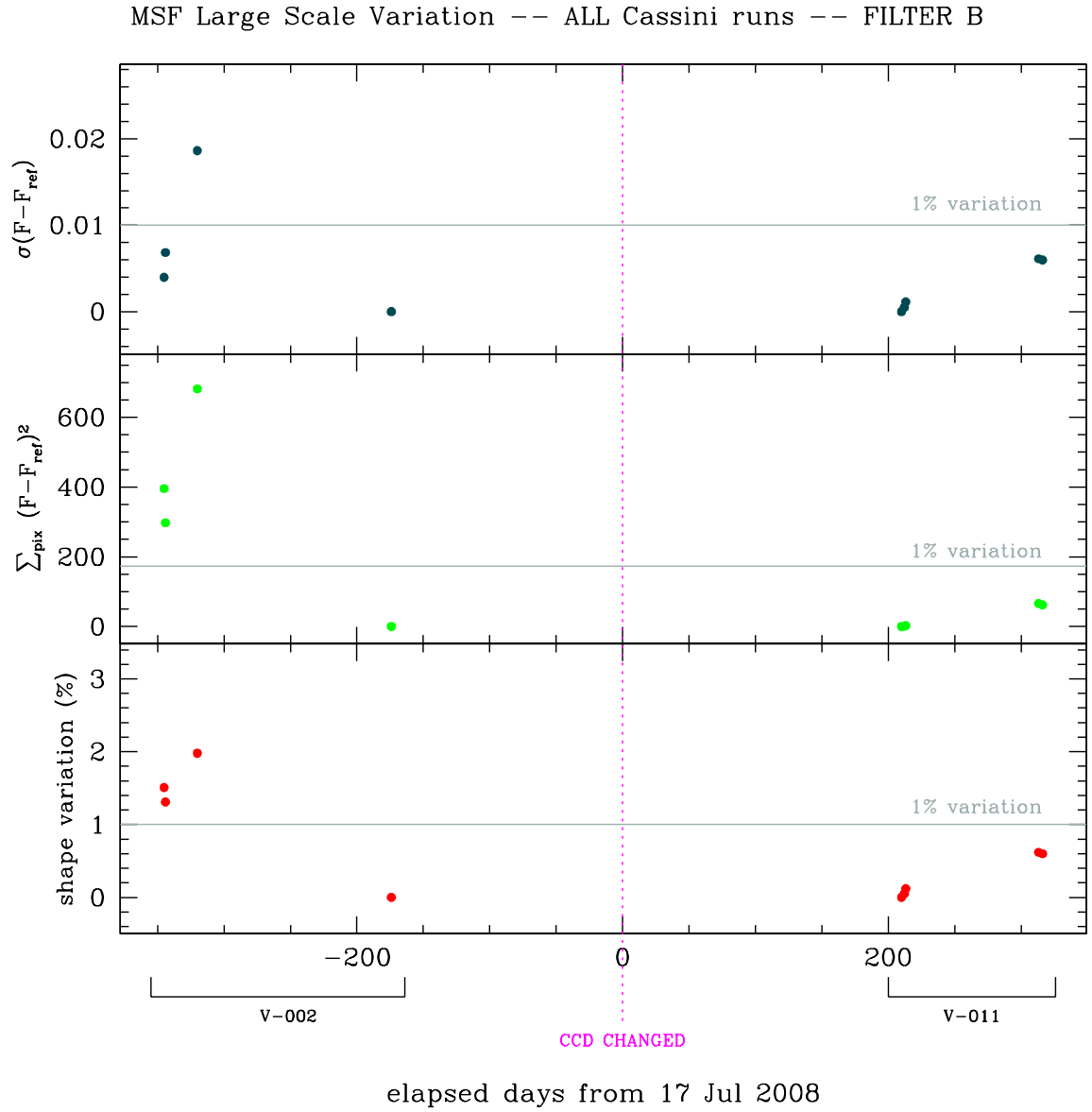

FIGURE 16: Long-time large scale variability test performed on all sky masterflats produced with the B filter during the first four V-runs in Loiano. Owing to the CCD change between run V-005 and V-008, two reference frames have been chosen: the sky masterflat produced using frames acquired in the last night of run V-002 is the reference frame for all sky masterflats acquired using the old CCD, while those acquired in the first night of run V-011 is the reference frame for the new CCD. No skyflats was acquired during runs V-005 and V-008. The stability of sky masterflats is very good for the new CCD while, for the old one,we can consider them stable only during each of the two halves of run V-002.

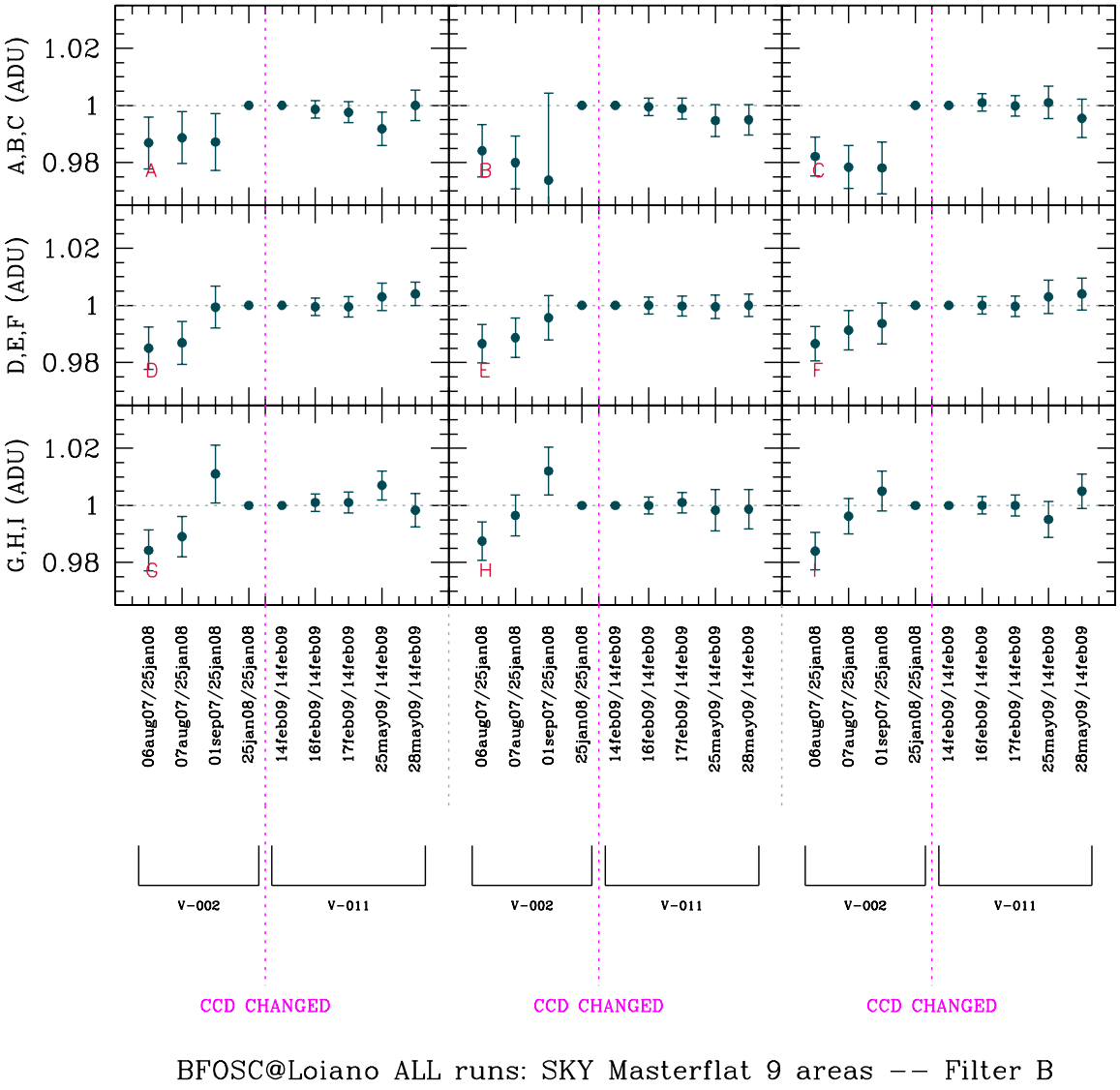

FIGURE 17: Long-time 9 areas test performed on all sky masterflats produced with the B filter during the first four V-runs in Loiano. The reference frames for each CCD used are the same of Fig. 16. Obviously, the big grain of dust is present also on the sky masterflat produced on 01-09-2008, as shown in the panel B of this plot.

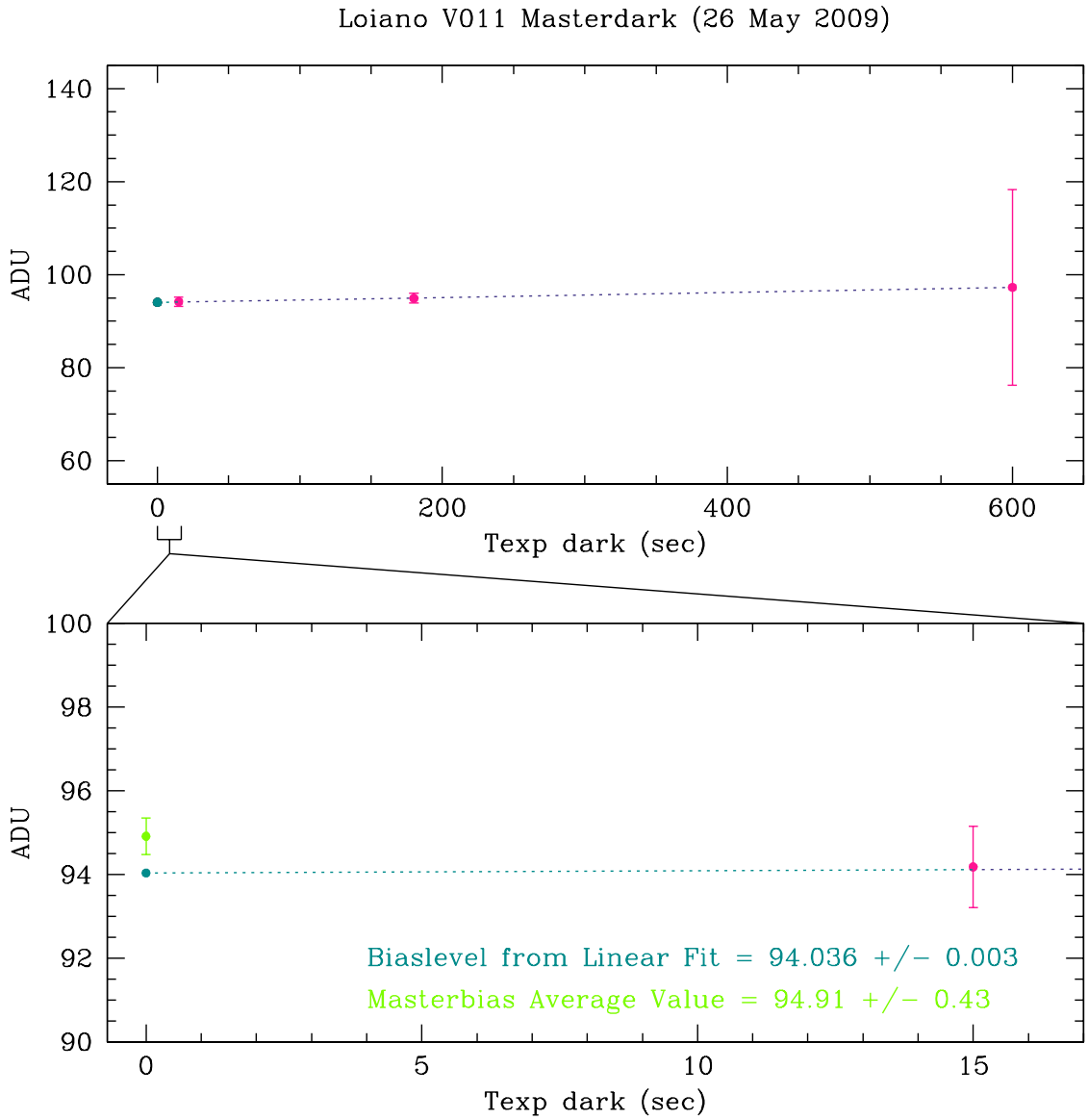

FIGURE 18: Quality Control on masterdark frames of run V-011@Loiano. The mean value of each masterdark is plotted against the exposure time. In the bottom panel a zoom is shown in order to compare the bias level extrapolated from the linear fit with that measured directly from the masterbias frame. No masterdark correction is needed for Loiano data.

B CAFOS@CAHA2.2m Calibration Frames IFP results

B.1 Masterbias

We checked the bias level (Fig. 19) and the two-dimensional stability trend (Fig. 20) during the first four runs (P-003, M-001, M-003 and M-006) performed with CAFOS in Calar Alto, both for the photometry and spectroscopy CCD trimming sections. The two-dimensional stability of masterbias frames is quite good (within $\sim 1\%$), while the long-term study (about 1.5 yr) of bias level shows an increasing trend. We recommend not to use masterbias produced during one run to pre-reduce data acquired during other runs.

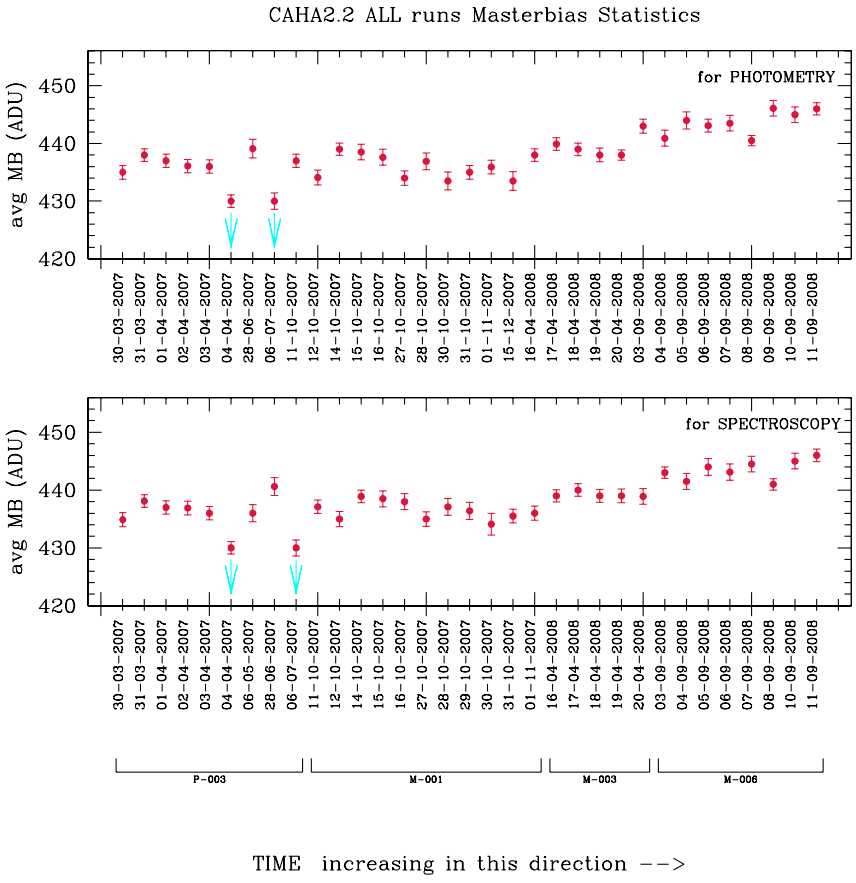

FIGURE 19: Long-time trend monitoring of the bias level produced using data acquired with CAFOS@CAHA in the four labelled runs. The masterbias frames produced on 04-04-2007 and 06-07-2007 (run P-003) show a median value lower with respect to the others ($\sim$110 ADU). For this reason in the plot they are labelled with cyan downward arrows.

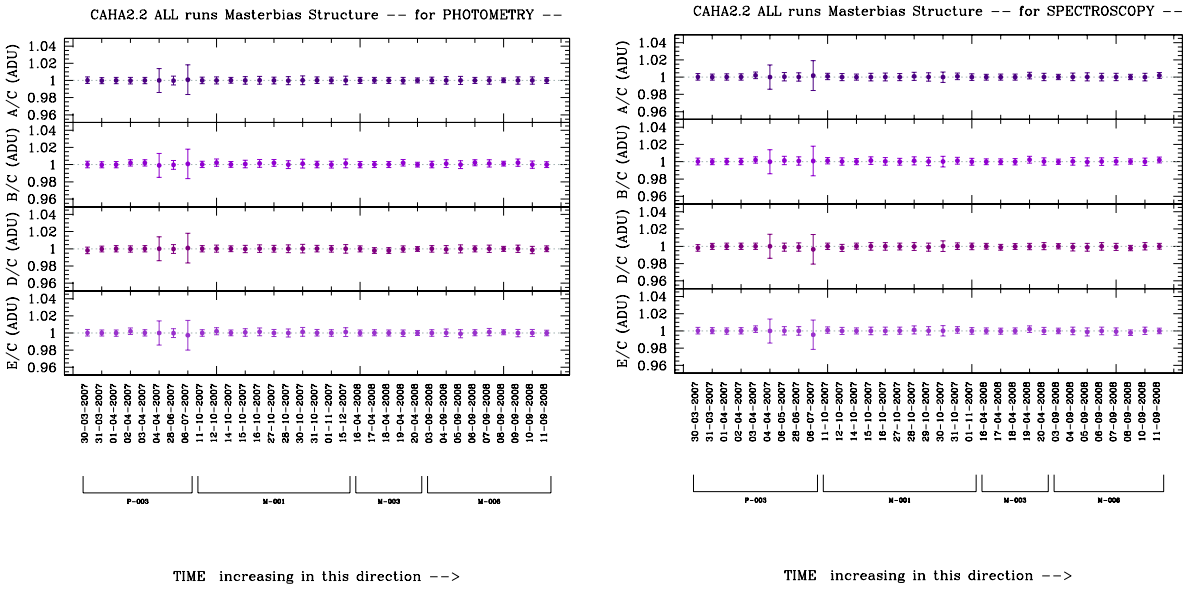

FIGURE 20: Two-dimensional structure long-time trends of masterbias frames produced using data acquired with CAFOS@CAHA in the four monitored runs. Two masterbias frames present large error-bars: they are the same frames which have low counts level in Fig. 19

B.2 Photometric Masterflat

The tests to study the short-term stability of photometric flats were performed for both dome and sky masterflats using data produced during runs P-003, M-001, M-003 and M-006: all these plots are available, at usual, in WikiBo. Here, we show as an example the monitoring plots for dome and sky masterflats produced during two runs (M-001b and M-006) using the B filter (see Fig. 21 and 22 respectively). In all filters, both dome and sky masterflats produced during the first three runs (P-003, M-001 and M-003, see all monitoring plots in WikiBo) are totally unstable, showing differences in shape as high as $\sim$4.5% in consecutive nights (as shown, for example, in the upper panels of both Fig. 21 and 22 for run M-001), and the masterflats behaviour varies significantly from run to run. Only from run M-006 both dome and sky masterflats seem to be stable, as shown in the bottom panels of Fig. 21 and 22 (and in WikiBo for all other filters). For this reason we recommend to acquire photometric flat frames *strictly* every night, and not to use masterflat frames produced for one night to pre-reduce images acquired in other nights, at least until run M-006 (see below).

In Fig. 23 we show, as an example, the long-term trend study on the large scale variation performed on filter B dome masterflat frames produced during runs M-001, M-003 and M-006[11].

[11]The dome masterflats produced during both run P-003 and the last night of run M-001 are not present in the plot because they were acquired with a different window (see SMR-001)

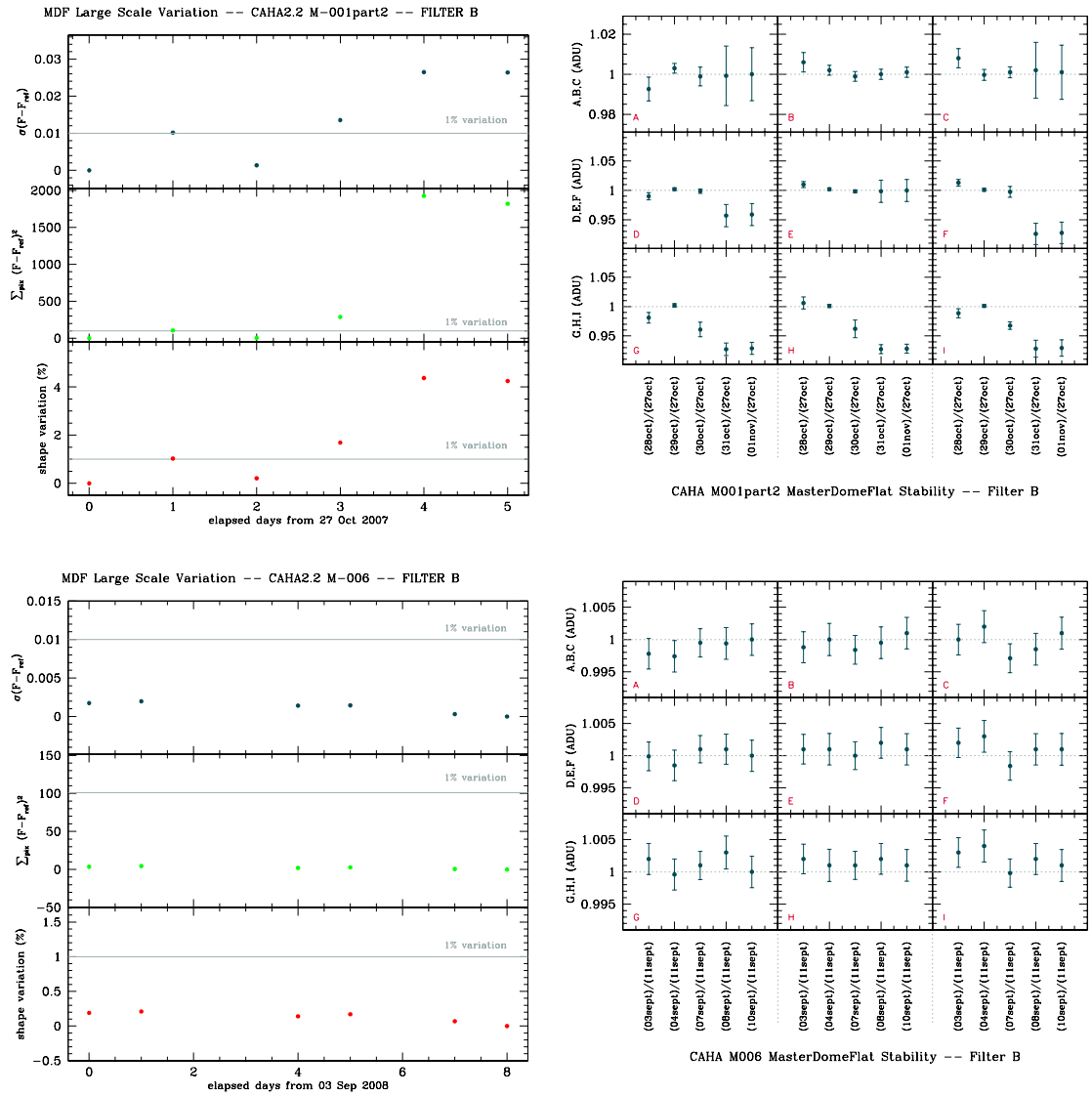

FIGURE 21: Short-time stability monitoring (see SMR-001) for dome masterflat frames (filter B) produced during runs M-001b (*upper panel*) and M-006 (*bottom panels*). The dome masterflats produced during run M-001 are strongly unstable, showing differences in shape as high as ≃4.5%. This behaviour is similar also for runs P-003 and M-003 (see WikiBo), while dome masterflats produced during run M-006 are stable, with differences in shape smaller than 0.3%. This is probably due to a refurbishment of the instrument between run M-003 and run M-006. As usual, the short-term monitoring plots for all runs and all filters are available in WikiBo.

The dome masterflat produced using frames acquired in the last night of run M-006 (11-09-2008) is the reference frame used to perform the test. The inter-run variation is clearly visible, as well as the night-by-night shape variation in runs M-001 and M-003. This is even more evident in Fig. 24: the difference in shape of the various regions of M-001 and M-003 masterflats

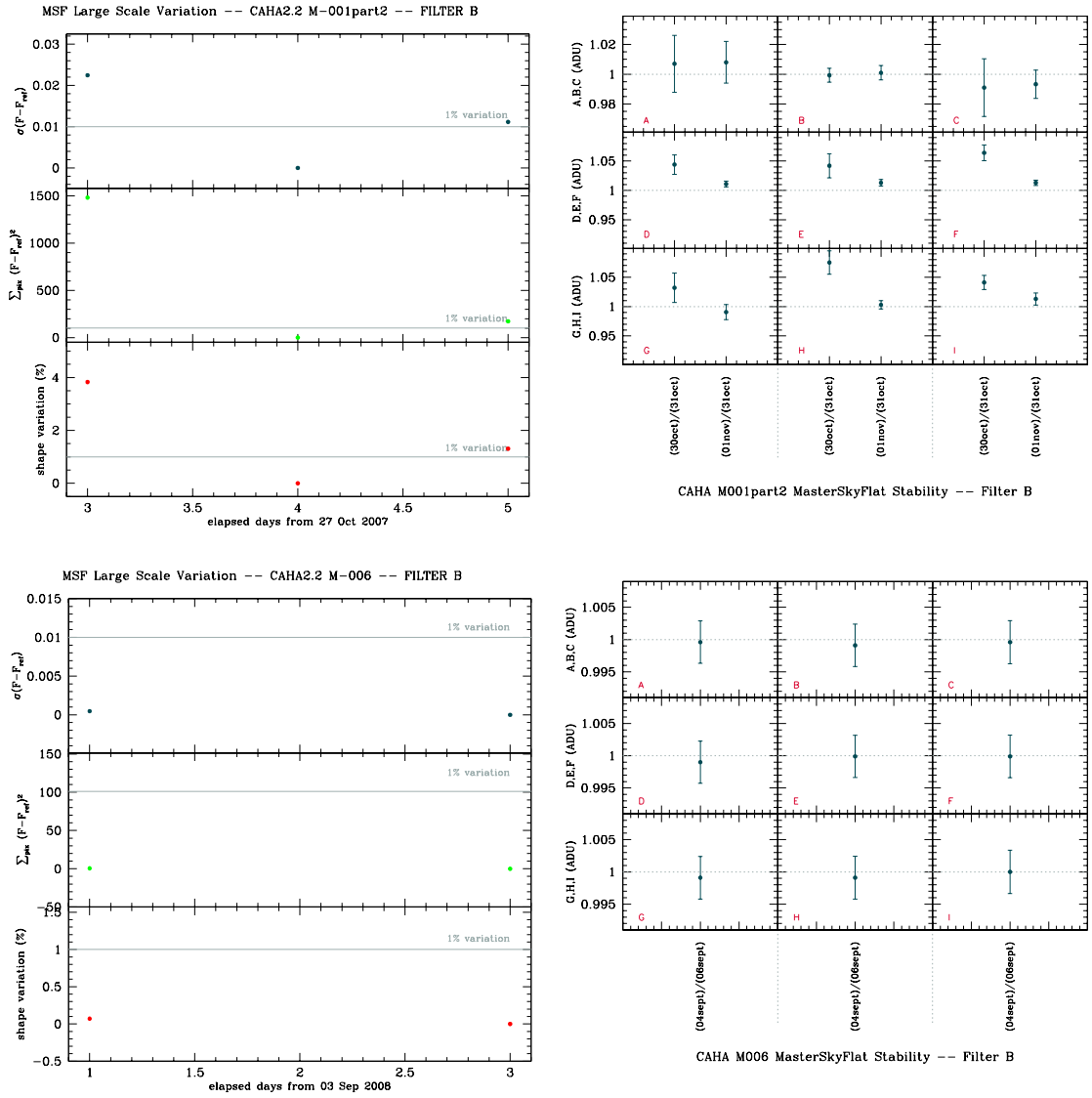

FIGURE 22: Short-time stability monitoring (see SMR-001) for sky masterflat frames (filter B) produced during runs M-001b (*upper panel*) and M-006 (*bottom panel*). Also for sky masterflats, the improvement in data quality from run M-001 and M-006 is evident: M-006 sky masterflats show a difference in shape smaller than 0.1%.

is due to the strange variable structure present in each masterflat produced during these runs, as shown in Fig. 25. On the contrary, M-006 is a very stable run.

Fig. 26 and 27 show the same tests performed on filter B sky masterflats produced during the same runs. The variable structure is present also in sky masterflats (see Fig. 28) indicating that, probably, it is not due to a non uniform illumination of the screen used for the production of domeflats. In any case, the problem affecting the first two M-runs in Calar Alto seems to be

resolved before the beginning of run M-006: apparently, a refurbishment of the instrument was performed between run M-003 and run M-006. From this latter run, if flats for a determined night are lacking for some reason, those of adjacent nights can be safely used in data pre-reduction. But we want to stress that for the first three runs in CAHA (P-003, M-001, and M-003) the masterflat frames produced for one night must not be used to pre-reduce images acquired in other nights.

B.3 Spectroscopic Masterflat

In Fig. 29 we report the monitoring for the spectroscopic masterflats frames produced during run M-003. The blue (grism B200) spectroscopic masterflats are quite stable, both for the narrow and the wide slits adopted[12] (left and right upper panels in the figure). In the bluer part of the blue grism (showed in the three upper boxes of each plot) the difference in shape between masterflats produced in different nights is $\simeq$2% in the worst case, due to the low S/N reached in this region. The red spectroscopic masterflats (grism R200, left and right bottom panels) are strongly affected by both fringing and internal reflections. The only region stable at the 1% level is the central one (see central boxes of each plot).

For these reasons we recommend to acquire spectroscopic flat frames every night, and not to use masterflats produced in one night to pre-reduce spectra acquired in other nights.

B.4 Masterdark

In Fig. 30 the check on the linear growth of masterdark frames with the exposure time is shown using data acquired during run M-003. With increasing exposure time, the CAFOS dark frames stay very stable; therefore, no dark correction is needed for scientific data. We suggest to repeat the test once every year in order to monitor the dark current behaviour.

[12] Usually, for this instrument, the adopted narrow slit is 2” and the wide slit is 11.7”.

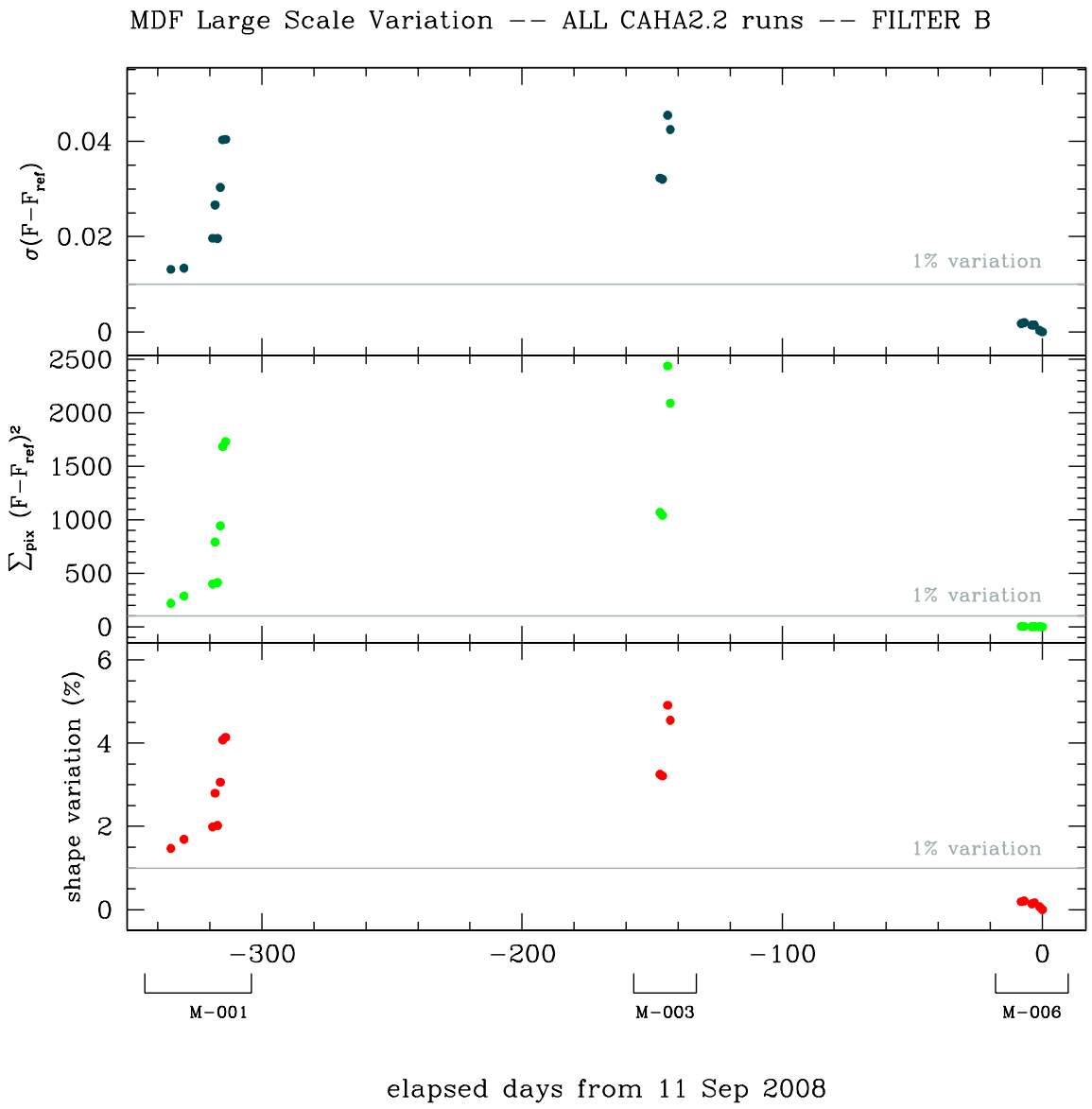

FIGURE 23: Long-time large scale stability test performed on all dome masterflats produced with the B filter during the first three CAHA runs of the Main Campaign. The dome masterflat produced using frames acquired in the last night of run M-006 (11-09-2008) is the reference frame. The inter-run variation of the dome masterflat frames is clearly visible, as well as the significant night-by-night shape variations in runs M-001 and M-003.

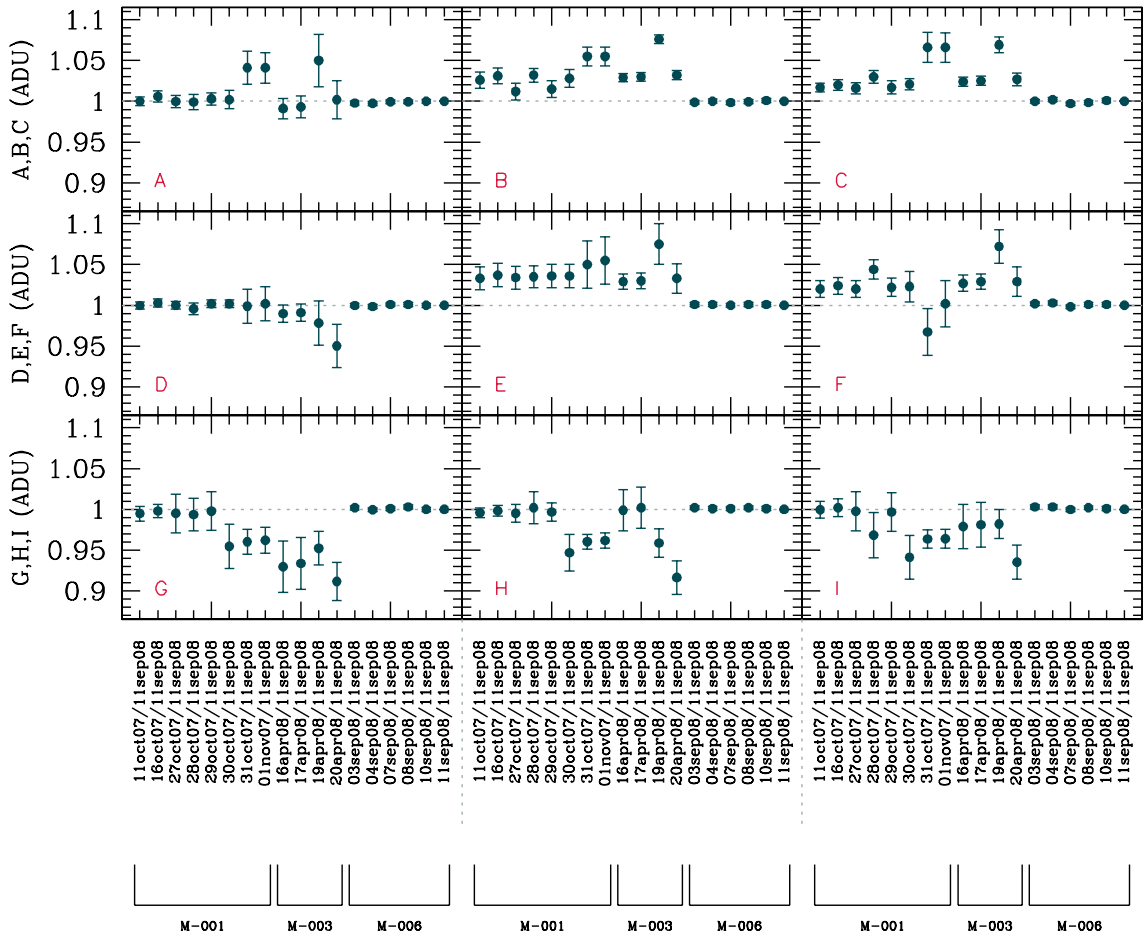

FIGURE 24: Long-time 9 areas test performed on all dome masterflats produced with the B filter during the first three M-runs in Calar Alto. The reference frame is the same of Fig. 23. The shape of dome masterflats produced during both runs M-001 and M-003 is quite different, and only run M-006 shows a good stability in its dome masterflats.

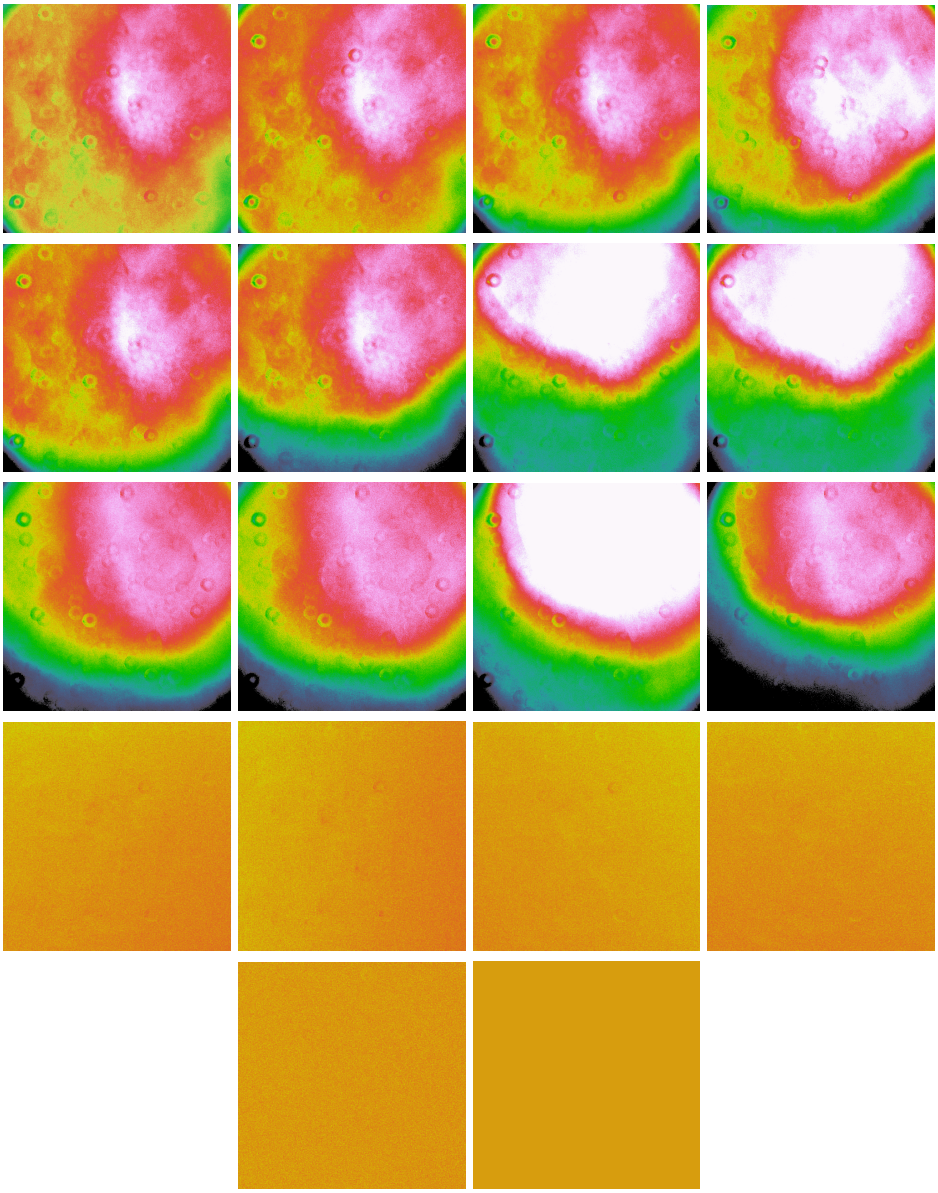

FIGURE 25: Ratio between each dome masterflat produced during the first three M-runs in Calar Alto and the reference one (the dome masterflat produced in the last night of run M-006) with the B filter. The display cuts are the same for all the images. The M-001 (the first 8 images) and M-003 (from image 9 to image 12) dome masterflats show a strange and variable structure, while those of run M-006 are very stable, as shown also in Fig. 24.

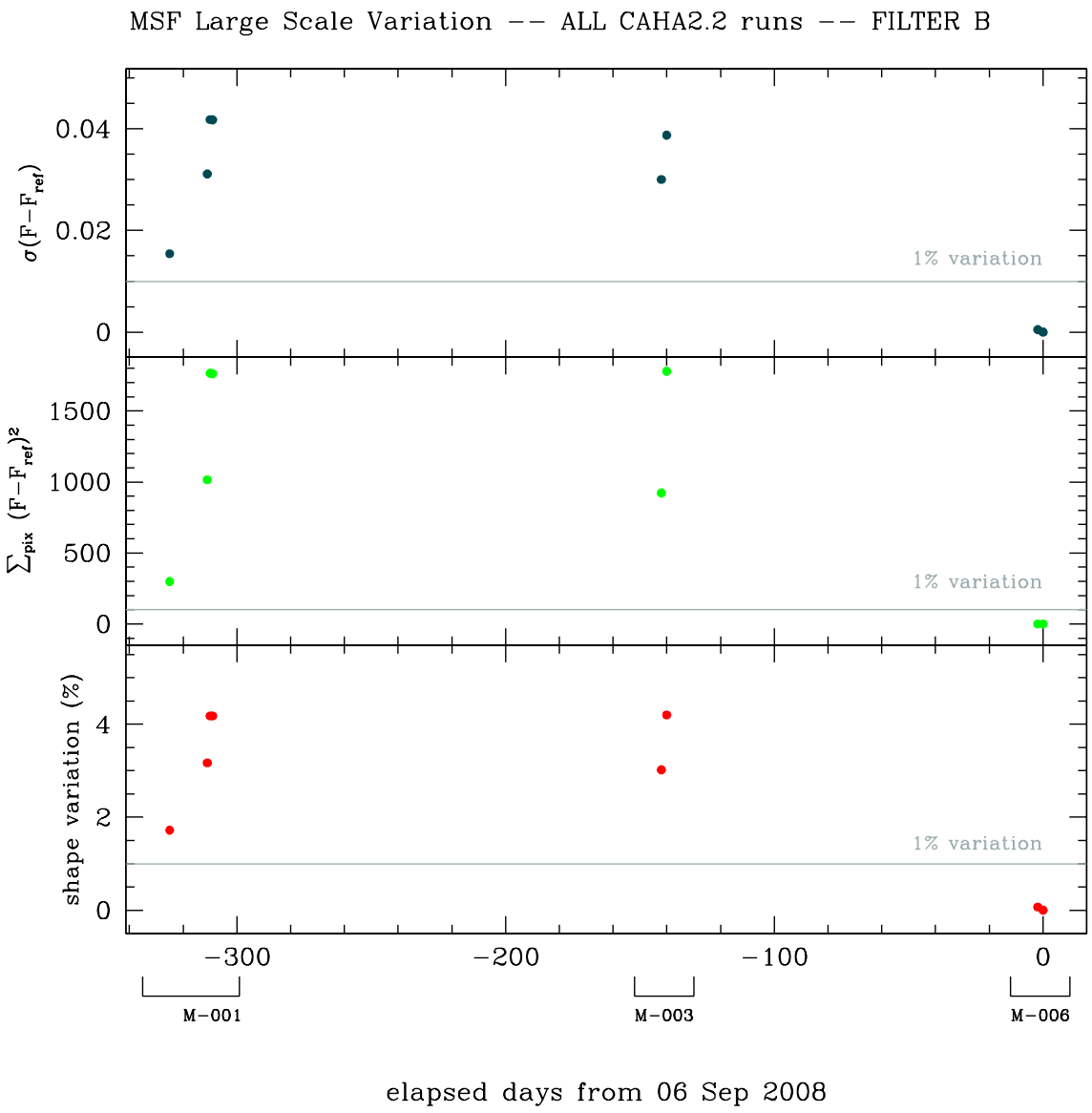

FIGURE 26: Long-time large scale stability test performed on all sky masterflats produced with the B filter during the first three CAHA runs of the Main Campaign. The last sky masterflat produced using frames acquired in run M-006 (06-09-2008) is the reference frame. The inter-run variation of the sky masterflat frames is clearly visible, as well as the significant night-by-night shape variations in runs M-001 and M-003.

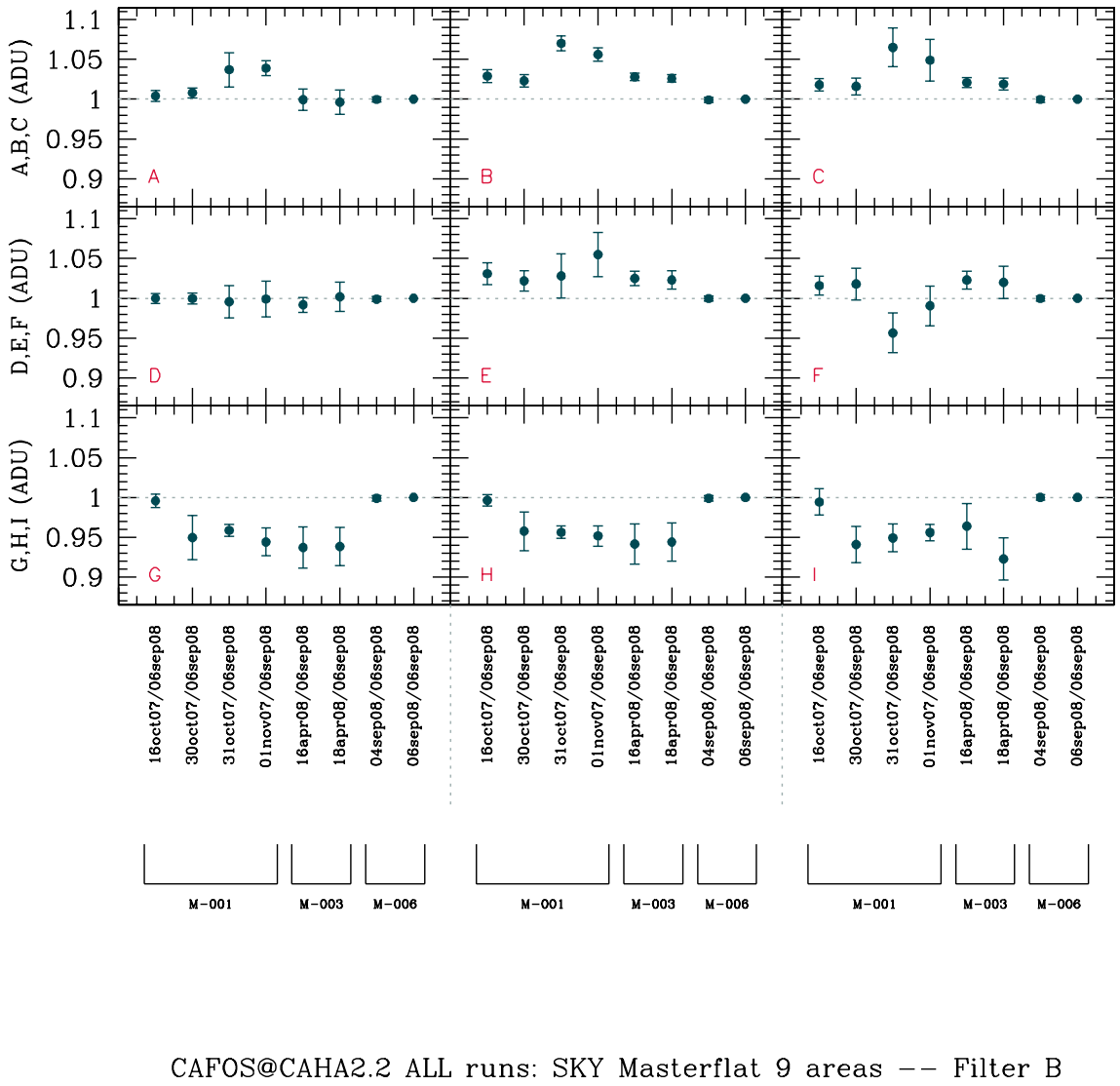

FIGURE 27: Long-time 9 areas test performed on all sky masterflat produced with the B filter during the first three M-runs in Calar Alto. The reference frame is the same of Fig. 26. The shape of sky masterflats produced during both runs M-001 and M-003 is quite different, and only run M-006 shows a good stability in its sky masterflats (as shown also in Fig. 26).

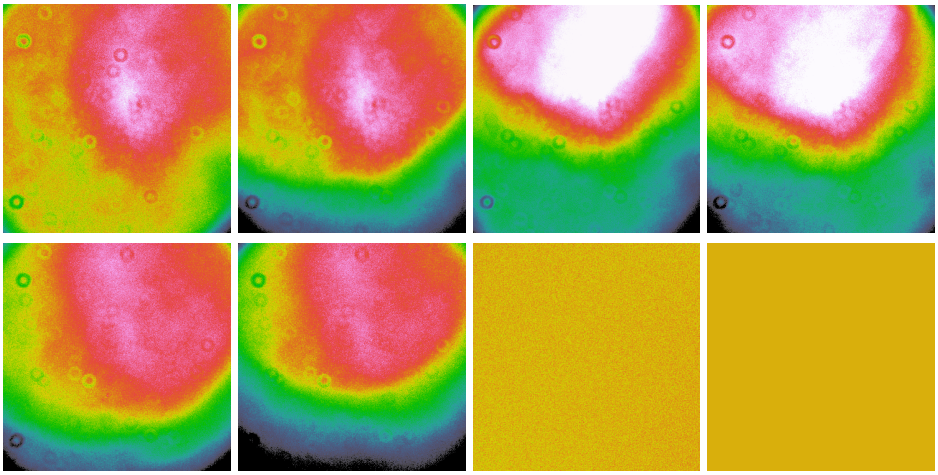

FIGURE 28: Ratio between each sky masterflat produced with the B filter during the first three M-runs in Calar Alto and the reference one (see Fig. 26). The display cuts are the same for all images. Also for sky masterflats, the M-001 ones (from image 1 to 4) and the M-003 ones (the next two images) show a strange and variable structure not present at all in M-006 sky masterflats.

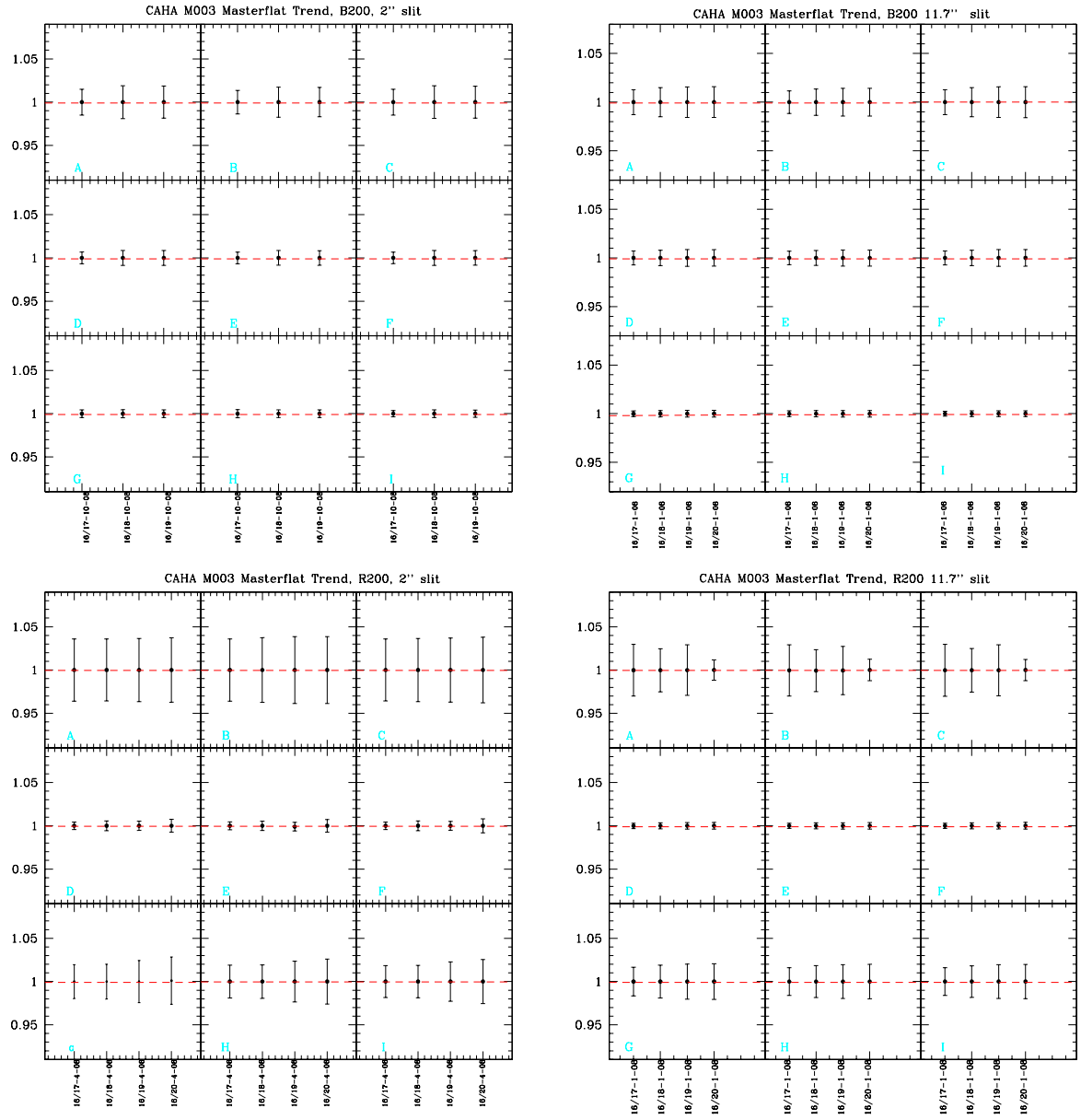

FIGURE 29: Stability test for spectroscopic masterflat frames produced during run M-003 for the blue grism B200 (top plots) and red grism R200 (bottom plots).

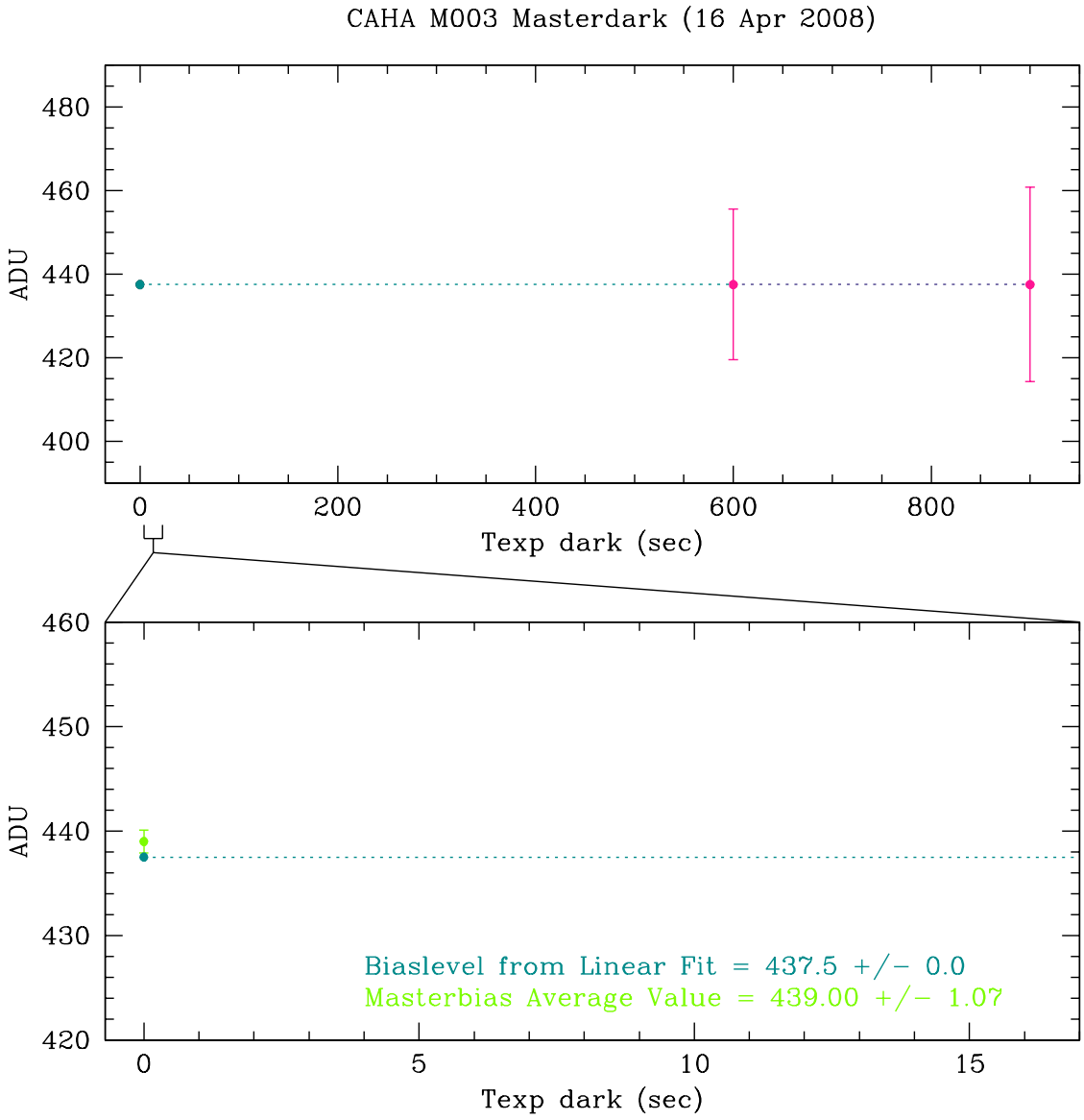

FIGURE 30: Quality Control on masterdark frames of run M-003@CAHA. The mean value of each masterdark is plotted versus the exposure time. In the bottom panel a zoom is shown in order to compare the bias level extrapolated from the linear fit (dark green point) with that measured directly from the masterbias frame (light green point). No masterdark correction is needed for CAHA data.

C DoLoRes@TNG Calibration Frames IFP results

C.1 Masterbias

We monitored the bias level and the two-dimensional stability trend during the first seven runs (P-004, M-002, M-005, M-008, M-009, M-012 and M-015) performed in La Palma (Canary Island, Spain) using DoLoRes@TNG (see Fig. 31). Between runs P-004 and M-002, a new CCD was mounted in DoLoRes[13]: the improvement in the data quality is clearly visible in the two-dimensional stability trend plot. DoLoRes masterbias are often characterized by bright and dark horizontal and/or vertical stripes (about ±5 counts from the average) with a pattern that changes with time (see SMR-001). For this reason, it is strongly recommended not to use bias taken during one day to correct data acquired during other days of the same run.

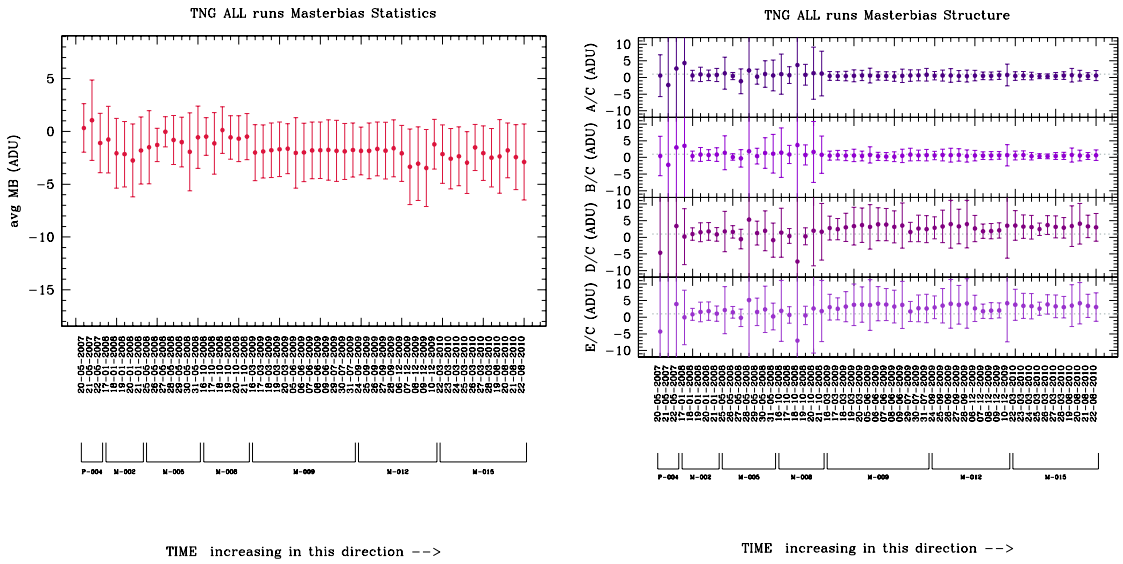

FIGURE 31: Long-time trend monitoring of the bias level (*left panel*) and two-dimensional structure (*right panel*) produced using the data acquired with DoLoRes@TNG in the seven studied runs.

C.2 Photometric Masterflat

DoLoRes@TNG is primarily dedicated to spectroscopy. Photometric skyflats have been acquired, if any[14], only during nights in which photometric observations have been performed.

[13]The original DoLoRes detector, an E2V4240, was replaced with a similar E2V4240 in December 2007.

[14]Because with TNG it is not possible to acquire skyflats during sunrise, often no flats are available if the observing mode was switched from spectroscopic to photometric during the night. No domeflats are acquired due

In Fig. 32 we report the tests performed in order to study the stability of photometric sky masterflat frames (for the B filter) acquired during run M-015. Fortunately, sky masterflats at TNG seem to be very stable within 0.3%, at least over one run (normally lasting 4-5 nights). So, if we do not have skyflats for one night, we can safely use those acquired during other nights in the same run.

In Fig. 33 we show the long-term trend study on the large scale variation performed on filter B sky masterflat frames produced during runs M-009, M-012 and M-015. The stability of DoLoRes sky masterflats is very good: the variation in shape is lower than 0.5% over a period greater than 200 days.

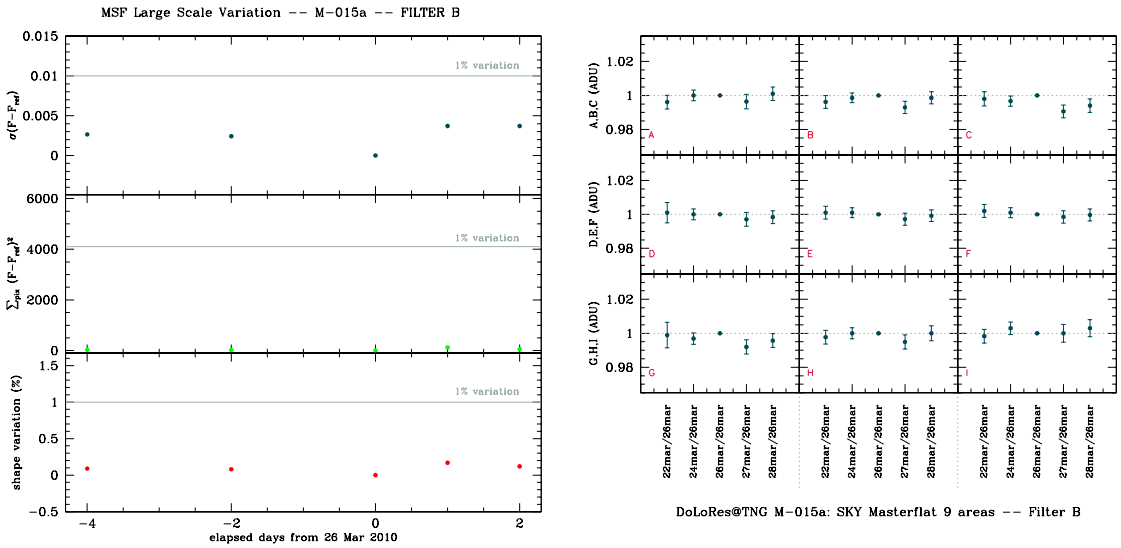

FIGURE 32: Stability tests for sky masterflat frames produced during run M-015 for the B filter.

The long-time trend of the *9 areas* plot for the B sky masterflats produced during the same runs is shown in Fig. 34: the large errorbars in the B region of all M-015 masterflats are due to a little but strong "imperfection" present in the reference frame (and also in the M-012 masterflats) but not in M-015 masterflats (see Fig. 35).

Similar studies and results, both for short and long time trends, performed for filter V and R can be found in Wiki-Bo.

to the low stability of the halogen lamp (see EP-003).

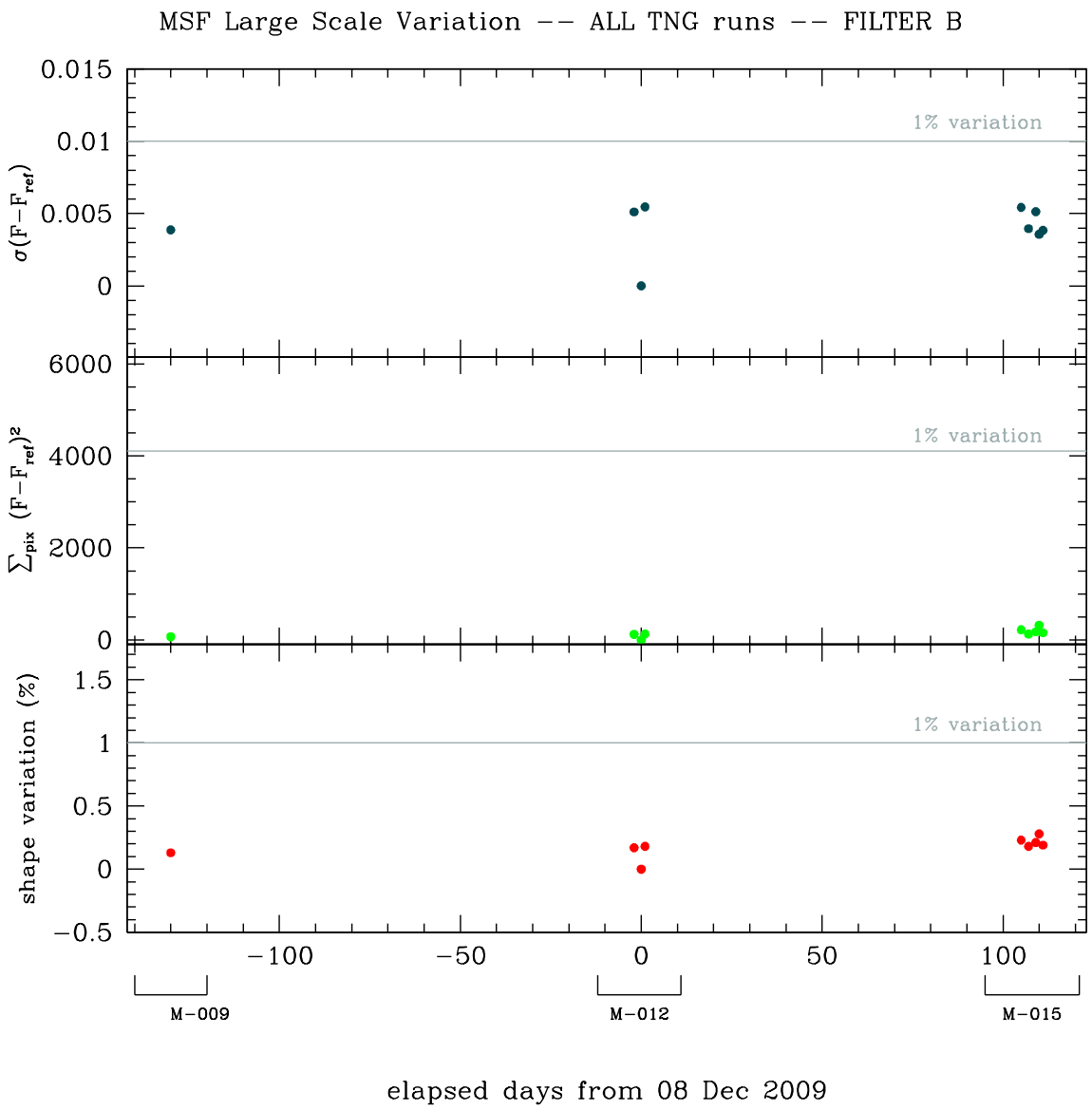

FIGURE 33: Long-time large scale stability test performed on all sky masterflats produced with the B filter during three TNG runs. The sky masterflat produced in the central night of run M-012 (08-12-2009) is the reference frame. The shape variation of sky masterflats is lower than 0.5% over a period of about 250 days.

C.3 Spectroscopic Masterflat

In Fig. 36 we report the stability for the spectroscopic masterflat frames produced during runs M-005 with DoLoRes@TNG. As usual, the monitoring plots for all other runs can be found

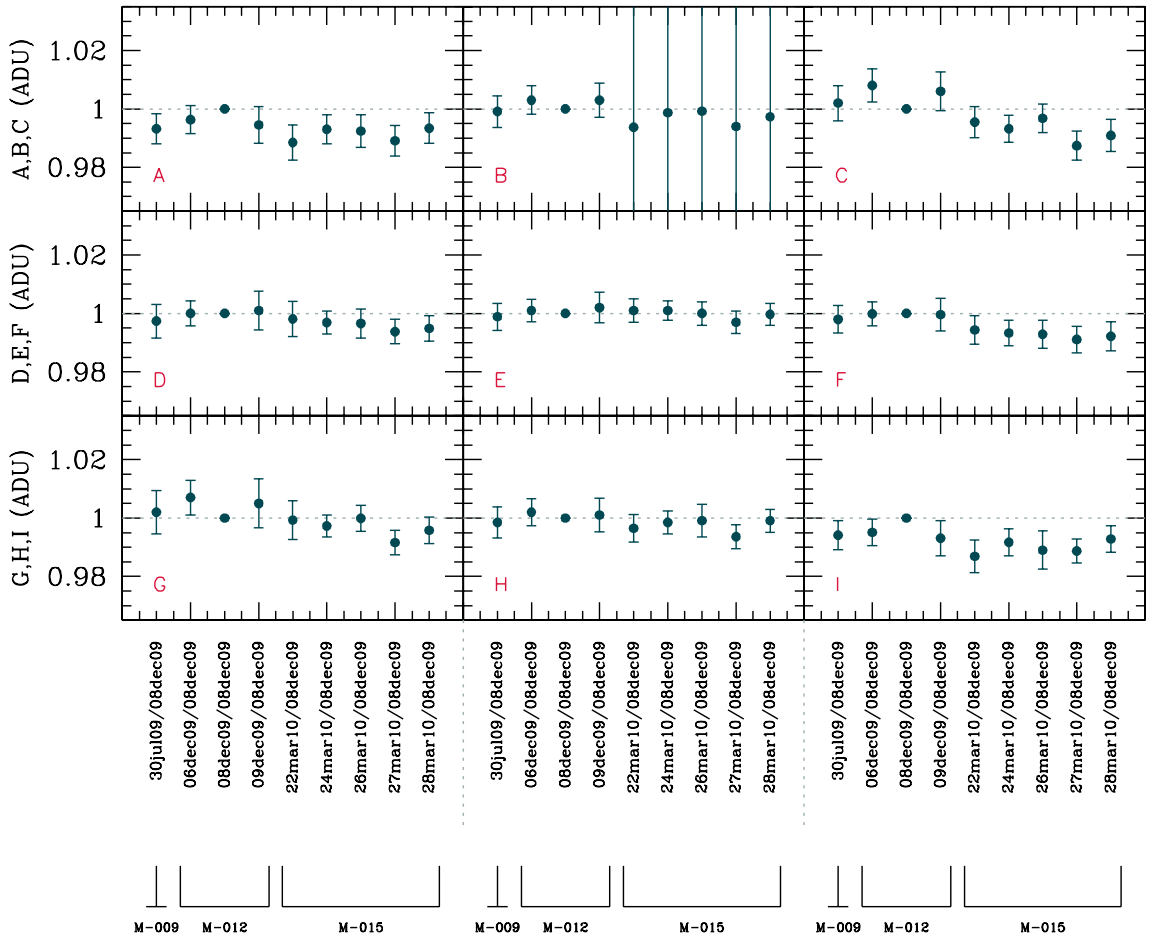

FIGURE 34: Long-time 9 areas test performed on all sky masterflats produced with the B filter during three TNG runs. The reference frame is the same of Fig. 33. The large errorbars in the B region of all M-015 masterflats are due to a little but strong "imperfection" present in all master frames of the previous runs which disappears in M-015 masterflats (see Fig. 35).

in Wiki-Bo. The blue (grism LR-B) spectroscopic masterflats are quite stable, both for the narrow and the wide slits adopted[15] (left and right upper panels in the figure). In the bluer part of the blue grism (showed in the three left boxes of each blue plot) the difference in shape between masterflats produced in different nights is ∼3-4% in the worst case, due to the low S/N

[15]Usually, for this instrument, the narrow slit is 2" and the wide slit is 5" (10" from M-009).

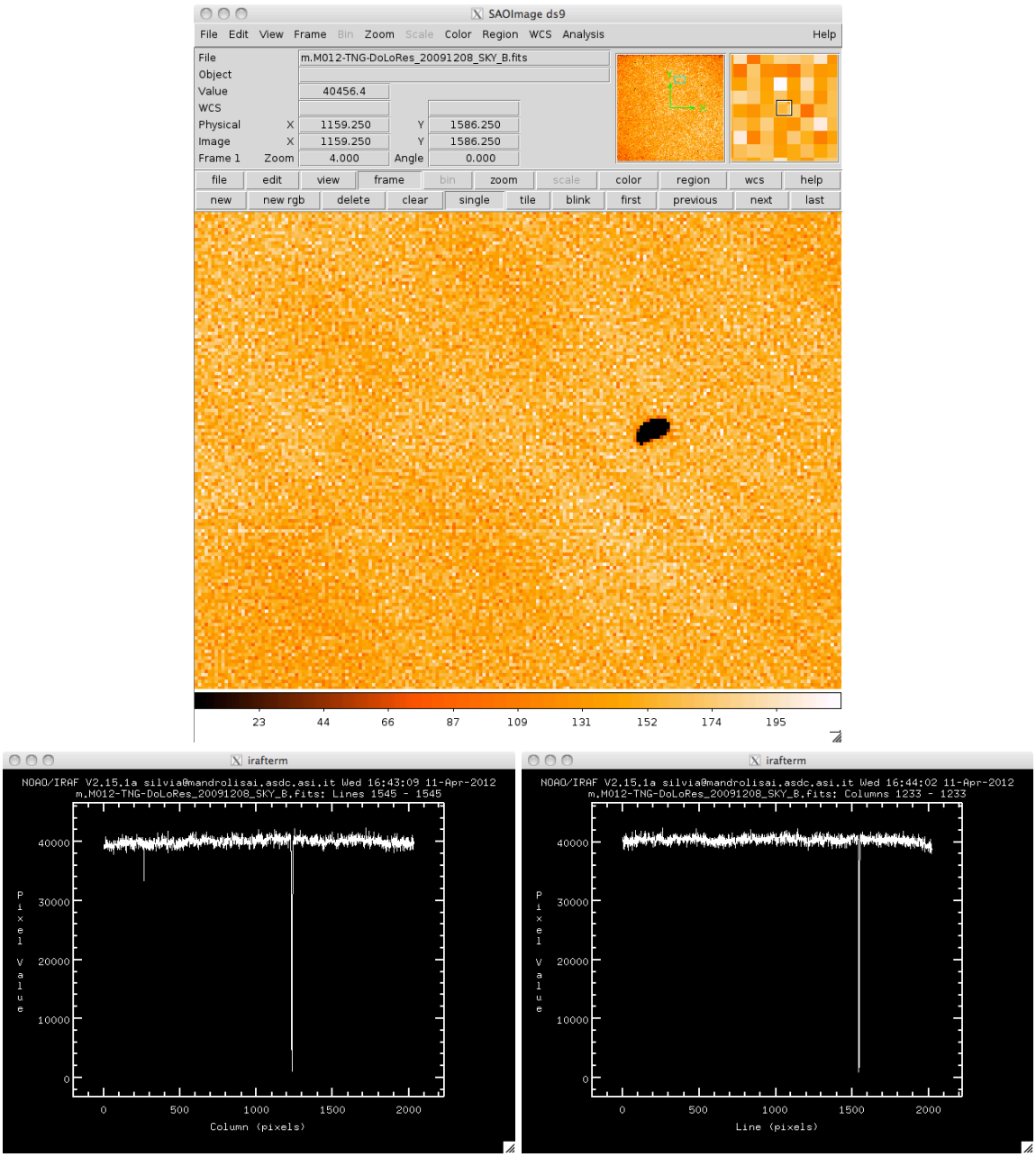

FIGURE 35: Zoom of the little "imperfection" (of about 10×14 pixels) on the reference masterflat used to produce both the 9 areas and the large scale variability plots. On the bottom part of the figure, a line and a column crossing the imperfection are plotted in order to show the deep hole produced in the counts: this is the origin of the strong errorbars in the B region of the 9 areas plot.

reached in this region. The red spectroscopic masterflats (grism LR-R, left and right bottom panels) are affected by both fringing and internal reflections (the latter are effectively removed during the pre-reduction, see GCC-001). The fringing pattern appears to be quite stable, but we recommend to be careful in using grism LR-R masterflats produced for one night to pre-reduce spectra acquired in other nights.

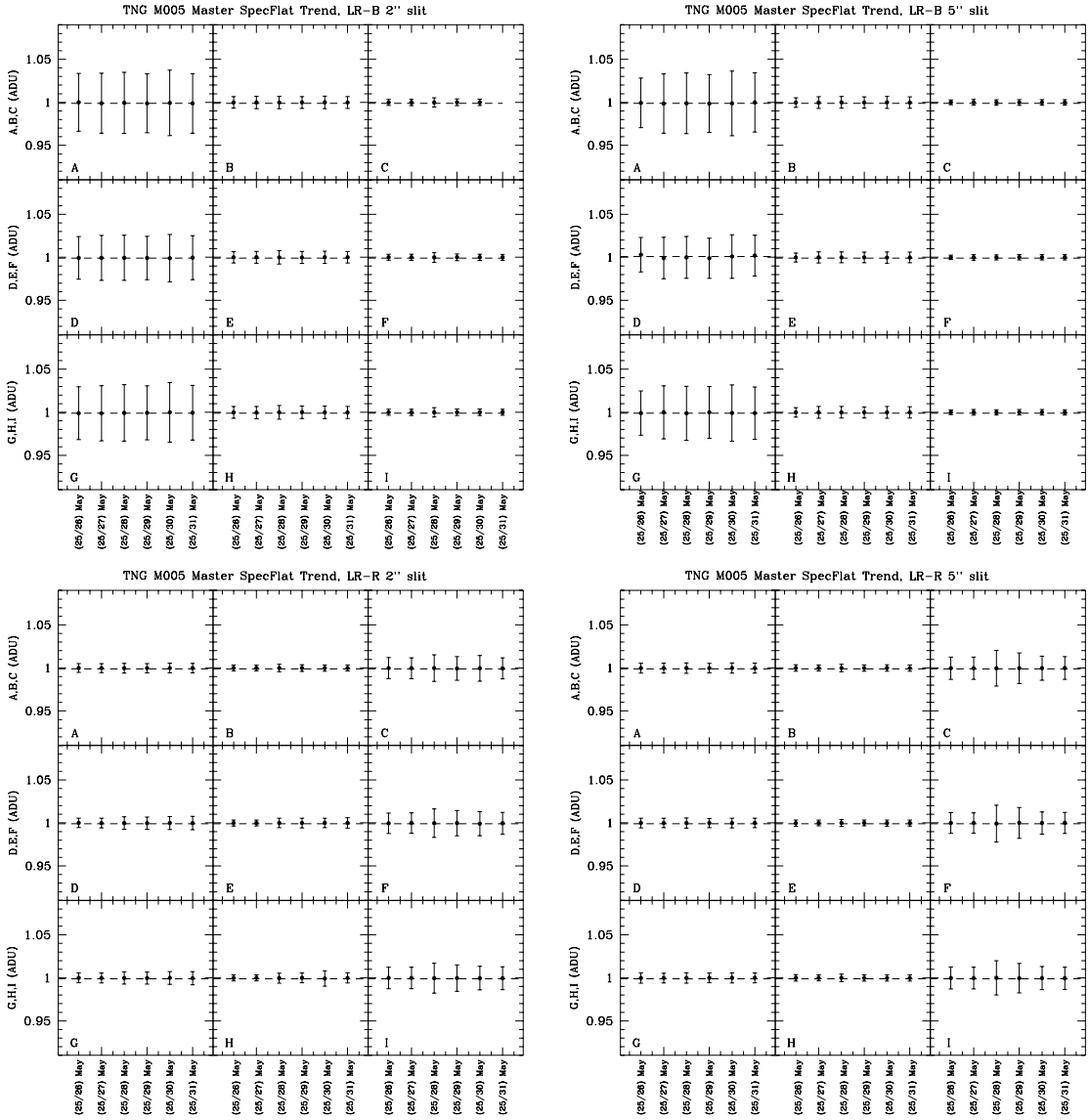

FIGURE 36: Stability test for spectroscopic masterflat frames produced during run M-005 for the blue grism LR-B (*upper plots*) and red grism LR-R (*bottom plots*).

C.4 Wavelength Lamp Flexures

We performed a test to measure the DoLoRes lamp flexures on 31 January 2008, when the instrument was equipped with three separate calibration lamps (He, Ne, Ar) that could not be switched on simultaneously, and the procedure to obtain an high signal-to-noise ratio calibration lamps for each single star was very time consuming (about 20 minutes). The time-consuming problem of acquiring a set of good S/N wavelength calibration arcs for each single observed star could be solved by acquiring a large number of lamps with high S/N during day time, and only one arc with lower S/N after each scientific spectrum. This solution is viable only if the high S/N calibration spectrum can be easily shifted to the wavelengths of the lamp acquired for each star by applying a simple linear shift, as explained in GCC-001. Presently, a new set of lamps is available for DoLoRes (He, Ar, Ne+Hg and Kr). All these lamps can now be switched on at the same time.

For the measurements, we used the LR-R grism, the 2” slit and the Ar lamp. Triplets of arc frames were acquired at different positions of the derotator, covering a complete derotator circle: from -260 up to + 100 degrees in steps of 10 degrees forward, and from +95 up to -255 degrees in steps of 10 degrees backwards. This way, the derotator performed a complete circle in steps of 10 degrees each. The median of the three acquired lamp frames was calculated for each derotator position and corrected for the overscan. The lines used for the test are shown in Fig. 37.

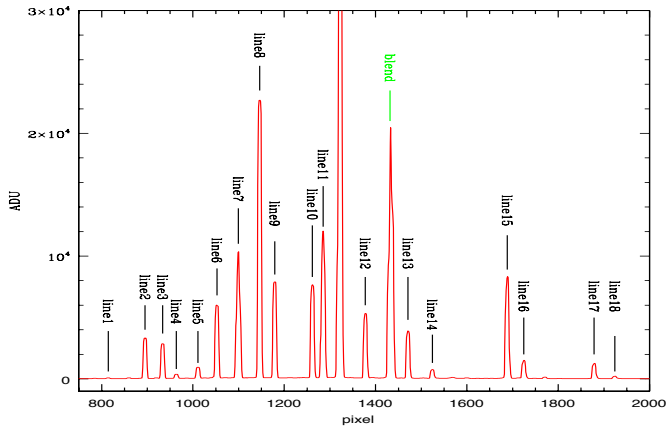

FIGURE 37: Lines used to measure lamp flexures, obtained with Ar lamp, slit 2” and grism LR-R. The line labelled in green is a blend not used for the test.

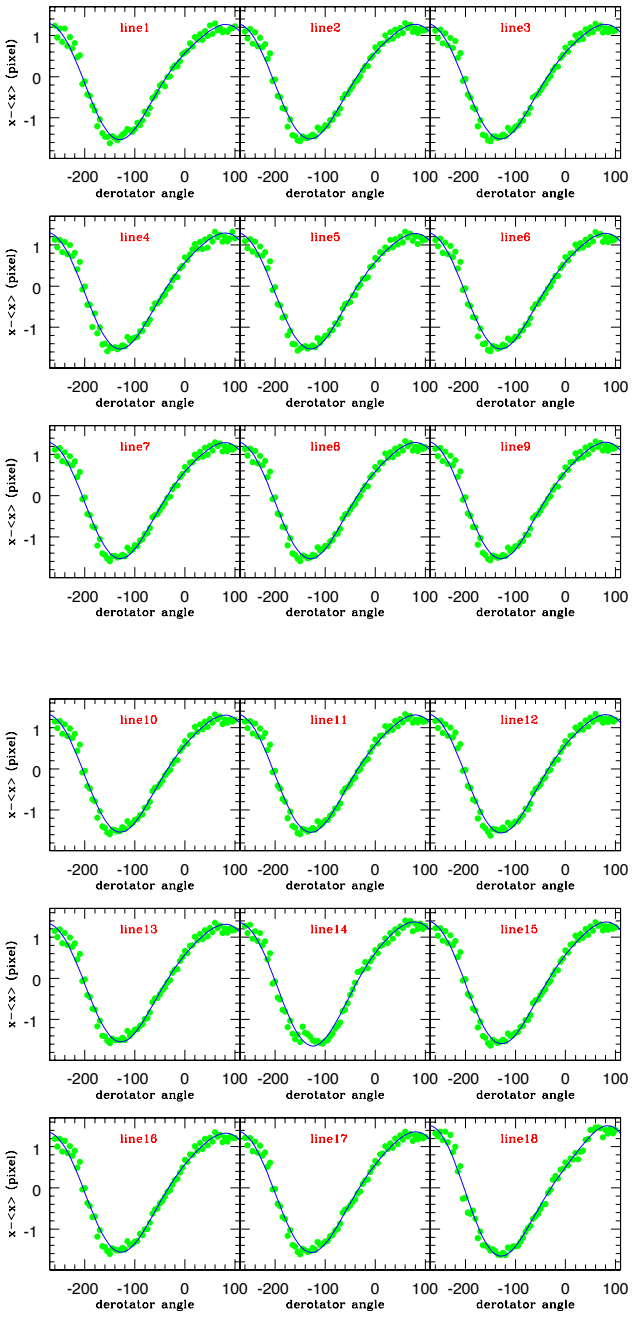

FIGURE 38: Displacement of different lines from their mean position (in pixel) versus derotator angle (green points). Each panel corresponds to a different emission line from Fig. 37. The blue line in each panel is the fit of the green points.

The position of lines as a function of the derotator angle are characterized by a quasi-sinusoidal trend, as shown in Fig. 38. Taking one lamp as a reference, we can estimate the shift that we need to apply to each line of all the other lamps to align them to the reference lamp. If the shift is perfectly rigid one would expect to measure, for each derotator position, the same shift in the position of each observed line, with respect to the reference lamp spectrum. In practice, the error on the position of each line, estimated with a gaussian fit, is quite large. For this reason, an average shift was estimated for each lamp by calculating the mean on the shift measured for each line. The reference spectrum obtained during day time can now be properly compared with the calibration spectra (acquired during night time for each observed star), by applying this average shift. The uncertainty resulting from this method is typically larger in the external parts of the spectrum and smaller in the central parts as shown in Fig. 39. This is probably due to a small non linearity of the dispersion relation. In any case, this uncertainty is small enough if compared with the typical error of the wavelength calibration (in particular if a 2" slit is used, as in our case).

As a result of this test, our observing (EP-006) and spectra pre-reduction (GCC-001) protocols foresee the use of one arc observed close to the target during night-time in order to shift (if necessary) the solution found with the calibrations arcs taken in day time.

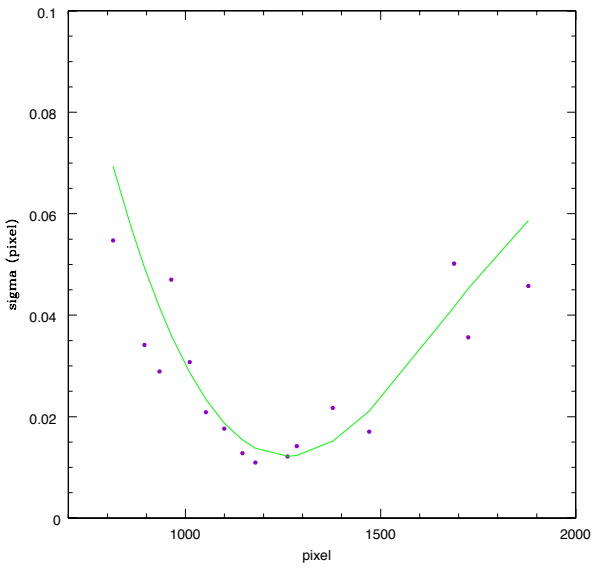

FIGURE 39: Uncertainty in lines positions (see text).

C.5 Masterdark

The check on the linear growth of masterdark frames with exposure time is shown in Fig. 40 using data acquired during run M-005. Only one example is shown here: other dark sequences were taken during this and other runs, and their analysis is available in Wiki-Bo. With increasing exposure time, the DoLoRes dark frames remain stable and close to the bias level. No dark correction is therefore necessary for scientific data. We suggest to repeat the test once every year in order to monitor the dark current behaviour.

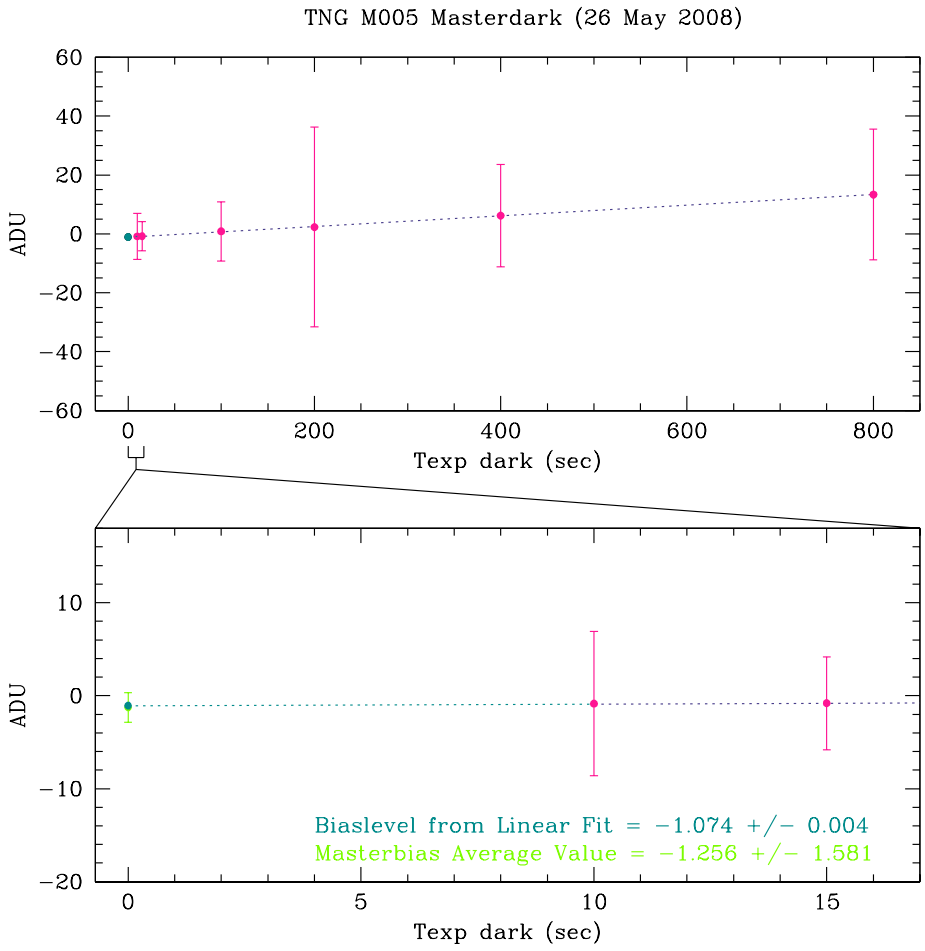

FIGURE 40: Growth plots of masterdark frames of run M-005@TNG. The mean value of each masterdark is plotted versus exposure time. In the bottom panel of the plot, a zoom is shown in order to compare the bias level extrapolated from the linear fit (dark green point) with that measured directly from the masterbias frame (light green point). No masterdark correction is needed for TNG data.

D EFOSC2@NTT Calibration Frames IFP results

D.1 Masterbias

In Fig. 41 and Fig. 42 we reported the bias level and the two-dimensional stability trend during the first two runs (M-007 and M-010) performed in La Silla (Chile) using EFOSC2@NTT, for both the photometric and spectroscopic binning factors. The two-dimensional stability of masterbias is very good for both binnings, but the long-term study of bias level shows an oscillating trend in the spectroscopic 2×2 binning, probably due to problems with electronics when the CCD is used applying this binning factor. Probably, the problem could be solved if overscan correction could be applied: unfortunately the overscan section is very irregular and it is impossible to select a reliable overscan section (see SMR-001).

We recommend not to use the masterbias produced for spectroscopy (binning 2x2) during one day to pre-reduce data acquired during other days of the same run.

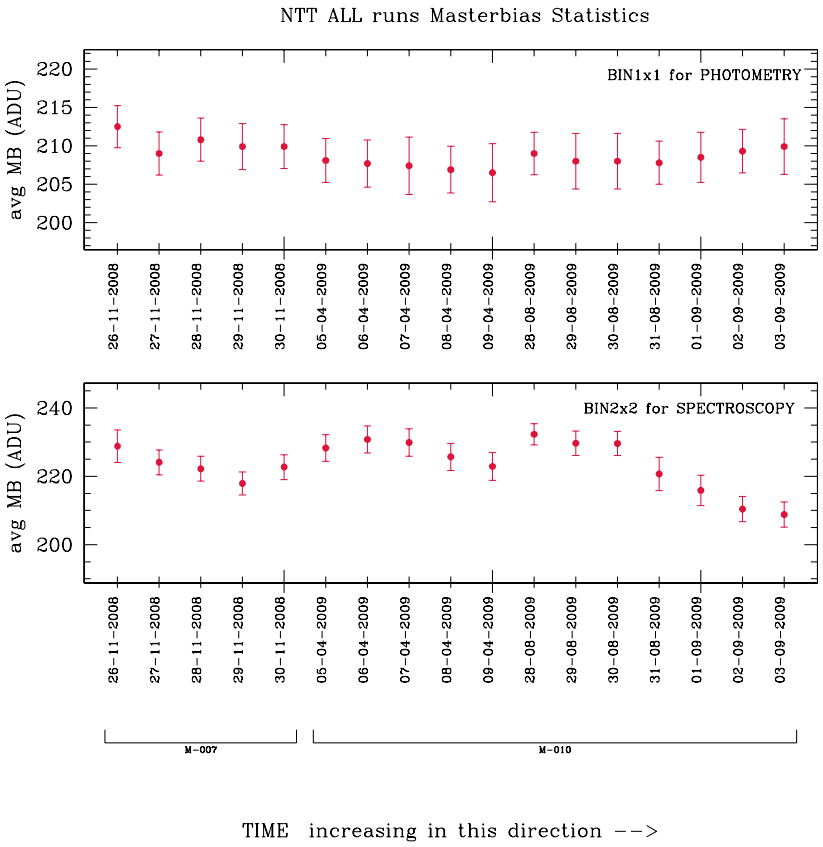

FIGURE 41: Long-time trend of the bias level produced using data acquired with EFOSC2@NTT during runs M-007 and M-010.

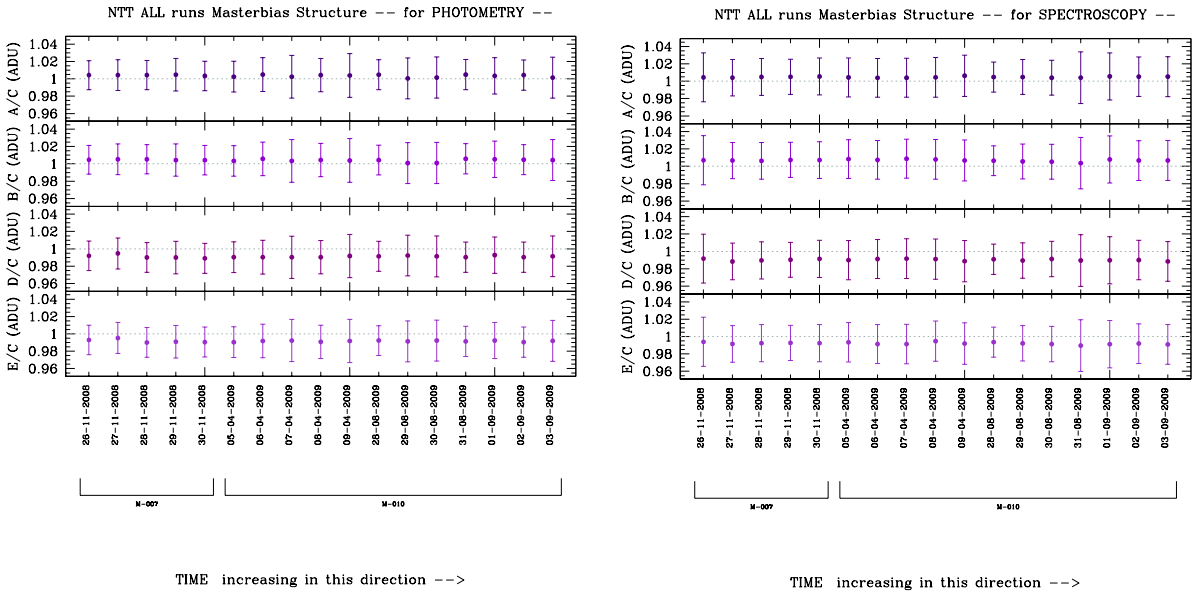

FIGURE 42: Long-time trend of the two-dimensional structure stability produced using the data acquired with EFOSC2@NTT during runs M-007 and M-010.

D.2 Photometric Masterflat

We show, as an example, the tests performed in order to study the short-term stability of photometric flats (for the B filters) for both dome and sky masterflat produced during run M-010b (see Fig. 43). As usual, the short-term monitoring plots for all runs and filters can be found in Wiki-Bo. In all filters, both dome and sky masterflats appear to be very stable, showing differences in shape lower than $\simeq$0.4% for skyflats and lower than $\simeq$0.3% for domeflats. So, if we do not have flat frames (dome or sky) for a particular night, we can safely use those acquired during other nights in the same run.

In Fig. 44 and 46 we show the long-term trend study on the large scale variation performed on filter B dome and sky masterflats respectively, produced during runs M-007 and M-010. The stability of EFOSC2 dome and sky masterflats is good: in both cases, the variation in shape is lower than 0.7% over a period greater than 250 days. The long-time trend of the *9 areas* plot for the B dome and sky masterflats produced during the same runs are shown in Fig. 45 and 47, respectively. In the EFOSC2 CCD, the overscan section is very irregular and it is impossible to select a reliable overscan section (see SMR-001): a little portion of the overscan section still remains in the upper left corner of the CCD also after the trimming[16]. As shown in Fig. 48, the intensity of this region is variable (but remains quite stable in each single run), and produces the large errorbars in the A window of the 9 areas plots. Similar studies for the long-time trend performed for filter V and R can be found in Wiki-Bo.

[16]Due to both the position and the shape of this "bad" CCD region, the trimming section was chosen in order to preserve the greatest possible portion of CCD.

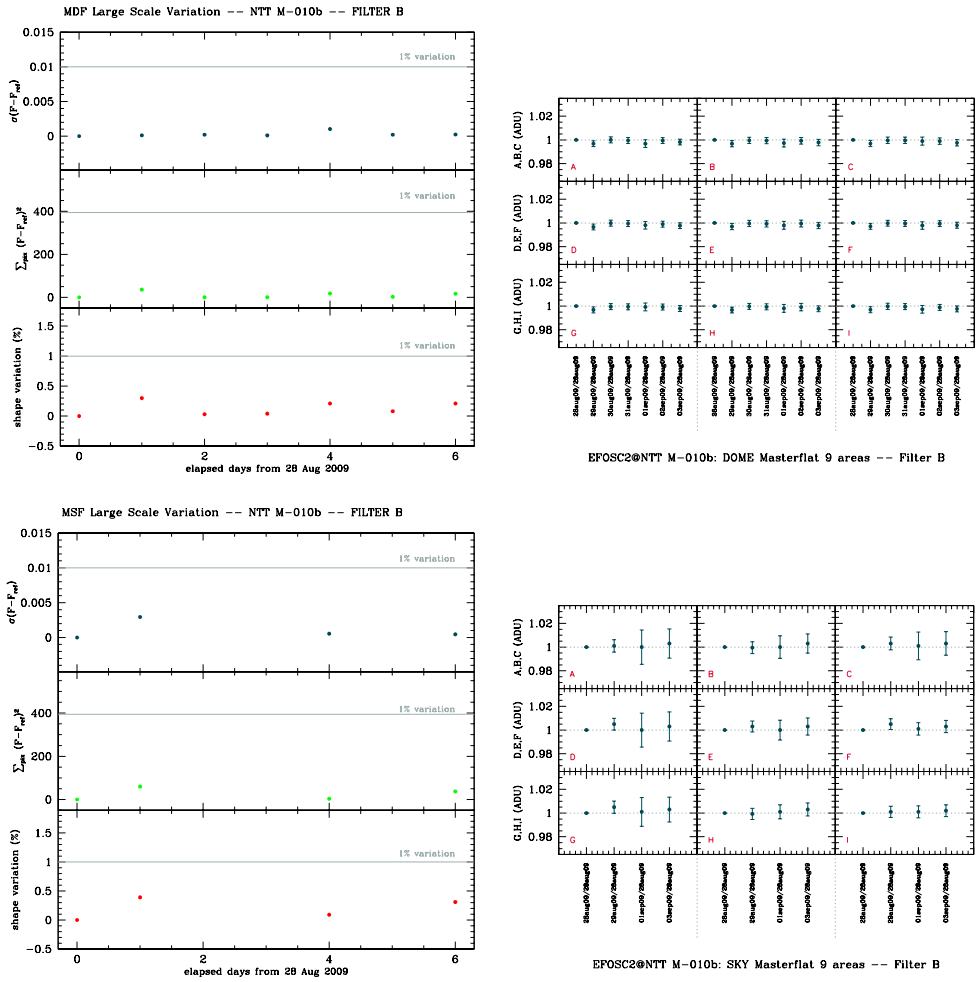

FIGURE 43: Short-term stability plots (see SMR-001) for dome (*upper panels*) and sky (*bottom panels*) masterflat frames produced during run M-010b using the B filter. The monitoring plots for all others runs and filters can be found in Wiki-Bo.

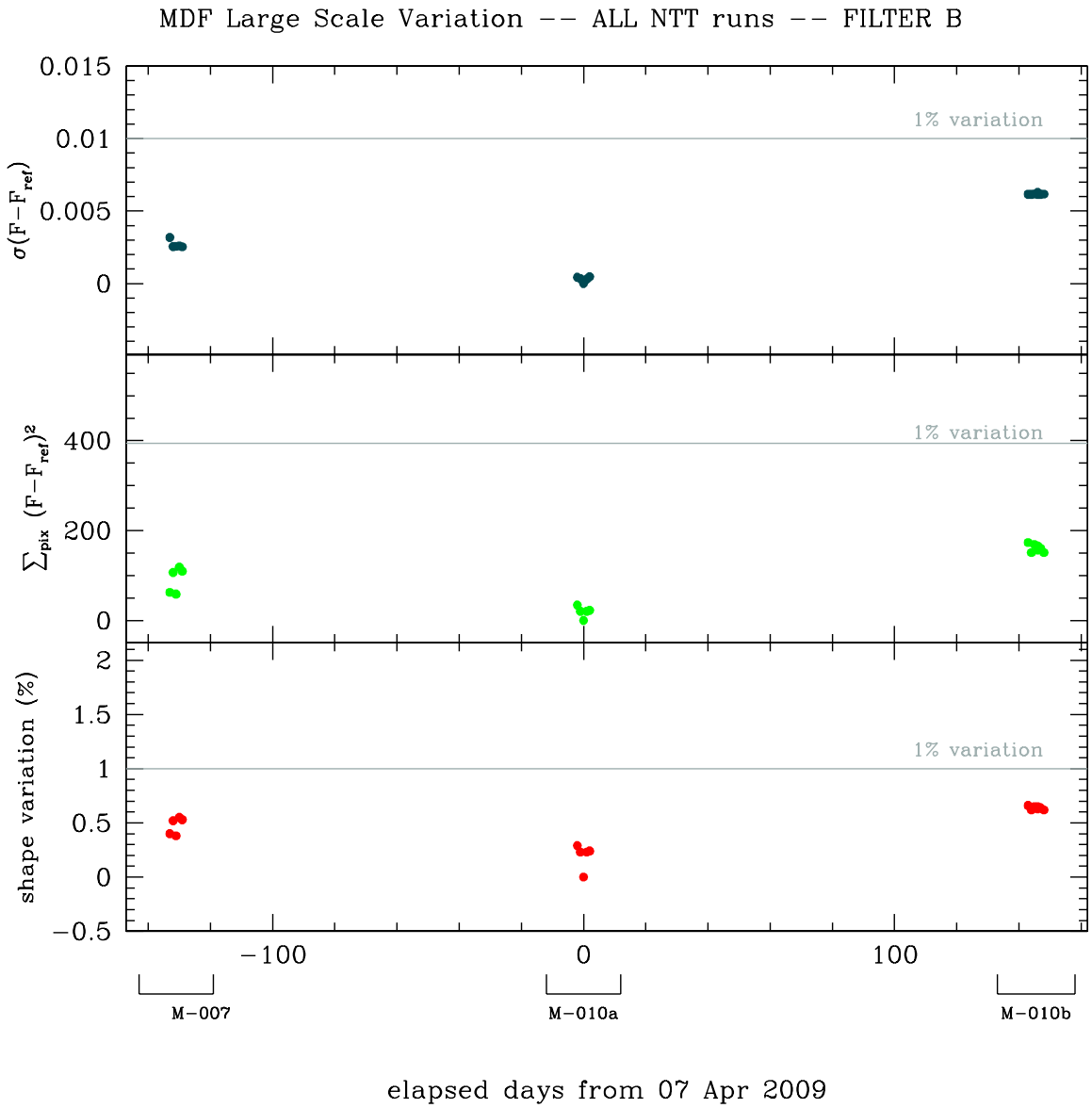

FIGURE 44: Long-time large scale stability test performed on all dome masterflats produced with the B filter during two NTT runs. The dome masterflat produced in the central night of run M-010a (07-04-2009) is the reference frame. The variations of dome masterflats are lower than 0.7% over a period of about 280 days.

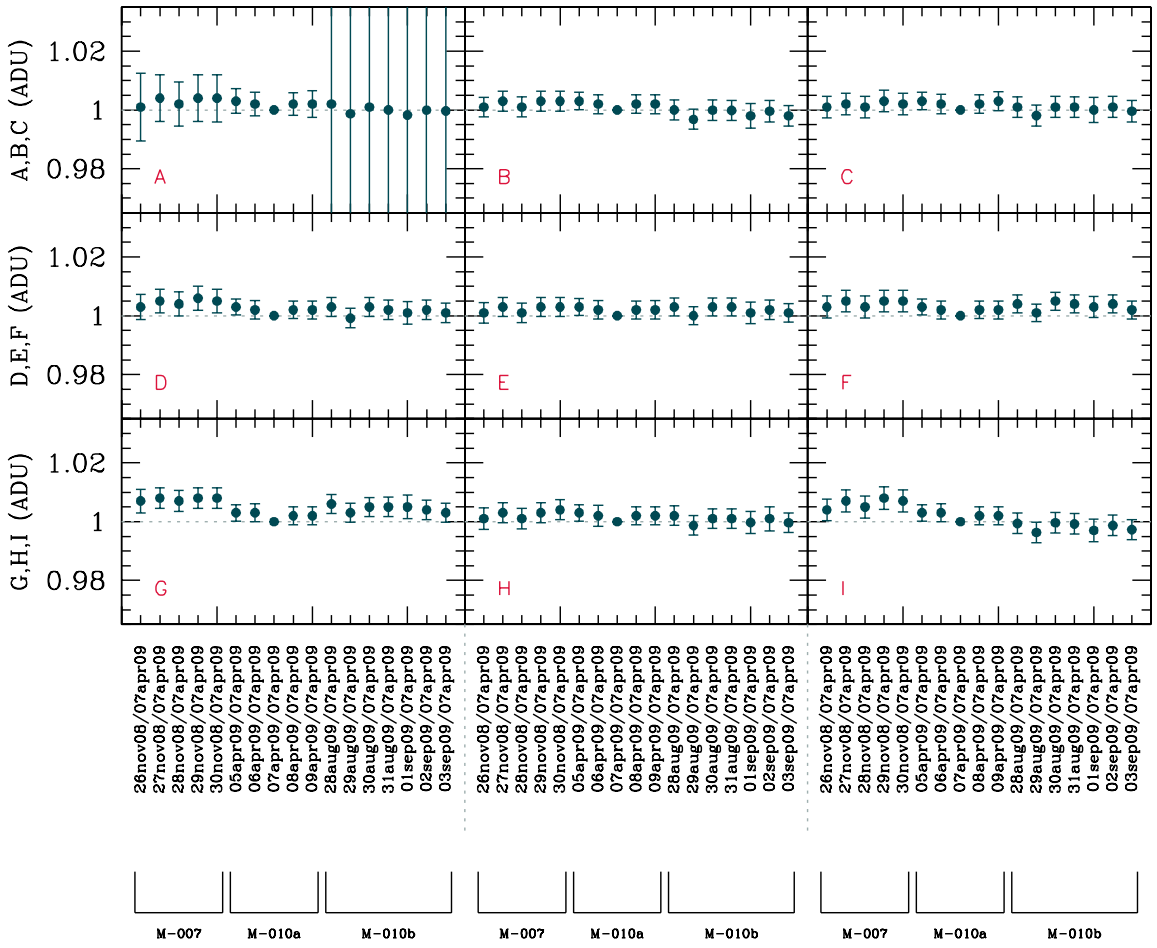

FIGURE 45: Long-time 9 areas test performed on all dome masterflats produced with the B filter during the first two NTT runs. The reference frame is the same of Fig. 44. The huge errorbars in the A region of all masterflats (more evident for the M-010b ones) are due to a little portion of the very irregular overscan section of the CCD which survives to the trimming procedure (see Fig. 48).

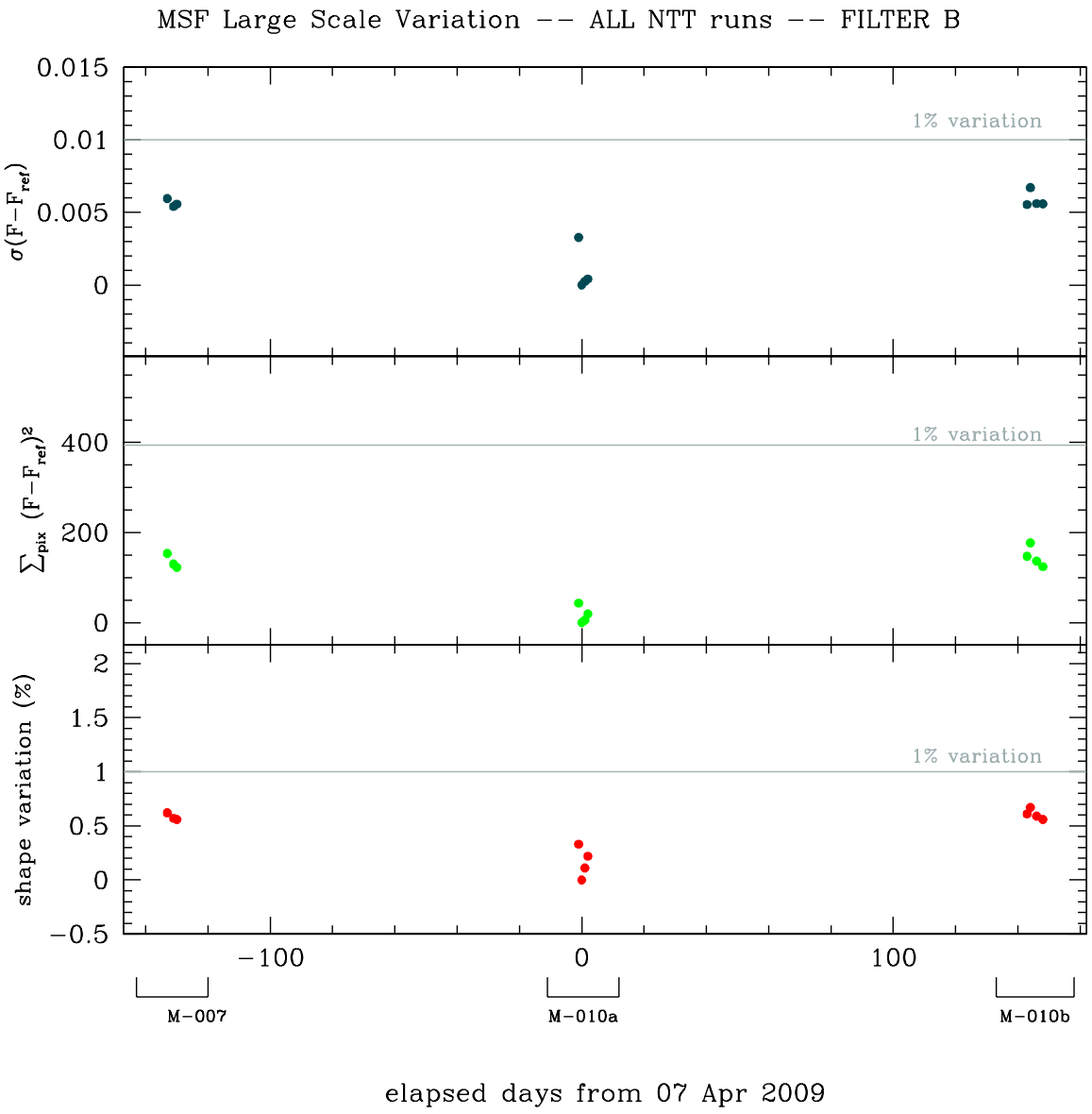

FIGURE 46: Long-time large scale stability test performed on all sky masterflats produced with the B filter during the first two NTT runs. The sky masterflat produced in the central night of run M-010a (07-04-2009) is the reference frame. Also for sky masterflats, the variation in shape is lower than 0.7% over a period of about 280 days.

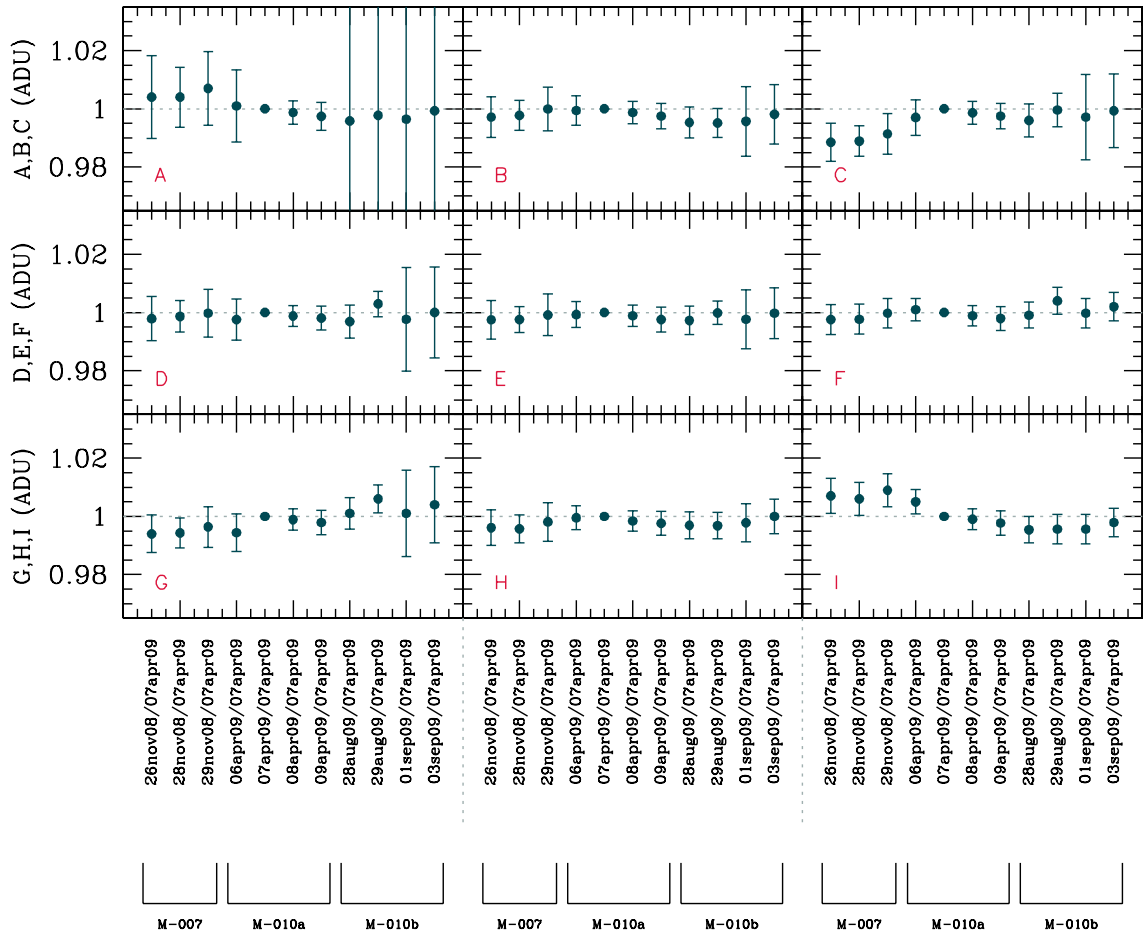

FIGURE 47: Long-time 9 areas test performed on all sky masterflats produced with the B filter during the first two NTT runs. The reference frame is the same of Fig. 46. Also in this case, the huge errorbars in the A region of all masterflats are due to a little portion of the very irregular overscan section of the CCD which survives to the trimming procedure.

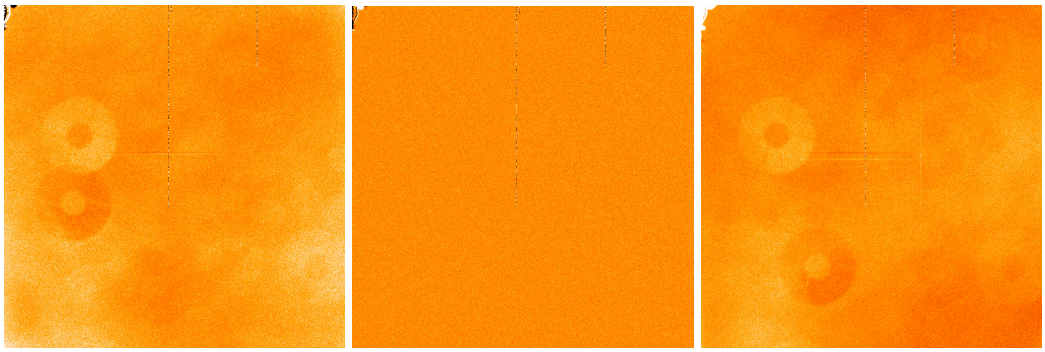

FIGURE 48: Ratio between three different dome masterflats (in the *left panel* the dome masterflat produced for the last night of run M-007, in the *central panel* the dome masterflat produced for the last night of run M-010a, and in the *right panel* the dome masterflat produced for the first night of the run M-010b) and the reference one. The display cuts are the same for all the images (z1=0.98 and z2=1.02). The upper left corner of the CCD shows the little portion of the overscan region which is responsible of the large errorbars in the A region of the 9 areas plots.

D.3 Spectroscopic Masterflat

We monitored the stability of the spectroscopic masterflat frames produced during run M-007 (Fig. 49 and 50). The blue spectroscopic masterflat frames (grism G11) are quite stable, both for the narrow and the wide slits adopted[17] (top and bottom panels in the Fig. 49 respectively). In the bluest part of the blue grism (showed in the three lower boxes of each plot) the difference in shape between masterflats produced in different nights is $\simeq$2-3% in the worst case (ignoring the deviant point in the central lower region of the first plot), caused by the low S/N usually reached in this region.

The NTT staff recommends to acquire lamp flats in the red grism (G16) for each star spectrum. The masterflats produced for each observed star during 2008-11-30 are shown in Fig. 50 (for both the narrow and wide slits) and are labelled with the proper star ID. The red spectroscopic masterflat frames are strongly affected by fringing: the effect is clearly visible and appears unstable in flats acquired with the narrow slit (points affected by large errors). The fringing pattern in spectroscopic flats acquired using the wide slit is much more stable, as reflected by the smaller errorbars. We agree with the NTT staff on the need of acquiring flats frames (red grism) for each observed star spectrum, in particular when using the narrow slit. We thus recommend to acquire spectroscopic flat frames for each setup during the afternoon. Just after each star spectrum, it is mandatory to acquire lamp flats using the red grism and the narrow slit setup. For safety, we also recommend to acquire flat frames using the red grism and the wide slit setup because sometimes and with random frequency flat fields can be significantly unstable (see, for example, the first 2 points in the bottom plot of Fig. 50)

[17] Usually, for this instrument, the narrow slit is 1.5" and the wide slit is 10".

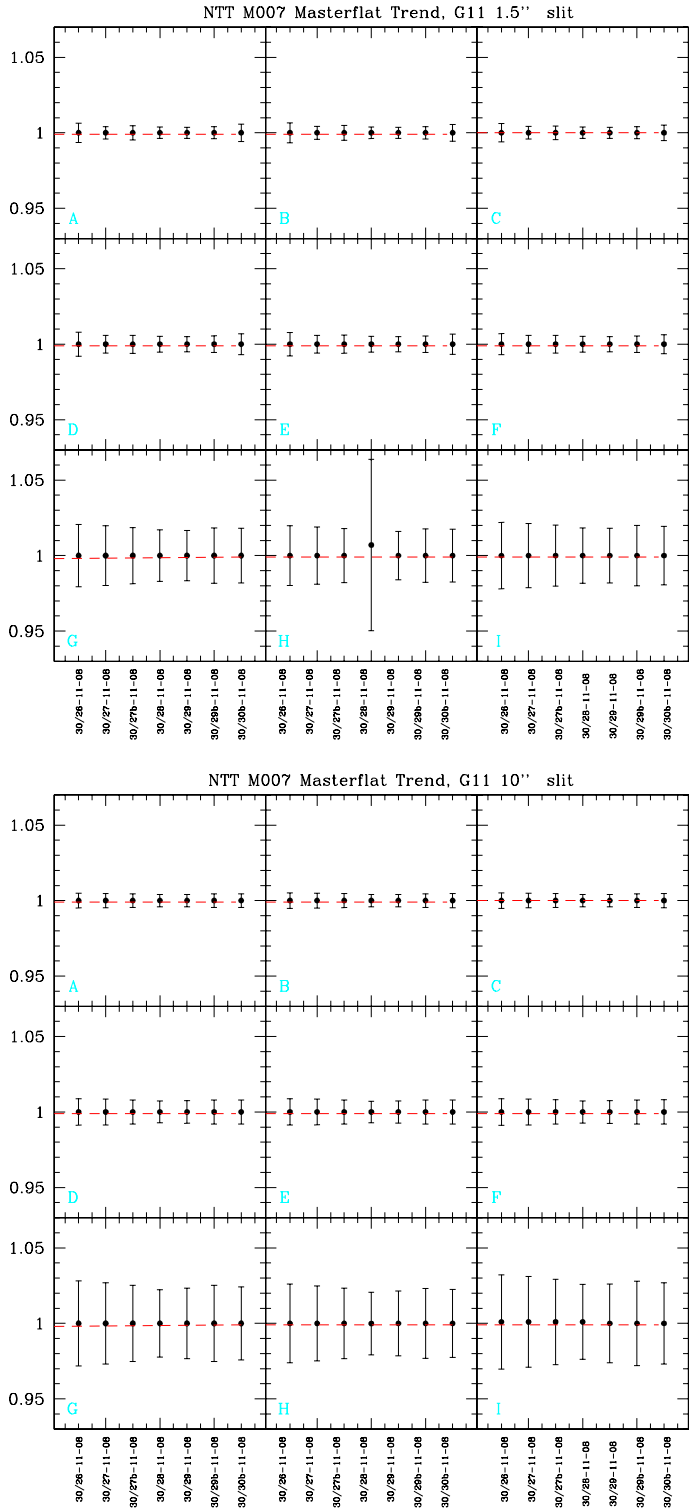

FIGURE 49: Stability test for spectroscopic masterflat frames produced during run M-007 for the blue grism G11. In all plots, the "b" label following the day number indicates masterflats produced using flat frames acquired by the NTT staff during the day.

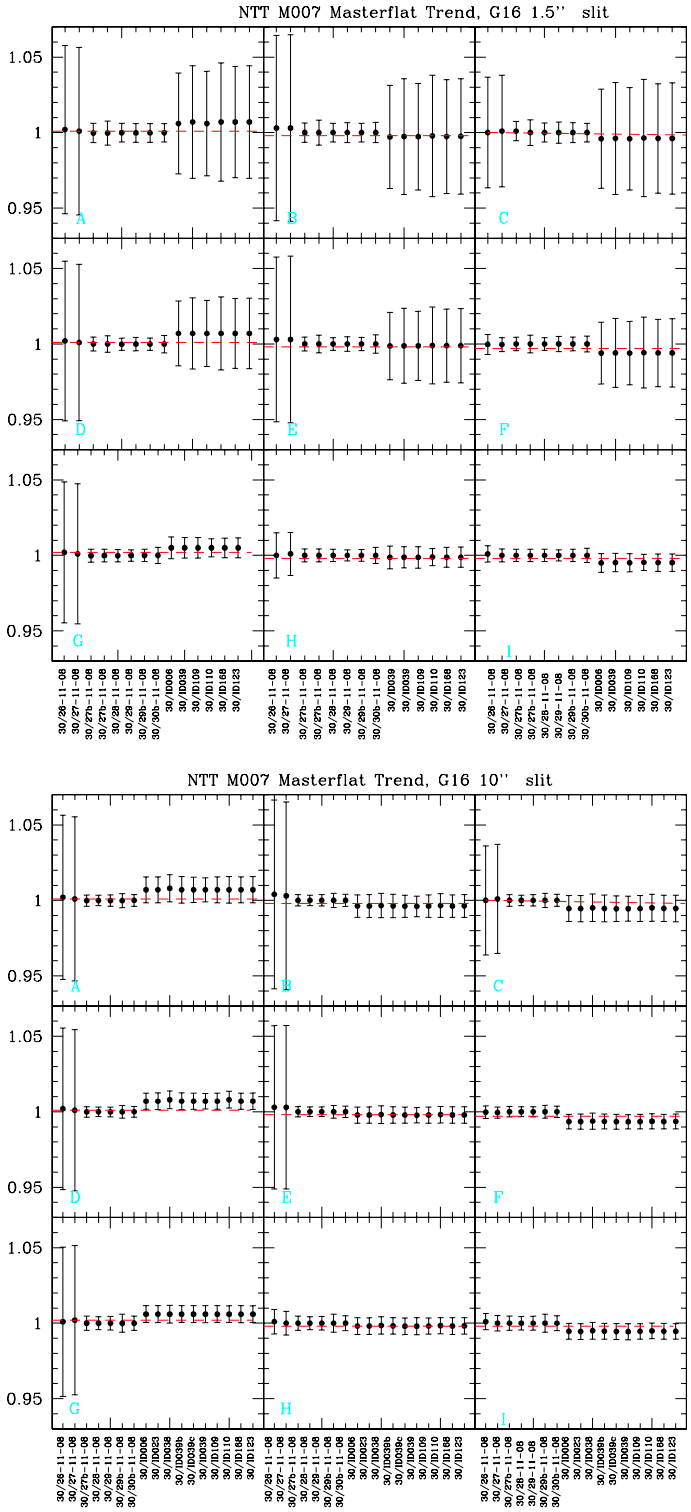

FIGURE 50: Stability test for Spectroscopic masterflat frames produced during run M-007 for the red grism G16. In all plots, the "b" label following the day number indicates masterflats produced using flat frames acquired by the NTT staff during the day. The masterflats produced for each observed star during 2008-11-30 are also reported.

D.4 Masterdark

The linear growth of masterdark frames counts with exposure time is shown in Fig. 51, built with data acquired during run M-007. There is no difference in counts between masterdark frames produced with increasing exposure times, and therefore no dark correction is needed for scientific data. We suggest to repeat the test once for year in order to monitor the dark current behaviour.

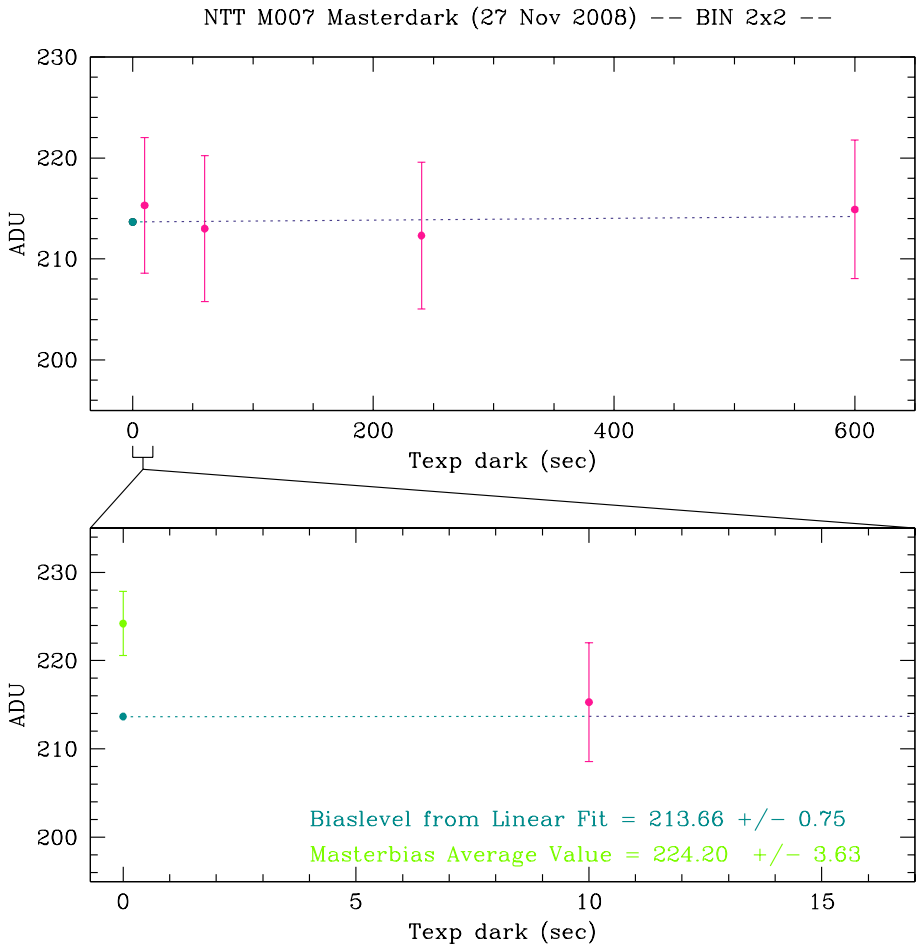

FIGURE 51: Quality control on masterdark frames of run M-007@NTT for the 2x2 binning factor. The mean value of each masterdark is plotted versus exposure time. In the bottom panel of the plot, a zoom is shown in order to compare the bias level extrapolated from the linear fit (dark green point) with that measured directly from the masterbias frame (light green point). Similar plots for other runs and for the 1x1 binning factor can be found in Wik-iBo.

E LaRuca@SPM1.5m Calibration Frames IFP results

E.1 Masterbias

We monitored the bias level and the two-dimensional stability trend during all runs performed in San Pedro Mártir (Mexico) using LaRuca mounted at the 1.5m Telescope (Fig. 52 and 53).

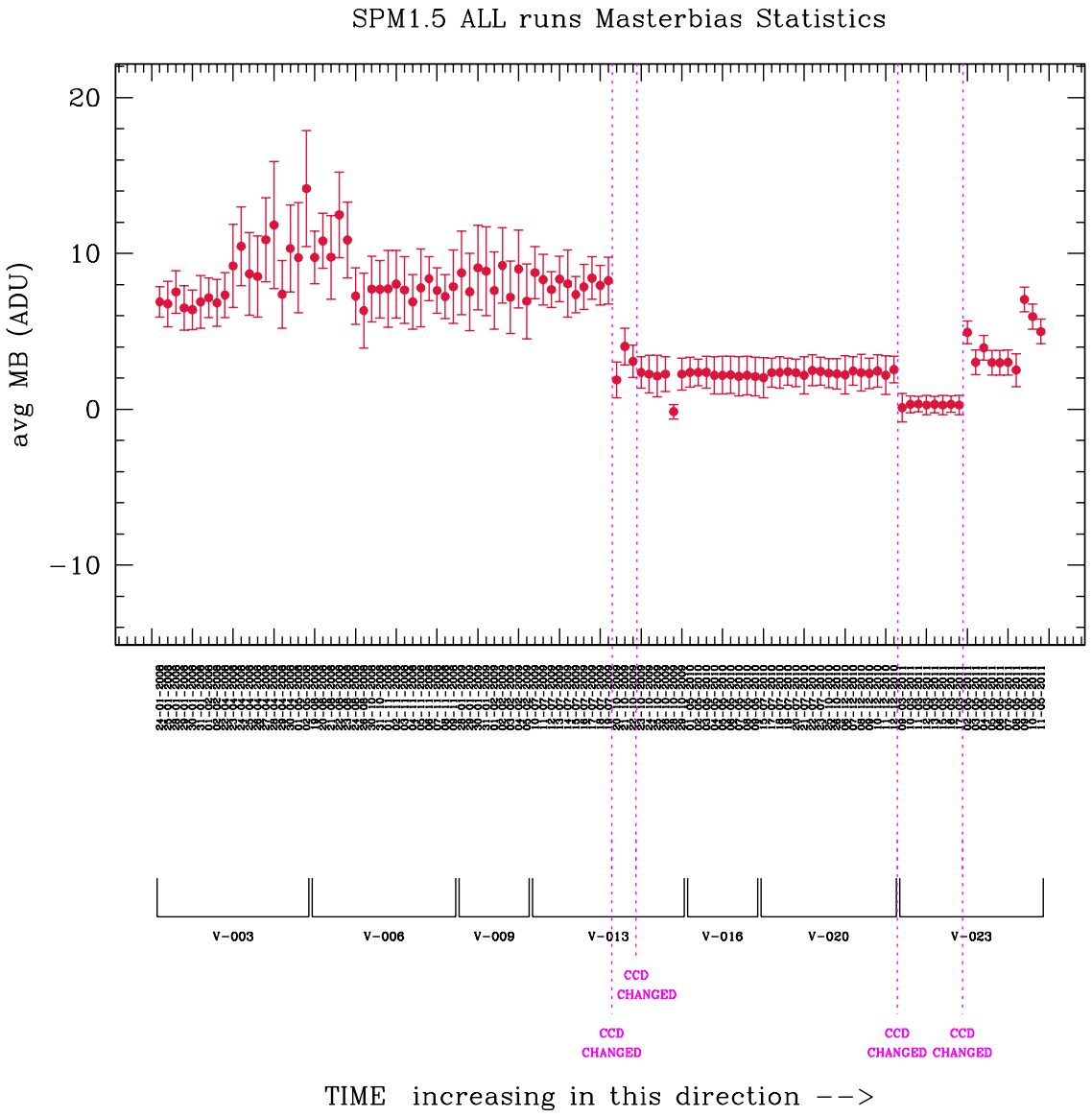

FIGURE 52: Long-time trend of the bias level of all the masterbias produced during the SPM campaigns using different CCDs. All the CCD changes are shown in the plot. ESOPO and SITE4 points are arbitrary shifted (see text) to match the ADU scale of the other CCDs.

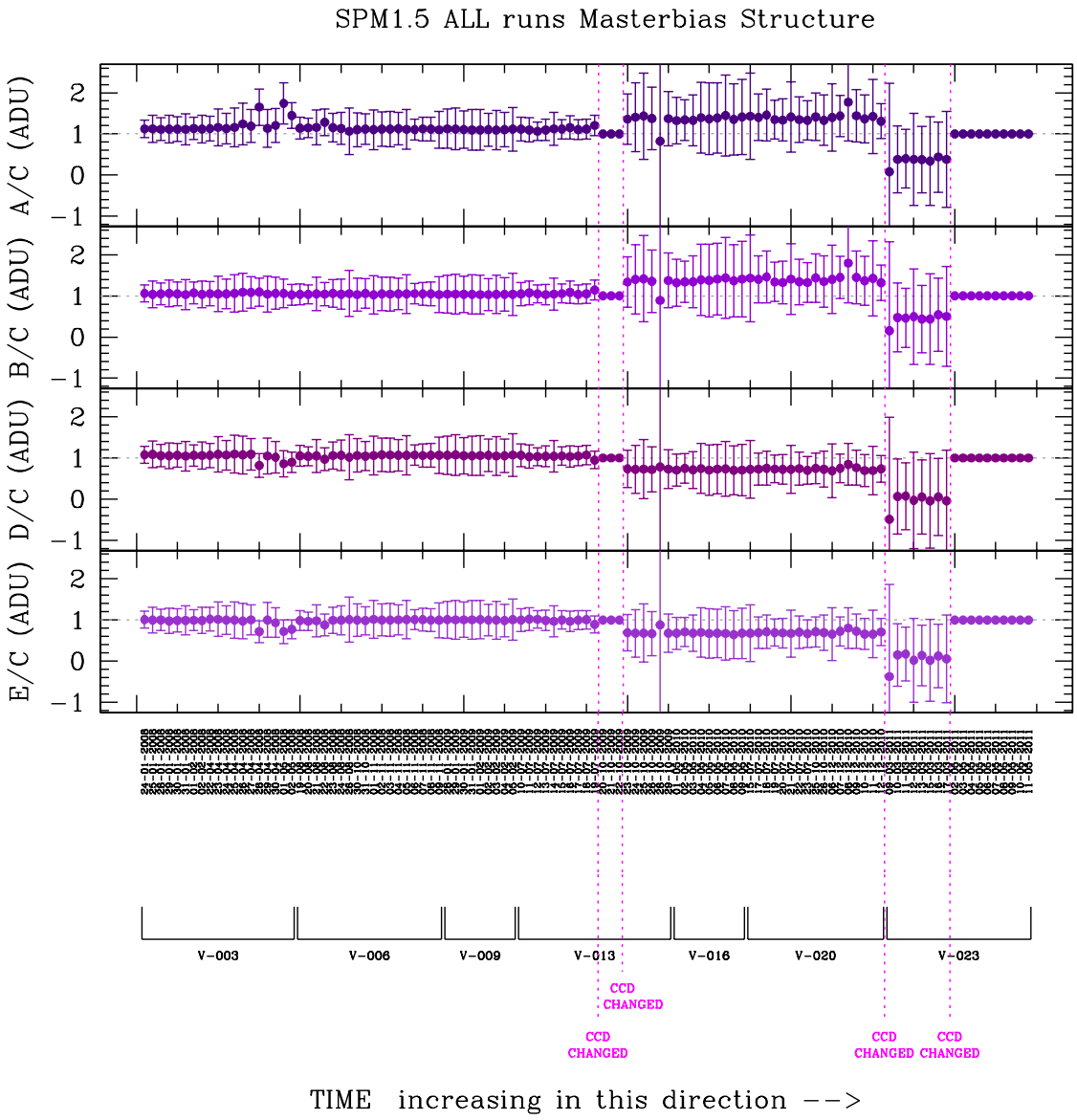

FIGURE 53: Long-time trend of the two-dimensional structure of all the masterbias produced during the SPM campaigns using different CCDs (see text). All the CCD changes are shown in the plot.

Five different CCDs were used with LaRuca. In October 2009, the SITE1 CCD was replaced for three night by the ESOPO CCD and then by a new Marconi1 CCD. This last CCD was used until the end of December 2010 (run V-020). In the next SPM run (V-023) two different CCDs were used: in the first part the Marconi2 CCD, and in the second part the SITE4 CCD. Because the ESOPO and the SITE4 CCD do not have any overscan strip, their bias level is very different from that of the other CCDs (which is computed after overscan correction). In order to show all

masterbias frames on the same scale, preserving their intensity trend with time, we subtract an arbitrary constant value to masterbias produced using ESOPO and SITE4 CCD.

For all CCDs used with LaRuca, the masterbias frames appear to be quite stable in shape, but often not so stable in the absolute global level. For this reason, at least when using the SITE1, SITE4 and ESOPO CCDs, we recommend not to use masterbias produced during one night to pre-reduce data acquired during other nights. This recommendation becomes less rigid when the Marconi1 or the Marconi2 CCDs are used, because their bias level is much more stable in time.

E.2 Photometric Masterflat

The tests performed in order to study the short-term stability of photometric skyflats, are described in SMR-001 and can be found in Wiki-Bo. An example for the B filter is shown in Fig. 54 and 55: the first one is produced using data acquired during runs V-006b (SITE1 CCD) and V-016b (Marconi1 CCD), and the last using data acquired during runs V-023a (Marconi2 CCD) and V-023b (SITE4 CCD).

In all filters, the sky masterflats are quite stable, showing differences in shape of about 1-2% (depending on the filter) during one run, but the masterflat frames behaviour vary from run to run. For these reasons we recommend to acquire photometric flat frames every night, and to use masterflats produced in one night to pre-reduce images acquired in other nights only when this is the only option. In this case, since the masterflat behaviour for each run is normally quite similar in all filters, both the *LargeScaleVariability* and the *9areas* plots can be useful to decide which masterflat of adjacent nights is better to use in the pre-reduction process.

In Fig. 56 we show the long-time trend study on the large scale variation performed using B filter sky masterflats produced during all SPM runs. Owing to the multiple CCD changes during the SPM campaigns, we choose one reference frame for each CCD. The sky masterflat produced using frames acquired in the last night of run V-013a is the reference frame for all masterflats produced using the old SITE1 CCD. During run V-013b two different CCDs were used with LaRuca (ESOPO, only for three nights, and Marconi1): for both CCDs, we use as reference frame the masterflat produced in the first night in which each CCD was mounted. Also for Marconi2 and SITE4 CCDs, mounted during the first and the second part of run V-023 respectively, the first masterflat produced using each CCD is used as reference frame. The long-time trend of the *9 areas* plot for the B sky masterflats produced during the same runs is shown in Fig. 57. The inter-run variation of the sky masterflat frames is clearly visible for all CCDs, as well as the night-by-night shape variation present in all runs. Similar studies (and similar results) for the long time trend performed for filter V and R can be found in Wiki-Bo.

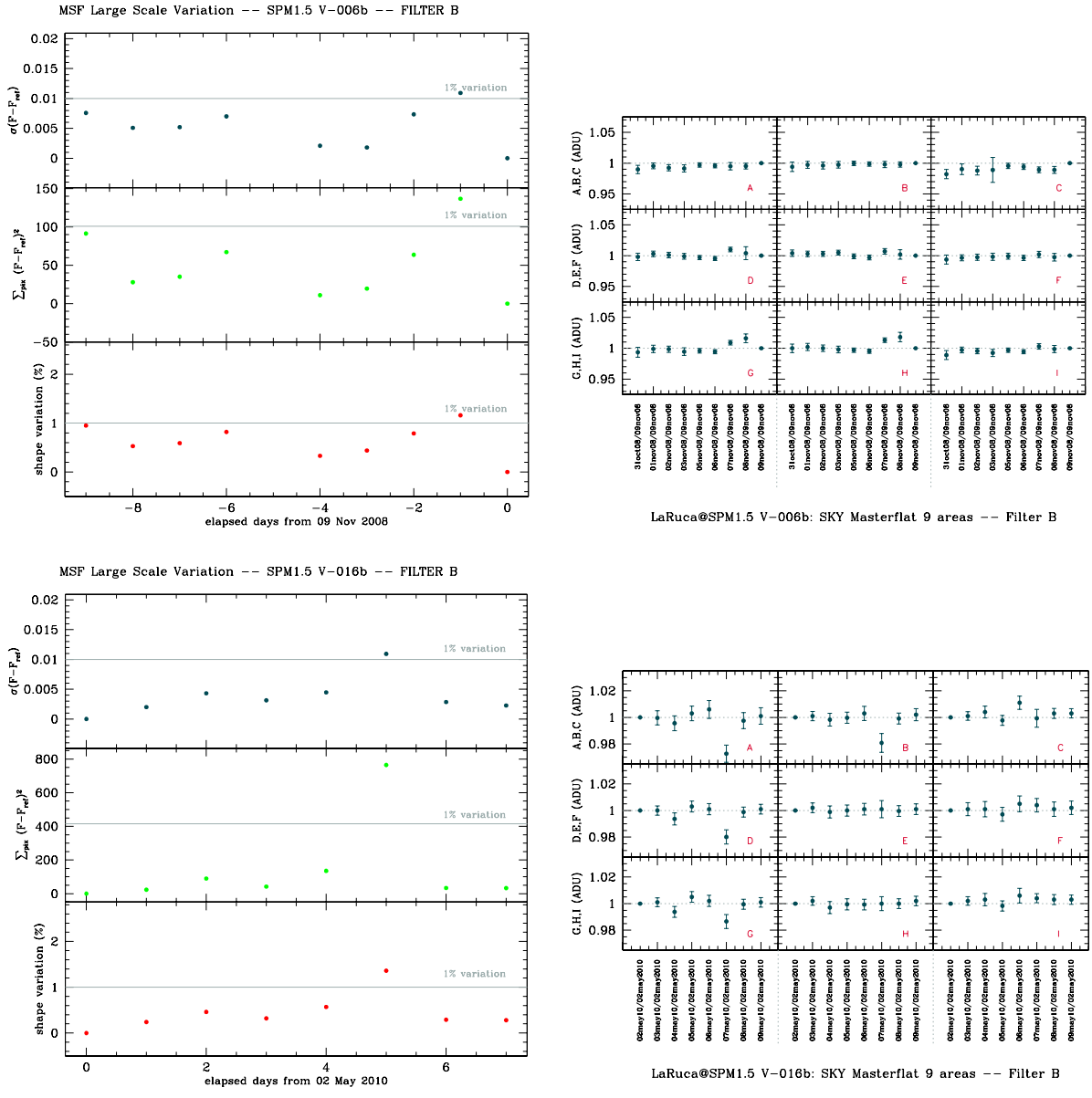

FIGURE 54: Stability tests for sky masterflat frames (B band) produced during run V-006b using the SITE1 CCD (*top panels*) and during run V016b using the Marconi1 CCD (*bottom panels*).

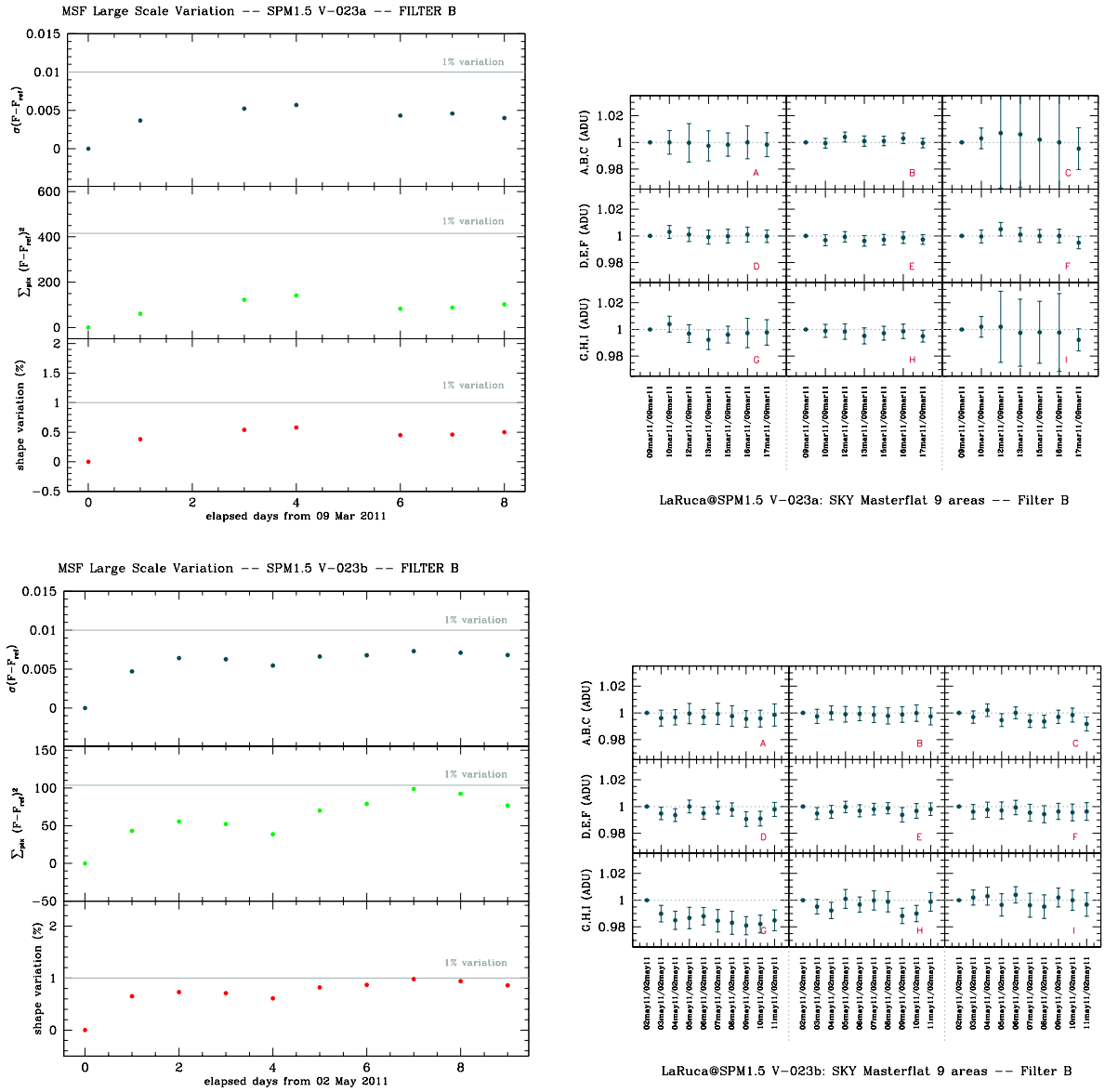

FIGURE 55: Stability tests for sky masterflat frames (B band) produced during run V-023a (*top panels*) and V-023b (*bottom panels*) using the Marconi2 CCDand the SITE4 CCD respectively.

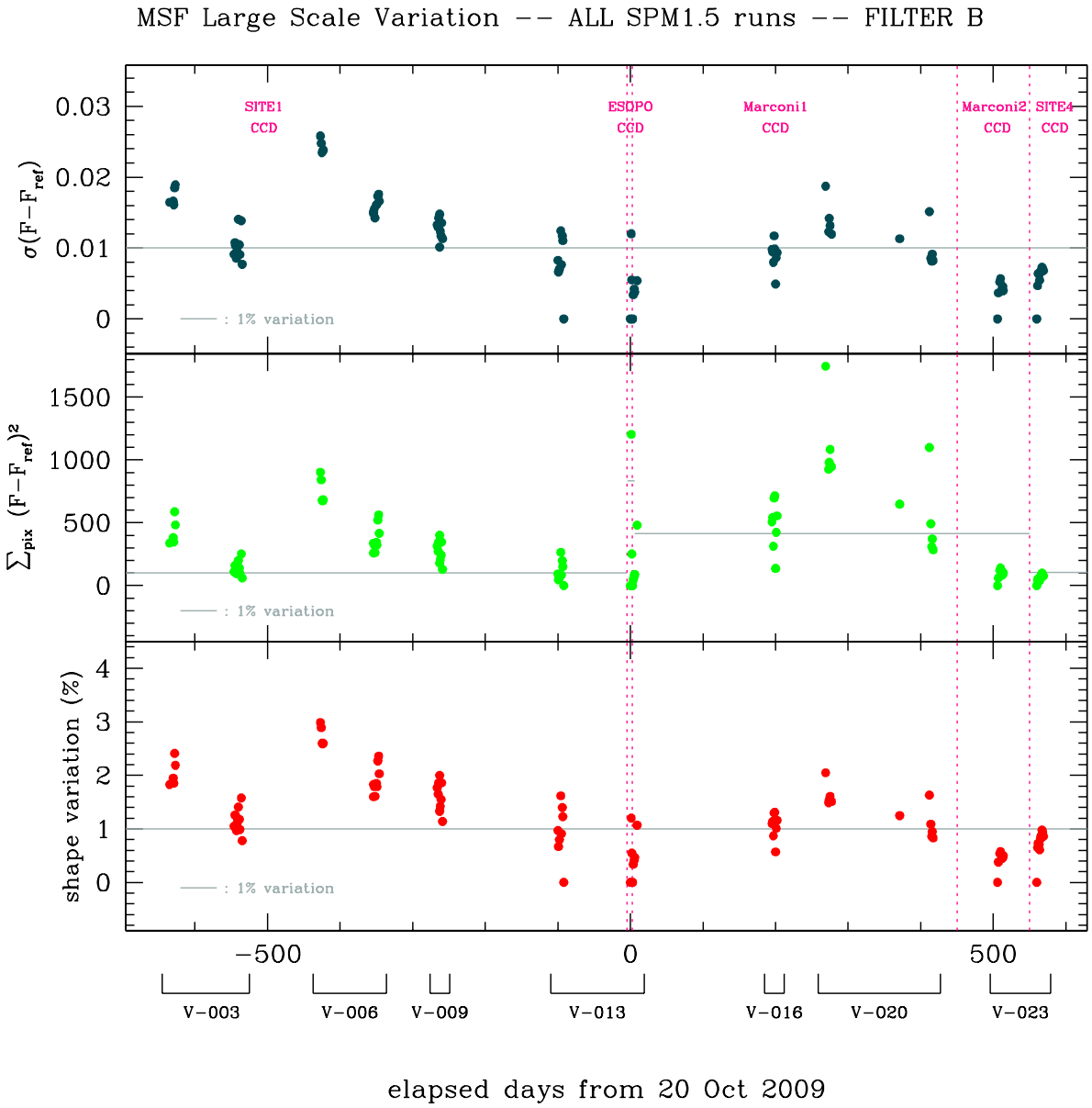

FIGURE 56: Long-time Large Scale Stability test performed on all sky masterflats produced with the B filter during all runs performed with LaRuca@SPM1.5 using different CCDs. Owing to the CCD changes, one reference frame for each CCDs has been chosen (see text). The inter-run variation of the sky masterflat frames is clearly visible for all CCDs, as well as the night-by-night shape variation.

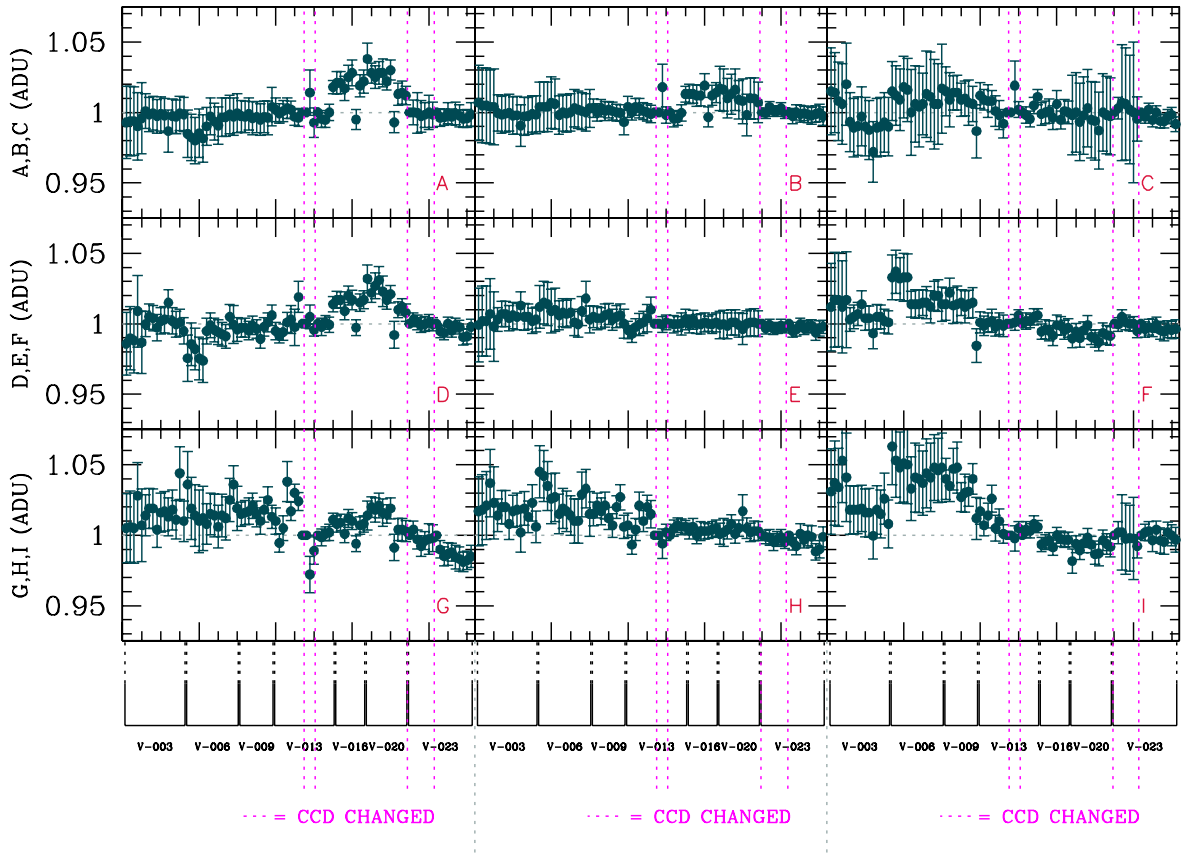

FIGURE 57: Long-time 9 areas test performed on all sky masterflat produced with the B filter during all runs performed with LaRuca@SPM1.5 using different CCDs. The reference frames for each CCDs used are the same of Fig. 56.

E.3 Masterdark

The check on the linear growth of Masterdark frames with exposure time was performed for all CCDs used with LaRuca, except for the SITE4 CCD because no darks were acquired during run V-023b. The test is shown in Fig. 58 using SITE1 data acquired during run V-003 and ESOPO data from run V-013. The same study, performed on darks acquired using the Marconi1 CCD (run V-020) and Marconi2 CCD (run V-023), can be found in Fig. 59 . For all used CCDs, there is no evident difference in counts between masterdark frames produced with increasing exposure times, and no dark correction is needed for scientific data. As usual, only few examples are shown here: other dark sequences were taken during SPM runs, and their analysis is available in Wiki-Bo.

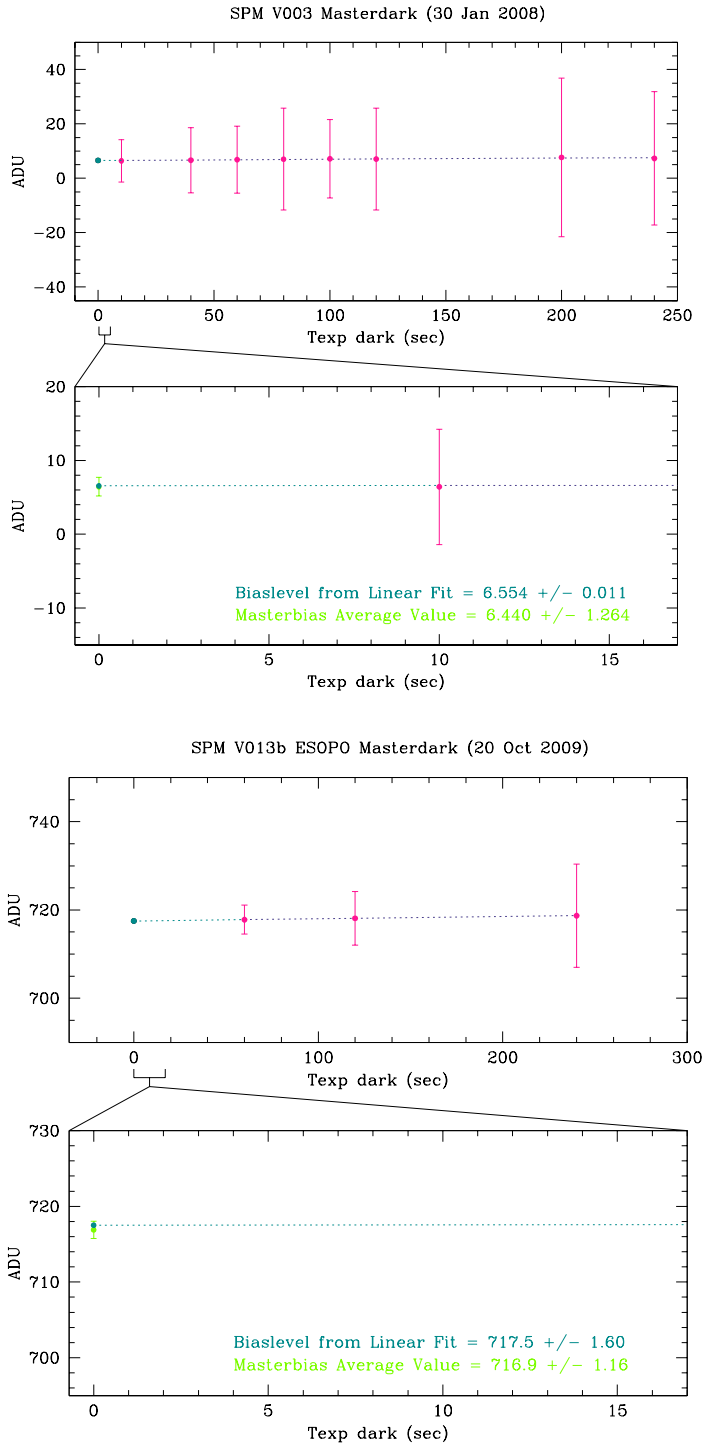

FIGURE 58: Quality control on masterdark frames of run V-003 and V-013@SPM1.5 produced using the SITE1 (upper plot) and the ESOPO CCD (bottom plot) respectively. The mean value of each masterdark is plotted versus exposure time. In the bottom panel of each plot, a zoom is shown in order to compare the bias level extrapolated from the linear fit (dark green point) with that measured directly from the masterbias frame (light green point).

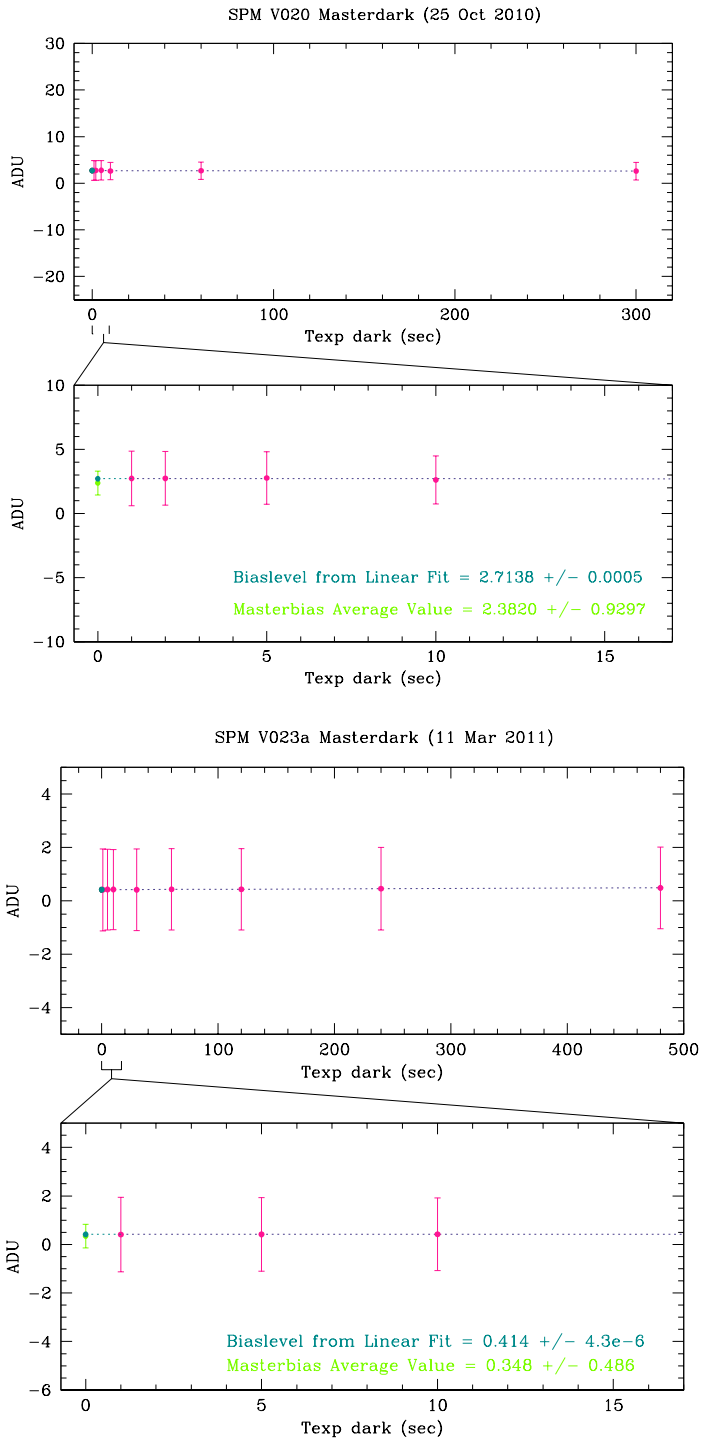

FIGURE 59: Quality control on masterdark frames of run V-020 and V-023@SPM1.5 produced using the new Marconi1 (upper plot) and the Marconi2 CCD (bottom plot) respectively. The mean value of each masterdark is plotted versus exposure time. In the bottom panel of each plot, a zoom is shown in order to compare the bias level extrapolated from the linear fit (dark green point) with that measured directly from the masterbias frame (light green point).

F ROSS@REM Calibration Frames IFP results

F.1 Masterbias

No bias frames are acquired for ROSS, beacuse the bias level and pattern is already included in dark frames (see EP-003).

F.2 Masterflat

Since we do not apply any masterflat correction to data acquired with ROSS@REM in our pre-reduction pipeline (owing to the light concentration problem, see SMR-004), we did not perform any study of the stability of these calibration frames.

F.3 Masterdark

Monthly Masterdark frames are produced by the REM team for exposure times of 1, 2, 3, 4, 5, 10, 15, 20, 30, 40, 60, 120, 240, 300 seconds. From our experience, we found that 180 seconds is a suitable exposure time for most of our targets, while 60 seconds are enough for the brightest targets ($V \leq 10.5$, see EP-003). The REM team does not produce routinely any 180 seconds monthly masterdark, so they have to be produced from 120 and 240 seconds darks, as explained in SMR-001.

We report, in Fig.60 and Fig. 61, the dark level (left panels) and the two-dimensional stability trends (right panels) for the 60 sec and 180 sec masterdarks respectively, acquired and produced during the first three REM runs (V-001, V-004 and V-007). Masterdark frames, for both exposure times, are very stable in shape, but the counts level shows seasonal changes. Therefore, our pre-reduction protocol (SMR-001) foresees the use of the closest available masterdark.

As an example, we show in Fig.62 the check on the linear growth of masterdark frames with exposure time for masterdark produced in July 2008 (run V-004). As usual, all tests performed on ROSS@REM masterdarks can be found in Wiki-Bo.

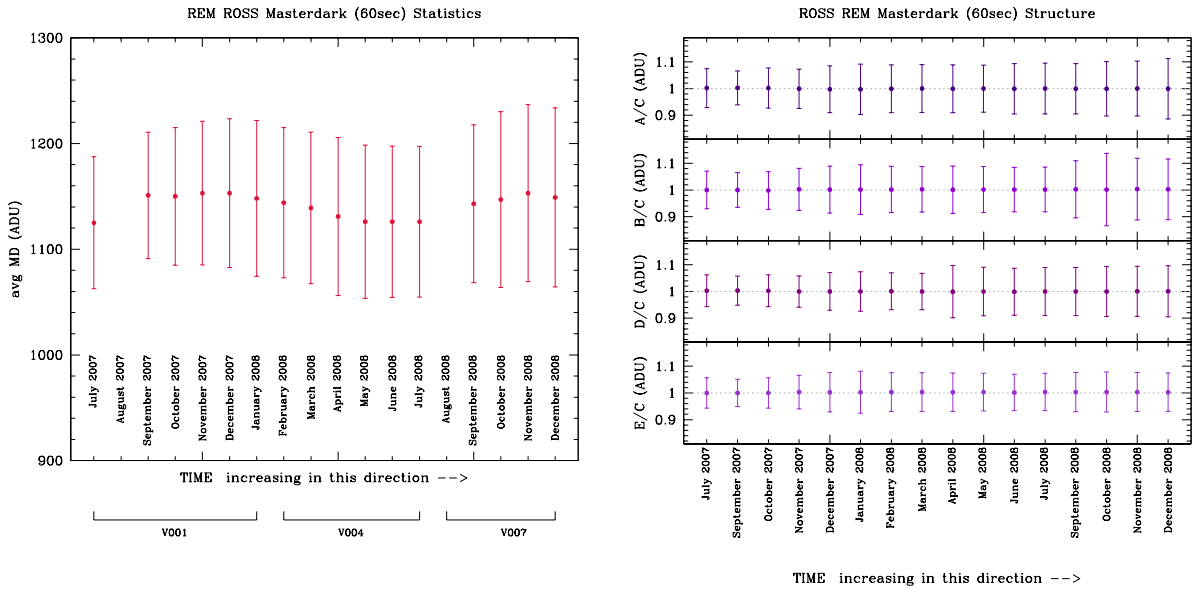

FIGURE 60: Long-time trend of the 60 sec dark level (*left panel*) and two-dimensional structure (*right panel*) produced using data acquired with ROSS@REM in the first three runs.

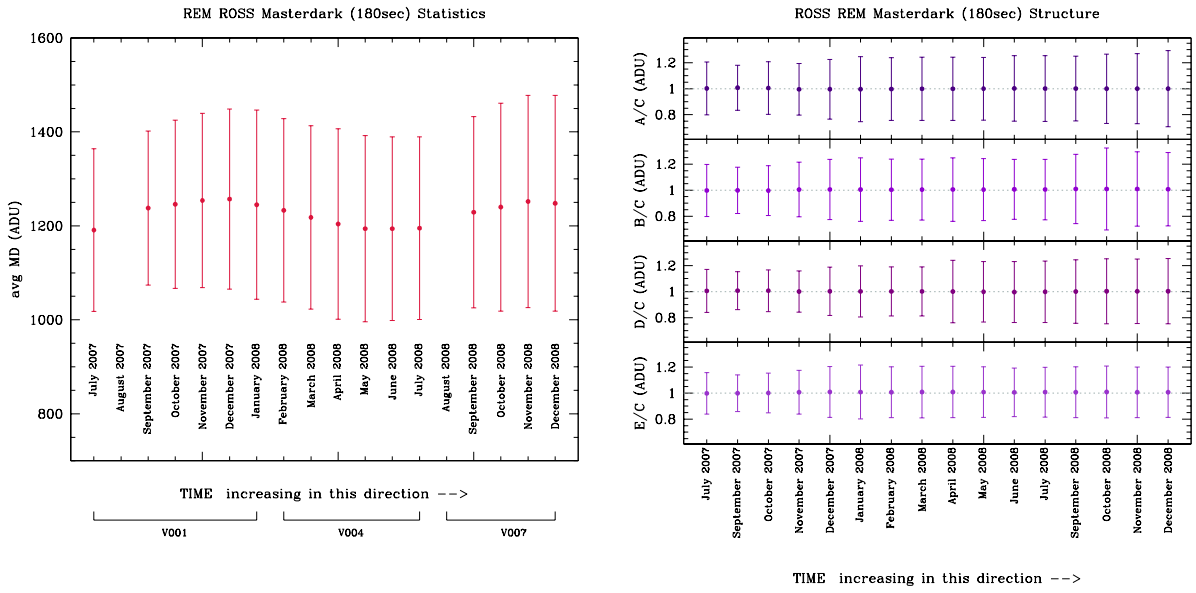

FIGURE 61: Long-time trend of the 180 sec dark level (*left panel*) and two-dimensional structure (*right panel*) produced using data acquired with ROSS@REM in the first three runs.

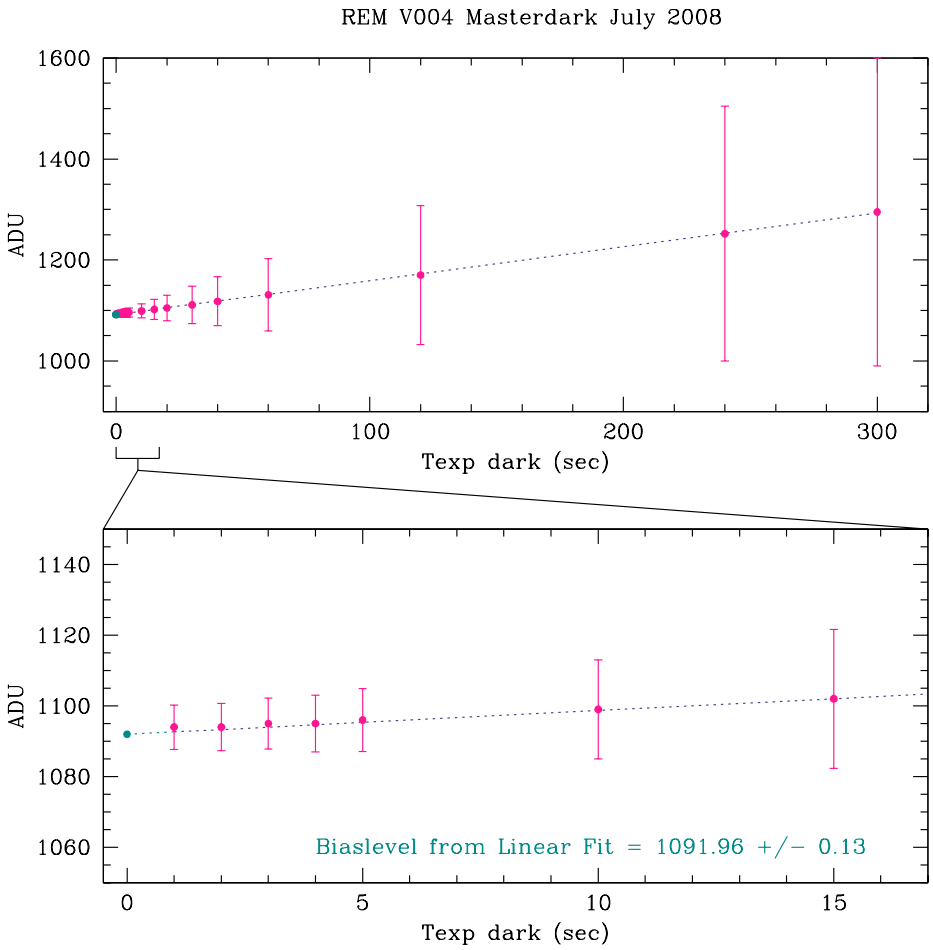

FIGURE 62: Quality Control on monthly masterdark frames produced by the REM team. The mean value of the July 2007 (run V-001) and July 2008 (run V-004) masterdark is plotted versus exposure time. In the bottom panel of each plot, the bias level extrapolated from the linear fit is reported.